ATMOSPHERIC STUDIES
BY
OPTICAL SCATTERING

Presented by

G.M.Shah,M.Sc.

for the degree of

DOCTOR OF PHILOSOPHY

of

THE GUJARAT UNIVERSITY

March 1982

Physical Research Laboratory,
Ahmedabad-9, India.

PREFACE

Studies in atmospheric ozone have been going on in India for a number of years now and various aspects of the subjects and of allied problems in the physics of the atmosphere have been engaging the attention of workers in the Physical Research Laboratory, Ahmedabad under the guidance of Professor K.R.Ramanathan. The author has been associated with this work since 1956 and the results reported in this thesis form part of this work.

Section I of the thesis gives an account of the author's work on atmospheric ozone. It includes a summary of the observations made computations and a discussion of the results, in relation to our present knowledge of the subject. In particular, the data of the IGY-IGC period are reviewed.

Section II of the thesis gives an account of author's studies on the scattering of light by aerosols in the atmosphere by measurements of the light scattered by the sky during twilight.

Certified that the thesis submitted by Mr.G.M.Shah is an account of the research work carried out by him at the Physical Research Laboratory, Ahmedabad.

Dated : 23rd March 1962.

(K.R.Ramanathan)

ACKNOWLEDGEMENTS

The ozone and twilight observations at Abu were made by the author from 1957-59. My colleague Shri P.D.Angreji has been responsible for taking ozone observations at Srinagar. Observers of the Indian Meteorological Department have been responsible for ozone observations at New Delhi and Kodaikanal. The Director of the Aerological Observatory at Tateno, Japan has been kind enough to send us the Aerological Bulletins which contain ozone and upper air data. I am thankful to all of them.

My thanks are also due to Dr.R.N.Kulkarni and Shri P.D.Angreji who helped me in taking moon observations. I am thankful to my colleague Shri P.D.Angreji for his help in preparing some diagrams.

I am thankful to the Council of Scientific and Industrial Research, New Delhi, India, for the award of a research assistantship during the course of study.

In the end, I wish to acknowledge my indebtedness to my Professor, Dr.K.R.Ramanathan under whose valuable guidance the work was carried out.

CONTENTS

SECTION I

STUDIES ON ATMOSPHERIC OZONE

SECTION II

DETECTION OF DUST LAYERS IN THE ATMOSPHERE BY TWILIGHT SCATTERING

SECTION I

STUDIES ON ATMOSPHERIC OZONE

CHAPTER I

CONTENTS

CHAPTER I

Part I

1. Introduction

The author has been engaged in studies on atmospheric ozone since 1956. He was in charge of the ozone observation station at Mt. Abu during the IGY and IGC. The results of his observations will first be discussed in relation to our present knowledge of the subject.

To-day the instrument most widely used for measurements of atmospheric ozone is the Dobson photo-electric photometer. A detailed description of the instrument and its working is given in IGY Annals, Vol.5 (1957-58).

Dobson spectrophotometer No.54 was received at the Physical Research Laboratory, Ahmedabad in the month of May 1956. It was assembled and tested at Ahmedabad in September 1956. The instrument has metallised optical wedges.

The wavelength settings were checked using the emission lines 3021 Å and 3129 Å from a Philips Hg discharge lamp and 3404 Å from a Cd lamp.

The wedges were calibrated by using perforated thin metal sheets whose transmission ratios were calculated by measuring the areas of the holes in defined areas.

New tables for the λ settings and for converting the dial readings R to log I/I'(N) were prepared from the calibration of the wedges at Ahmedabad in October 1956.

Both total-ozone and umkehr observations were made at Ahmedabad to test the consistency of the observations.

The instrument was transferred to Mt.Abu (24°N) in June 1957. The altitude of the station is 4000 ft. Ozone measurements were made with this instrument at Abu during IGY and IGC periods.

After the transfer to Abu, the instrumental adjustments were again tested and the wedge re-calibrated. Some small changes were necessary in the λ settings and these were made.

No appreciable change was found in the wedge calibration and the table for converting R to N prepared at Ahmedabad could be used at Abu. Regular observations

with the wavelength pairs λλCC' and λλAD were started at Abu from 1st July 1957 with Dobson spectrophotometer No.54. Umkehr measurements with wavelength pairs λλ A (3055/3254), λλ C (3114/3324) and λλD (3176/3383) were made on days of clear weather and especially when the total ozone amount was found to change rapidly.

An attempt was also made to measure the changes of ozone during night. The observations were made with moon light at Abu, during 1958-59, at Ahmedabad during 1960-61 and at Anand, 50 miles south of Ahmedabad during 1961.

Umkehr curves were obtained on about 100 days and out of these, a number was selected for calculating the vertical distribution. Corrections for multiple scattering were determined by the differential method using umkehr curves determined on the same days with A, C and D pairs of wavelengths.

Zenith sky intensity measurements with Dobson spectrophotometer were also made during 1957-58 on days when the zenith sky was covered with uniform clouds but direct sun observations also were possible within a few hours of the zenith sky measurements. The aim of these measurements was to connect up empirically the amount of total ozone obtained from zenith cloudy sky observations

with those obtained with the direct sun.

The observations presented in this thesis were made by the author during 1957-61.

2. Dobson's photo-electric spectrophotometer

2.1 General principle of the instrument

The amount of ozone in the atmosphere is determined by measuring with a spectrophotometer the relative intensities of two narrow bands of solar ultraviolet radiation, one well within the Hartley absorption band and the other just outside it.

The ratio is determined thus :

(a) The two bands of wavelengths are selected by slits in the focal plane of a monochromator.

(b) They are allowed to fall on the same photomultiplier alternately by means of a rotating sector.

(c) The intensity of the stronger beam is reduced in a known ratio by adjustable optical wedges so that the intensities of the two beams are equal.

(d) An A.C. amplifier amplifies the fluctuations in the current from the photomultiplier and the rectified current passes through a micro-ammeter. When the instrument indicates no current, the intensities of the two wave-length bands are equal.

Thus, the position of the wedge when the meter indicates zero is a measure of the ratio of the intensities of the two wave-length bands.

2.2 Description of the optical system of the Dobson spectrophotometer No.64[1]

Fig.1 gives a schematic diagram of the optical system of the Dobson spectrophotometer.

Light enters through a window (W) in the top of the instrument and is reflected in a right-angled prism (P). It then falls on the slit (S_1), of the first spectroscope. This spectroscope consists of a quartz lens which renders the light parallel, a 60° prism P_1 and a mirror M_1 which reflects the light back through the prism and lens to form a spectrum in the focal plane of the instrument. In actual observations, a quartz reflecting prism called the sun director

OPTICAL SYSTEM OF THE DOBSON SPECTROPHOTOMETER

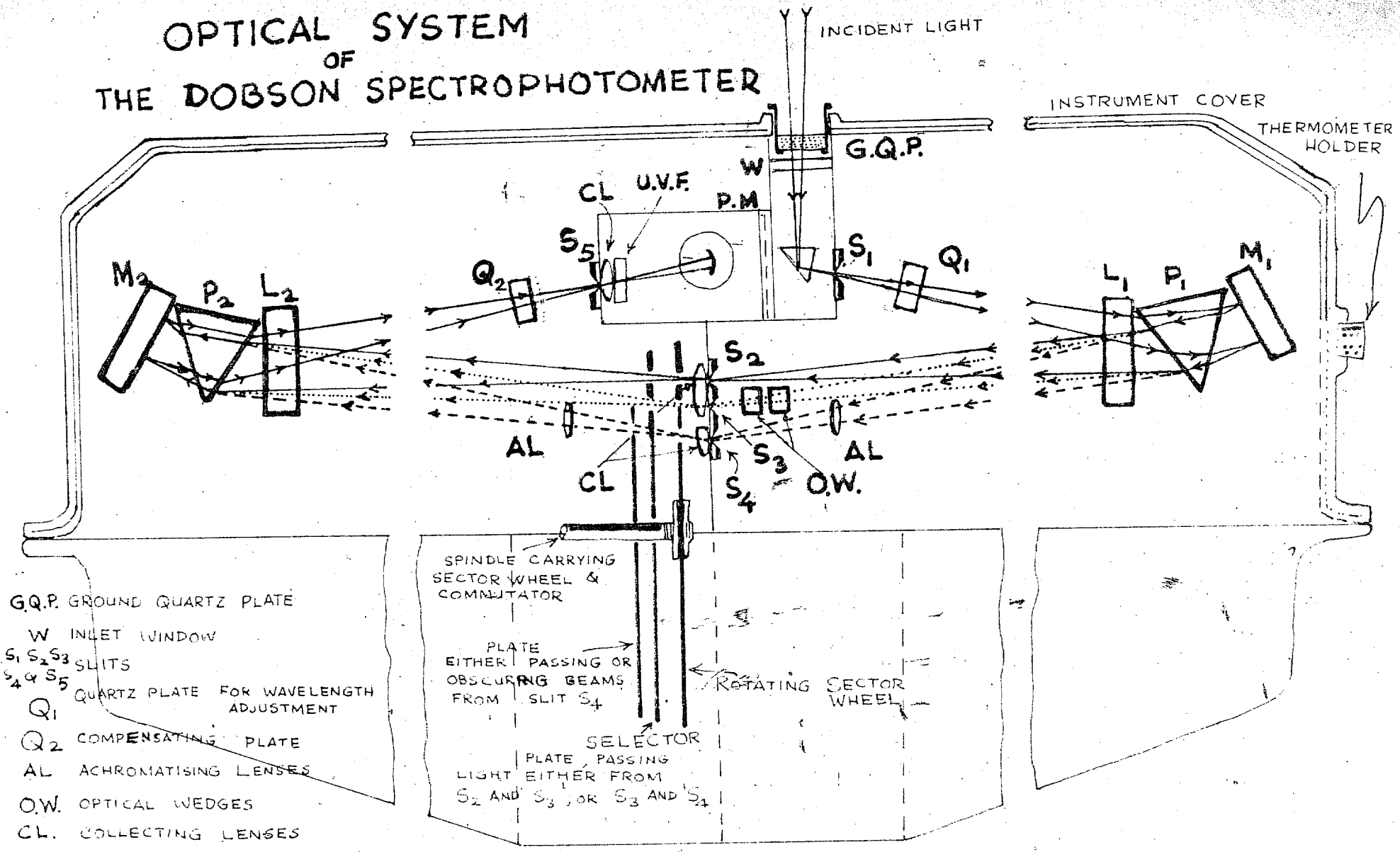

G.Q.P. GROUND QUARTZ PLATE
W INLET WINDOW
S_1 S_2 S_3 S_4 & S_5 SLITS
Q_1 QUARTZ PLATE FOR WAVELENGTH ADJUSTMENT
Q_2 COMPENSATING PLATE
AL ACHROMATISING LENSES
O.W. OPTICAL WEDGES
CL. COLLECTING LENSES
L_1 L_2 QUARTZ LENSES
P_1 P_2 QUARTZ PRISMS
M_1 M_2 MIRRORS
U.V.F. ULTRA VIOLET FILTER
P.M. PHOTO MULTIPLIER

FIG. 1

is used to throw direct sunlight on to the window. A ground quartz plate which fits over the inlet window is provided to even out and sometimes to reduce the intensity.

A thick plane parallel quartz plate Q_1 is mounted in front of slit S_1. It can be rotated about a horizontal axis and its inclination to the vertical is shown by a pointer which moves over the scale on the outside of the cover. The light passing through slit S_1 is reflected by Q_1 and displaced up or down depending on the angle of incidence of the ray with the quartz plate Q_1.

Three slits (S_2, S_3, S_4) are fixed in a plane at right angles to the axis of the instrument. These slits isolate the required wave-lengths from the spectrum. The slit that isolates the shorter wave-lengths is named S_2 and that isolating longer wave-lengths is named S_4. S_3 isolates intermediate wave-lengths. The wave-lengths passing through S_2, S_3 and S_4 can be changed within certain limits by changing the inclination of the quartz plate Q_1. The wave-lengths passing through S_2 can be changed from 3050 Å - 3250 Å and the wave-lengths through S_3 and S_4 are changed correspondingly.

I

The slits S_2, S_3 and S_4 are controlled by a rod which operates a shutter which blocks out either S_2 or S_4 slit , thus enabling only two wavelengths at a time to pass through.

The positions of the slits are adjusted in such a manner that only selected wavelengths pass through them, that is, when 3114 Å passes through S_2, 3324 Å must pass through S_3 and 4536 Å must pass through S_4.

After passing through S_2 or S_3, the light passes through a rotating sector driven by electric motor which allows the two wavelengths to pass alternately into a second spectroscope. It is an exact copy of the first. The purpose of the second monochromator is to reduce the effect of scattered light.

After passing through prism P_2, mirror M_2 and lens L_2 of the second spectroscope the light of wavelengths 3114 Å or of 3324 Å and 4536 Å passes through another thick quartz plate Q_2 and enters the slit S_5 and falls on the cathode of a photomultiplier. The purpose of Q_2 is to deflect the beams of light passing through S_2, S_3 so that the same wavelengths fall on S_5. An ultraviolet filter F is placed behind the slit S_5 to reduce further the effect of any scattered light in the longer wavelength.

Changes in refractive index of the prisms due to changes in temperatures are allowed for by adjusting the inclination of the quartz plates. Approximately 1° change in inclination of the quartz plate corresponds to 10° change in temperature

A lens L_3 has been fitted adjacent to slits S_2 and S_3. As the optical parts are set symmetrically in the two halves of the instrument the correct alignment of the beams through S_2 and S_3 depends on the focal length of the lens. The focal length is so adjusted as to refract the beams through S_2 and S_3 back to recombination as a single beam on emergence from the second prism.

The lens L_4 is set centrally behind the slit S_5, and the slit, lens and u.v. filter are placed in the photomultiplier box. The lens L_4 focusses the image of the prism P_2 on the photomultiplier, so that the bands through S_2, S_3 and S_4 fall at the same photosensitive surface of the photomultiplier.

To focus the wave band coming from λ4636 Å from the first spectroscope on S_4 in the plane of other slits S_2 and S_3, an achromatising lens A_1 is mounted in the path before the slit S_4. For symmetry another achromatising lens A_2 is mounted after the slit S_4.

It is to be remembered that slits S_2, S_3 and S_4 are such that the wave bands of 14 Å, 27 Å and 11 Å can pass through them respectively. If the slit S_2 is more wide the variation of the absorption coefficients of ozone over the range of the wavelengths passed by S_2 will introduce appreciable errors since the absorption coefficient changes much with the wavelength in that region.

A three stage A.C amplifier is used to amplify the

current from the photomultiplier. The amplified a.c. signal is rectified by a synchronous mechanical commutator mounted on the shaft driving the sector wheel and read on a D.C. micro-ammeter.

The wavelength 3324 Å is in the weak absorption region of ozone but 3114 Å passing through S_2 is in strong absorption region. Thus the light for wavelength 3324 Å produces greater photoelectric current. As the measurements consist in knowing the relative intensities of the two beams, the method of reducing the intensity of the less absorbed light by means of optical wedges has been adopted.

Metallised optical wedges are mounted in the path of the light 3324 Å coming from S_2. The intensity of light of this wavelength is reduced by optical wedges until the output from the photomultiplier is the same for both wavelengths and the meter indicates zero. This position of wedge is a measure of the relative intensities of the two wavelengths.

2.3 Calibration of spectrophotometer[2]

2.3.1 Checking up of Q values for λ settings

The checking up of Q values of the instrument is done inside a room. After seeing that the silica gel inside the instrument is blue and dry and the batteries supplying the filament current (2 volts), plate voltage for the amplifier

(105 volts dry battery) and the super-high tension for the photomultiplier (950 volts, regulated power supply unit) are all in good condition, it is examined whether the pointers connected to the quartz plates Q_1 and Q_2 read 34° when they are vertical as is required according to the instructions in the operator's handbook.

Owing to the change in the refractive index of quartz with temperature and the expansion of the metal of the instrument there is a small change required in the Q setting when the temperatures differ from 15° C. For every 10° C increase in temperature the setting of Q_1 should be increased by 1° when Q_2 is set at the value appropriate for 15° C.

The ground quartz plate is placed over the slit of the spectrograph inside the inlet window. The Hg discharge lamp was mounted over the inlet window with its length parallel to the slit so as to illuminate the window. The lamp is kept switched on for a few minutes to get constant emission before any adjustment is made or reading taken. The shutters in the instrument are then set so as to allow the light to pass through the slits S_2 and S_3 or S_3 and S_4. The light passing through the slit S_3 is reduced in intensity by keeping the thick end of the wedge in front of the S_3 slit, if light passing through S_2 is needed.

Then using the emission lines 3021 Å and 3125 Å from a Phillys mercury discharge lamp and 3404 Å from a Cd lamp,

I

the positions of Q_1 pointer on the scale were determined when 3021 Å and 3130 Å were passing through S_2 slit and 3404 Å through S_3 slit according to method described by Dobson and Normand in Annals of IGY, 5 (1957-58). The values of Q_1 for different temperature and wavelengths were determined using appropriate temperature factors as given in the same article, and a table was prepared to give Q_1 for different temperatures and wavelengths.

2.3.3 Calibration of optical wedges

Ideal wedge

An ideal optical wedge would be one in which any dial reading R changes to (R-100 log r) when the transmitted light increases r times. For example, if the transmitted intensity becomes twice the original intensity by a displacement of the wedge, $\log_{10} 2 = 0.3010$. On the dial, 0.3010 corresponds to $30^{\circ}.10$.

On calibrating the actual optical wedge, supplied with the instrument it is found that a correction, varying with the dial reading has to be applied in order to convert the observed dial readings to readings of an ideal wedge.

Actual optical wedges

In the instrument, there are actually two equal optical

wedges placed end to end as shown in the sketch. They are moved relative to each other across the wavelength selector slits. The optical wedges can be calibrated by interposing in the path of the light, a filter of known constant opacity and doing it for different initial positions of the wedge. The constant opacity takes the form of either a perforated metal plate of known transmission ratio or a Rhodiumised quartz plate which acts as a neutral filter. In India, direct sunlight near about midday from a clear sky is a very convenient source of light. A pair of standard lamps run under constant conditions can also be used.

The methods of calibrating the wedges by Rhodiumised plate and by lamps are described in the operator's handbook. The method used by the author for wedge calibration at Abu is described here.

Calibration of wedges

For calibrating the wedges of the Dobson spectrophotometer No.64, the following method was employed.

The instrument was set up so as to allow direct sunlight from the clear sky between 11 and 13 hours to enter the instrument through the sun director. Q_1 and Q_2 were adjusted so that light of wavelength 3324 Å fell on slit S_3. The deflection of the meter could be controlled by adjusting the photomultiplier voltage.

I

The wedge was moved to such a position that the deflection in the micro-ammeter was nearly full scale. A thin perforated metal gauze dull black was interposed in the path of the light, causing a decrease in the meter reading, and moved about continuously at right angle to the incident beam so as to average out the light passing. The now steady deflection was noted and the same steady deflection was then obtained by removing the metal gauze and readjusting the wedge. The difference between the first and second dial readings corresponds to the attenuation of the incident beam caused by the perforated metal gauze.

The operation was repeated a number of times. The wedge was then moved successively in steps to new positions, and for each position, after re-adjusting the sensitiveness of the amplifier and voltages on the photomultiplier so as to give nearly full-scale deflection without the screen, the correspondin change in the dial position was noted.

The dial readings R_1 and R_2 with and without the gauze were determined throughout the length of the wedge. These differences $\Delta R (= R_2 - R_1)$ were plotted against the mean dial readings $\frac{(R_1 + R_2)}{2}$.

The observations were repeated on a few clear days and with different initial positions of the wedge. The mean transmission ratio of the gauze which was determined to be 45.65 % corresponded to a value of $\Delta L = 0.3405$.

I

From the smoothed curve of ΔR against R (Fig.2), $\Delta L/\Delta R$ was calculated for each degree of the dial and the value of L for different values of R were determined by successive summations. By adding an appropriate constant, the zero of "L" was made to coincide with the zero of R.

A table was then prepared giving the value of Log I/I' (L) for every $0^{o}.1$ of a dial. Using the identity $100\ (L_{o} - L) \equiv N - N_{o}$ this table was converted into a table of N against R.

The value of N_{A} for another wavelength like 3254 Å can be determined by multiplying the N_{λ} value for 3324 Å by the relative opacity p_{λ} e.g.

$$N_{A} = p_{A} N_{C}$$

Determination of relative opacity of optical wedges p_{λ}

The wedge calibration were repeated with wavelengths 3254 Å, 3324 Å and 3388 Å, using the same perforated metal gauze (45.63 % transmission). The values of dial readings R_1 and R_2 with and without the gauze were found for different wavelengths. The corresponding values of N_1 and N_2 are found from R to N table. Then the relative opacity factor

$$p_{A} = \frac{(N_2)_{C} - (N_1)_{C}}{(N_2)_{A} - (N_1)_{A}}$$

$$p_{C} = 1$$

I

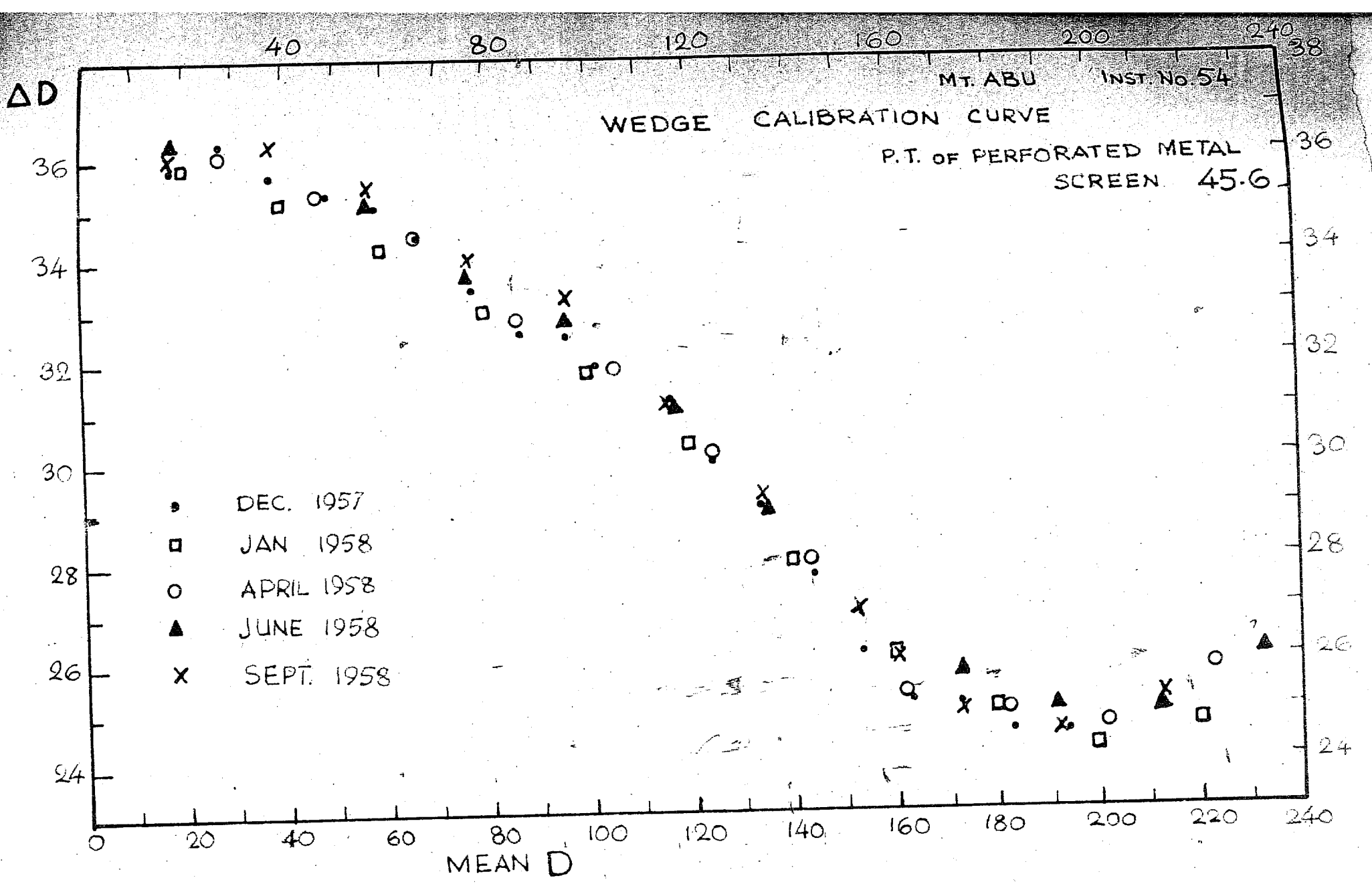
MT. ABU INST. No. 54
WEDGE CALIBRATION CURVE
P.T. OF PERFORATED METAL SCREEN 45·6
ΔD
MEAN D
DEC. 1957
JAN 1958
APRIL 1958
JUNE 1958
SEPT. 1958
0 20 40 60 80 100 120 140 160 180 200 220 240
24 26 28 30 32 34 36 38

FIG. 2

$$\text{and} \quad p_D = \frac{(N_2)_C - (N_1)_C}{(N_2)_D - (N_1)_D}$$

The values for p_A, p_C and p_D for the metallic wedge in instrument No. 34 were found to be 1.02, 1.00 and 0.03 respectively.

2.3.3 Determination of "N_0" values

Days when the ozone changes are small, are common at Abu. On such days direct sun observations with all the three wavelength pairs $\lambda\lambda A$, $\lambda\lambda C$ and $\lambda\lambda D$ were made over a large range of sun's zenith distances. The plot of $p_\lambda N_\lambda$ against μ the optical path of the light through ozone layer, the vertical to be taken as unity, is made. The graph of $p_\lambda N_\lambda$ against μ would give a good straight line and extrapolation to $\mu = 0$ gives the value of N_0 for A, C and D pairs (Fig.3), the value of N outside the atmosphere. "N'_0", the value of N' outside the atmosphere was determined by taking observations with longer wavelength.

Except for instrumental changes "N_0" is assumed to remain constant with time. By making periodical determinations of "N_0", the constancy of the instrument is tested.

3. Measurements of total amount of ozone using direct sunlight

3.1 Selection of wavelength

Ozone has absorption bands in the ultra violet, visible

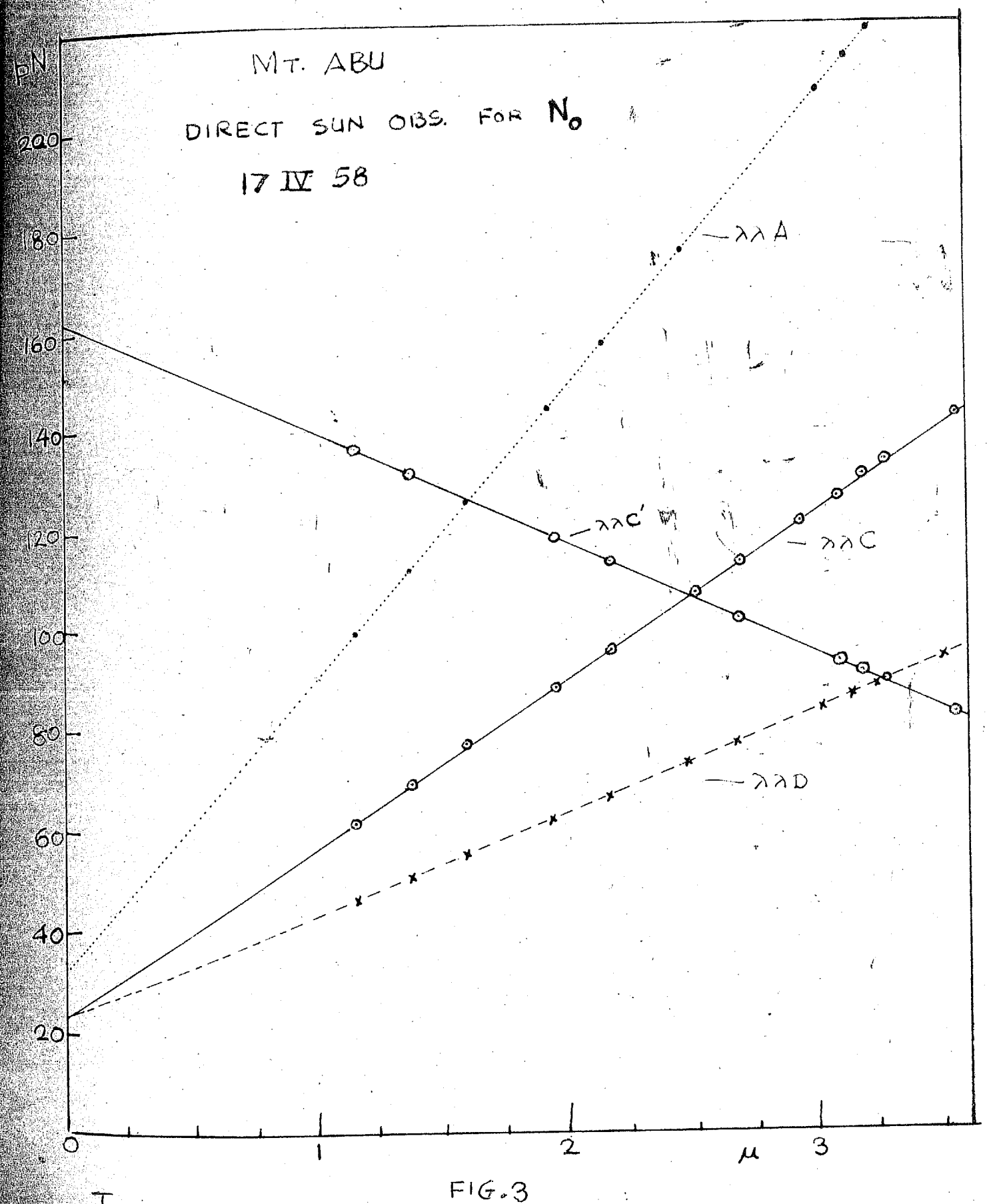
MT. ABU
DIRECT SUN OBS. FOR N_o
17 IV 58
pN
200
180
160
140
120
100
80
60
40
20
0
1
2
μ
3
λλA
λλC'
λλC
λλD

FIG. 3

I

and infrared regions. The strongest of these is the Hartley band in the ultraviolet extending from (3000 Å - 3000 Å). The Chappius band system in the visible is weak; the infrared band at 9.6 μ is important because it plays an important role in the radiation balance of the stratosphere. Overlapping the Hartley bands on the long wavelength side are the Shaver bands and Huggins bands occupying the regions 3200 Å - 3600 Å.

The property of differential absorption of ozone in the ultraviolet is used to estimate the total amount of ozone in the atmosphere. Thus the determination of the amount of ozone consists in determining the relative intensities of the light in two narrow bands of wavelengths (say near 3114 Å and 3324 Å) in the solar ultraviolet spectrum; one well within the highly absorbing region of the Hartley band and the other just outside it on the visible side.

Another pair of wavelengths (λ 3324 and λ 4636 Å) is such that the difference in their scattering is large but absorption in ozone is small, so that their relative intensities can be used to estimate the correction due to large particle scattering or haze.

3.2 List of symbols used in ozone calculations

I_o, I'_o, I''_o = Intensities of solar radiation in unit band-width at wavelengths λ, λ' and λ'' respectively outside the earth's atmosphere.

I

I, I', I'' = Intensities of λ, λ' and λ'' respectively outside the instrument.

X = The amount of ozone in a vertical column of unit area expressed as the thickness in cm which this amount of ozone would occupy if concentrated into a uniform layer of pure gas at S.T.P. It is expressed in milli-atmo-cm or Dobson units.

Z = The sun's zenith distance measured from the earth's surface.

m = The equivalent path-length of sunlight through the atmosphere allowing for refraction and curvature of the earth ($m = 1$ when $Z = 0$).

μ = The relative path-length of sunlight through the ozone gas ($\mu = 1$ when $Z = 0$). μ is calculated on the assumption that the c.g. of ozone is at a height of 22 km over a curved earth.

α, α', α'' = Decimal absorption coefficients of ozone for 1 cm of pure O_3 at N.T.P. for wavelengths λ, λ' and λ''.

β, β', β'' = Decimal scattering coefficients of clear air for λ, λ' and λ'' respectively. The scattering being due to air molecules and to particles which are small compared to λ and which therefore scatter light inversely as the fourth power of the wavelength.

δ , δ', δ'' = Decimal scattering coefficients of atmosphere at wavelengths λ, λ' and λ'' respectively due to particles which are large compared with λ and therefore tend to scatter all wavelengths equally.

R = Dial reading on the instrument when comparing the intensities of wavelengths λ and λ'.

R' = Dial reading when comparing wavelengths λ' and λ''.

L_o = Log I_o/I'_o

L'_o = Log I''_o/I'_o

L = Log I/I'

L' = Log I''/I'

p = The relative opacity of the optical wedge at different wavelengths being regarded unit for the standard wavelength λ' 3324 $\mathring{A}$.

3.3 Calculation of total ozone

The intensity I at the surface of the earth when I_o, the radiation of the extraterrestrial intensity of wavelength λ is subjected to absorption in the Hartley band is given by

$$I = I_o \cdot 10^{-\alpha x/\mu - \beta m - \delta m}$$

Thus the basic equations for calculating total ozone amount are

$$\text{Log } I = \text{Log } I_o - \alpha x\mu - \beta m - \delta m \qquad (3)$$

$$\text{Log } I' = \text{Log } I'_o - \alpha' x\mu - \beta' m - \delta' m \qquad (4)$$

$$\text{Log } I'' = \text{Log } I''_o - \alpha'' x\mu - \beta'' m - \delta'' m \qquad (5)$$

From (3) and (4) by substraction we get

$$\text{Log } I/I' = \text{Log } I_o/I'_o - (\alpha - \alpha')\, x\mu - (\beta - \beta')\, m - (\delta - \delta')m$$

$$\text{or} \quad L = L_o - (\alpha - \alpha')\, x\mu - (\beta - \beta')\, m - (\delta - \delta')m \qquad (6)$$

From (4) and (5) we get

$$\text{Log } I''/I' = L' = L'_o + \underline{\alpha' x\mu} + (\beta' - \beta'')\, m + (\delta' - \delta'')m \qquad (7)$$

where α'' is negligible.

Equation (6) can be written as

$$X = \frac{(L_o - L) - (\beta - \beta')m - (\delta - \delta')m}{(\alpha - \alpha')\mu} \qquad (8)$$

$$= \frac{(L_o - L) - (\beta - \beta')m}{(\alpha - \alpha')\mu}$$

This was the equation used by Fabry and Buisson[3] and developed by Dobson (Dobson and Harrison 1926[4], Dobson, Lawrence[5] 1927-29, Dobson 1930[6]).

I

The net attenuation coefficients for dust and haze, water droplets and other large particles, δ and δ' should each be zero on very clear days where haze and dust is absent, but if the atmosphere contains particles whose size is comparable to the wavelength used, and haze which is common for our latitudes in India, the values of $\delta - \delta'$ will vary from day to day.

This last equation used by Dobson was modified by Ramanathan and Karandikar[7] to take account of the haze.

From equation (7) we get

$$(\delta' - \delta'') = \left\{ \frac{L' - L_0'}{m} - \frac{\alpha x \mu}{m} - (\beta' - \beta'') \right\}$$

$$\text{If } K' = \frac{(\delta - \delta')}{(\delta' - \delta'')} = \frac{\lambda^{-n} - \lambda'^{-n}}{\lambda'^{-n} - \lambda''^{-n}}$$

$$= \frac{\log \lambda - \log \lambda'}{\log \lambda' - \log \lambda''} \quad \text{as } n \longrightarrow 0$$

Ramanathan and Karandikar assumed that scattering due to large particles is proportional to λ^{-n}. After discussing their extensive results at Delhi they came to the conclusion that the most suitable value for n would be zero.

For Abu value of K' turns out to be 0.210.

Now $$(\delta - \delta') = K'(\delta' - \delta'')$$

$$= 0.210 \left\{ \frac{L' - L_0'}{m} - \frac{\alpha' x \mu}{m} - (\beta' - \beta'') \right\}$$

∴ Equation (8) becomes

$$x = \frac{(L_0 - L) - (\beta - \beta')m}{(\alpha - \alpha')\mu} - \frac{0.210\,\bar{m}}{(\alpha - \alpha')\mu}(\delta' - \delta'')$$

$$= \frac{(L_0 - L) - (\beta - \beta')m}{(\alpha - \alpha')\mu} - \frac{0.210}{(\alpha - \alpha')}\left\{\frac{L' - L'_0}{m} - \alpha' x - (\beta' - \beta'')\right\}$$

$$\text{or} \quad x = \frac{(N - N_0)}{100(\alpha - \alpha')\mu} - \frac{(\beta - \beta')m}{(\alpha - \alpha')\mu} - \frac{0.210}{(\alpha - \alpha')}\left\{\frac{N'_0 - N'}{m} - \alpha' x - (\beta' - \beta'')\right\} \qquad (9)$$

where $100\,(L_0 - L) \equiv N - N_0$

The wavelengths employed during the course of study and the corresponding values of ozone absorption and molecular scattering coefficients are given in the following table.

Table 1.

Wavelengths and other constants

Designation of wavelength pair.		Mean wavelength A.U.		Ozone absorption coeff. α	α'	$\alpha - \alpha'$	Atmospheric scattering coeff. β	β'	$\beta - \beta'$
A	Short	3055		1.382	0.120	1.762	0.491	0.375	0.116
	Long		3234						
C	Short	3114		0.912	0.047	0.865	0.453	0.343	0.110
	Long		3324						
D	Short	3176		0.301	0.017	0.374	0.416	0.312	0.104
	Long		3393						
C'	Short	3324		0.047	Nil	0.047	0.343	-	-
	Long		4536						

I

The values of $(\beta - \beta')$ given above are for sea-level (1013 mb) and require modification for high altitude station. Mt.Abu is at an altitude of 4000 ft, the values of β, β' would be reduced at that level to 90 % of the values at sea-level.

4. Comparison of ozone values determined by $\lambda\lambda$ca' and by $\lambda\lambda$AD method

If we use any two pairs of wavelengths, which we may designate "A" and "D" instead of equation (9) we get

$$x_{AD} = \frac{\left[(N - N_o)_A - (N - N_o)_D\right]}{100\left[(\alpha - \alpha')_A - (\alpha - \alpha')_D\right]/\mu} - \frac{m\left[(\beta - \beta')_A - (\beta - \beta')_D\right]}{\mu\left[(\alpha - \alpha')_A - (\alpha - \alpha')_D\right]}$$

$$\text{or } x_{AD} = \frac{\left[(N - N_o)_A - (N - N_o)_D\right]}{F/\mu} - G\frac{m}{\mu}$$

$$\text{Where } F = 100\left[(\alpha - \alpha')_A - (\alpha - \alpha')_D\right]$$

$$\text{and } G = \frac{100\left[(\beta - \beta')_A - (\beta - \beta')_D\right]}{F}$$

If it is assumed that the haze corrections due to two wavelengths A and D are equal, the haze correction term $(\delta - \delta')$ is eliminated.

I

The total ozone amount determined by AD method was found to be a little higher than that obtained by the CC' method (Table 1). The mean difference ($x_{AD} - x_{CC'}$) as determined from the ozone data collected during IGY and IGC periods of Indian stations was 0.004 cm for Abu, 0.009 cm for Srinagar and 0.007 cm for Kodaikanal. Some larger differences are found in individual observations at Srinagar. There were also similar larger differences at Kodaikanal in the first ten months, but after a recalibration and re-setting of the wavelength positions, the mean difference came down to 0.005 cm.

Table 1.

Monthly mean differences $x_{AD} - x_{CC'}$ in D.U. at Kodaikanal, Abu and Srinagar, using Vigroux' values of absorption coefficients of Ozone (α, α'). The number of observations in each month is given in brackets.

Year	Month	Name of stations: Kodaikanal	Mt.Abu	Srinagar
1957	Jun	-	6 (25)	-
	Jul	-	6 (16)	-
	Aug	-	5 (14)	6 (28)
	Sep	-	4 (26)	12 (15)
	Oct	-	4 (28)	10 (21)
	Nov	-	4 (23)	10 (24)
	Dec	-	5 (29)	10 (17)

I

Table 1 (contd.)

Year	Month	Name of stations: Kodaikanal	Mt.Abu	Srinagar
1958	Jan	-	5 (29)	10 (20)
	Feb	-	4 (28)	10 (10)
	Mar	-	4 (31)	10 (21)
	Apr	-	5 (29)	10 (29)
	May	15 (17)	6 (31)	9 (30)
	Jun	14 (13)	3 (26)	4 (30)
	Jul	13 (13)	3 (4)	4 (22)
	Aug	14 (4)	3 (16)	6 (31)
	Sep	14 (20)	4 (9)	5 (28)
	Oct	10 (11)	4 (25)	4 (29)
	Nov	11 (23)	3 (28)	8 (28)
	Dec	11 (23)	3 (29)	6 (9)
1959	Jan	11 (22)	3 (28)	14 (10)
	Feb	11 (20)	3 (26)	11 (20)
	Mar	6 (30)	3 (27)	10 (27)
	Apr	6 (17)	4 (29)	14 (29)
	May	5 (16)	4 (29)	8 (16)
	Jun	4 (10)	4 (23)	9 (30)
	Jul	3 (8)	-	8 (28)
	Aug	7 (12)	-	8 (30)
	Sep	7 (13)	4 (5)	6 (25)
	Oct	9 (9)	5 (18)	4 (28)
	Nov	6 (13)	3 (24)	9 (29)
	Dec	2 (16)	4 (29)	6 (31)

12
+6

Table 1 (contd.)

Year	Month	Name of stations: Kodaikanal		Mt. Abu		Srinagar	
1960	Jan	4	(21)	5	(20)	5	(24)
	Feb	6	(14)	3*	(24)	6	(17)
	Mar	5	(22)	4*	(24)	7	(21)
	Apr	4	(20)	5*	(27)	13	(26)
	May	5	(10)	5*	(28)	14	(27)
	Jun	5	(14)	5*	(20)	11	(27)
	Jul	5	(7)	5*	(7)	10	(29)
	Aug	5	(12)	5*	(3)	12	(23)
	Sep	7	(8)	5*	(22)	11	(28)
	Oct	6	(6)	5*	(26)	12	(29)
	Nov	4	(7)	4*	(28)	11	(27)
	Dec	5	(22)	5*	(24)	6	(18)
Average		7		4		9	

* The observations marked with an asterisk were made at Ahmedabad.

I

5. "Ozone observations with light from clear and cloudy zenith skies". This was published as a note by G.M.Shah in the Indian Journal of Meteorology and Geophysics, Vol.12, No.2, 345 (April 1961).

Reprinted from Vol, 12, No. 2, April 1961, of the Indian Journal of Meteorology and Geophysics pages 345 to 346

551.510.534

Ozone observations with light from clear and cloudy zenith skies

G. M. SHAH

Physical Research Laboratory, Ahmedabad

(*Received 12 January 1961*)

To make effective use of ozone measurements in Meteorology, *daily* observations of total ozone at a number of suitably distributed stations is necessary.

Dobson has shown that on days when the sky is clouded, measurements can be made with the light from the zenith sky. This method is followed at many stations in middle and high latitudes but has not generally been used in tropical latitudes. To try out whether the same method can be used with cloudy skies in tropical latitudes, zenith sky measurements were made during the period June 1957 to June 1958 at Mt. Abu (24°N) on days which were cloudy but on which direct sun observation could also be taken within a few hours of the zenith sky observation. For comparison, zenith sky measurements were made on many occasions along with direct sun observations when the zenith sky was blue.

The measurements were made with the wavelength pair $\lambda\lambda$ CC' and also with the pairs A and D in the manner suggested by Dobson and Normand. The amount of ozone was calculated from each direct sun observation. Fig. 1 (a) shows the plot of N_C and N_{A-D} against μ on days with blue zenith skies for different values of ozone ranging from 0·221 to 0·255 cm. These are divided into three groups—

(*i*) 0·250 to 0·255 cm, (*ii*) 0·237 to 0·242 cm and (*iii*) 0·221 to 0·228 cm.

Fig. 1 (b) shows a similar plot of N_C and N_{A-D} against μ on days with uniform thick clouds for different values of ozone. The range of ozone values is the same as in Fig. 1 (a).

With direct sunlight, ozone measurements can be made with a relative error of about 1 per cent (Dobson and Meetham 1934). In the absence of direct sunlight also, the ozone amount can be determined from observations on the zenith sky, but with less accuracy. Errors in total ozone which may occur with observations made on the zenith blue or cloudy sky have been discussed by Tonsberg and Olsen (1944) and Langlo (1952).

From Fig.1 (a) relating to blue zenith skies, it is clear that the N values show systematic variations with μ with a possible error of $\pm$ 0·005 cm when the average value of ozone is 0·240 cm.

From the chart relating to cloudy zenith skies (Fig. 1 b), it is noticed that :

(*i*) Points on both $\lambda\lambda$ CC' and $A-D$ curves are more scattered than those on blue zenith sky curves.

(*ii*) An estimated maximum error of $\pm$0·010 cm can occur with $\lambda\lambda$ CC', if the sky is clouded with uniform clouds of nearly constant illumination. The error would be markedly less with $A-D$.

Most of the days in sub-tropical latitudes are clear, but if the zenith is covered with thick uniform clouds, the ozone amount can be determined with reasonable accuracy using Fig. 1(b).

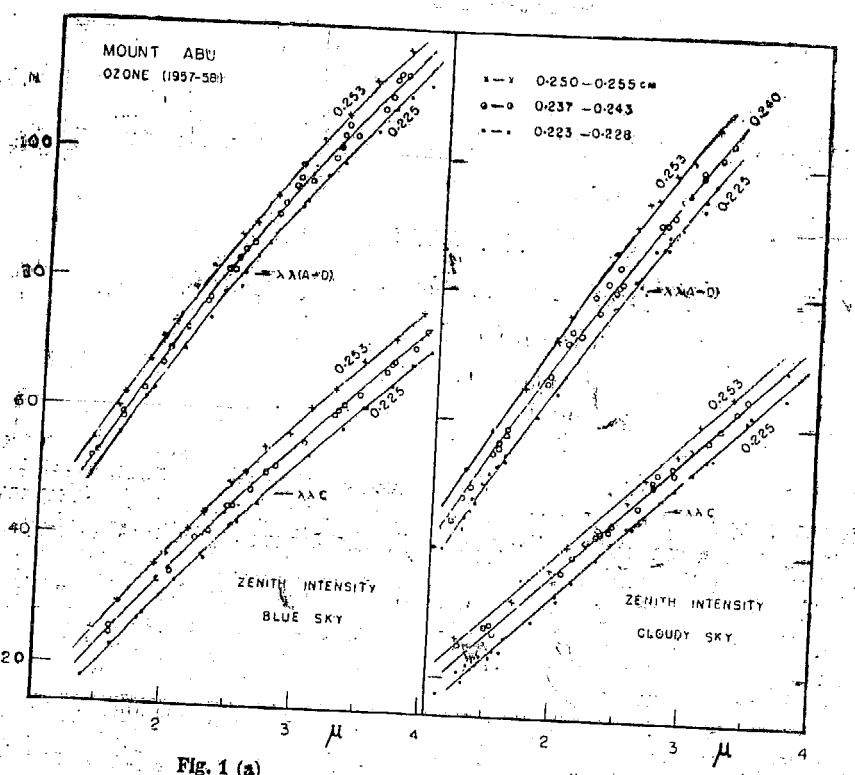

Fig. 1 (a) Fig. 1 (b)

The author is grateful to the Council of Scientific and Industrial Research for the award of a Research Assistantship during the course of this study. He also takes this opportunity to express his indebtedness to Prof. K. R. Ramanathan for suggesting the problem and for valuable guidance.

REFERENCES

Dobson, G. M. B.	1957-58	*Annals of IGY*, 5.
Dobson, G. M. B. and Meetham, A. R.	1934	*Quart. J.R. met. Soc.* 60, p. 265.
Langlo, K.	1952	*Geophys. Publ.*, 8,6.
Tonsberg, E. and Olsen, K. L.	1944	*Ibid*, 13, 12.

J25DGOb—30—29-9-61—GIPS

CHAPTER I

Part II - Apparent variation of ozone during night-time

As the day to day variations of ozone amount in middle and high latitudes are large, the systematic difference, if any, in the ozone amount between day and night cannot be firmly established without prolonged observations. In low latitudes, however, both the total ozone content and the day to day changes are small during most of the year, any systematic change in ozone content during night should be possible to determine.

Dobson[9] himself made some measurements at Oxford in November and December 1948 and they showed some type of variations of ozone on some nights. The variations, however, were not systematic. He concluded that they were such as might be expected from the meteorological conditions. Detailed study and prolonged series of observations at different places were necessary to justify any conclusion regarding the variation of ozone at night.

Ramanathan and Raman Murthy[9] reported in 1953 the results of ozone measurements made at Abu with moon light. In each of the 17 sets of observations they showed an apparent increase of absorption during night proportional

to sec Z and this was interpreted to mean that the ozone amount increased during night by about 0.030 cm.

In Quetta Fournier d' Albe(10) and his collaborators made observations with moon light and found that the night ozone value was greater than that at day. The increase in ozone was of the order of 0.003 cm to 0.050 cm. The extra terrestrial constants were assumed to be same for day and night.

It is important to be sure that the observations during the day and night are made under identical conditions, so far as possible.

To study this, night-time increase in ozone more carefully, observations with moon light were made at Abu during the period 1958-59 with at least two pairs of wavelengths $\lambda\lambda$ C and $\lambda\lambda$ D, and at a number of zenith distances of moon.

The observations were repeated with all the three wavelengths pairs at Ahmedabad in 1960-61 and at Anand (50 miles south of Ahmedabad) in 1961 with Dobson spectrophotometer. The direct sun observations were also made on the same and succeeding days with all the three wavelengths.

Method of observations

The Dobson spectrophotometer was checked for λ setting

I

and wedge calibration before each set of observations as described in part (I) of chapter I, to make sure that the constancy of the instrument is maintained.

The ground quartz plate necessary for direct sun observation was removed and a quartz lens fitted in the sun director and generally kept at the lowest position during the sun observation was raised in the sun director tube to the position at which it forms an image of moon on slit S_1. As the slit cannot be easily seen through the viewing hole at the bottom of the sun director, a small reflecting prism is mounted at the top of the sun director, supplied with Inst. No.54 through which the slit and the moon's image can be easily seen.

It is necessary to set the moon's image very carefully and centrally on the slit and to allow for the movement of the moon, so that the slit will bisect the image of the moon half-way through the observation. In the sun director there is an arrangement to make slow movements of the prism so that the image of the moon can be adjusted very accurately and centrally at the slit S_1, observing through the reflecting prism during the observation.

It was observed that slight defocussing of the image did not have any effect on reading, but if the image of the moon was not maintained in the centre of the entrance slit S_1, considerable error could be caused. All possible care was therefore taken to avoid such errors and each observation was repeated number of times.

During the day the observations were made with unfocussed sunlight falling on the entrance slit S_1 through a ground quartz plate, while during the night, the moon is focussed on the slit and the ground quartz plate is removed. Hence observations are not identical during day and night.

Effect of focussed image

Dobson[11] pointed out that there is a small constant difference between the value of N for any wavelength pair obtained with the ground quartz plate and the focussed image methods, and hence a correction should be applied to the N values observed with focussed sun or moon.

An attempt was made to estimate the effect on the measured amount of ozone of focussing the sun on the slit and removing the ground quartz plate. This could be done provided the intensity of the sun was reduced. A perforated zinc plate with a very small percentage transmission was employed to reduce the intensity.

When the ground quartz plate was removed and the screen introduced, the value of N was reduced by the same amount at all angles of the sun. There was no change in the slope of the line N against μ and thus there was no significant effect on the apparent total ozone amount. Focussing the sun did not show any change in the value of N and also of N_0.

I

Results and discussion

Fig.1 shows the plot of N against μ, where μ is the thickness of ozone traversed by the incident light at different zenith distances of the sun or moon at Abu, Ahmedabad and Anand. The "N_0" values were determined from the plots for sun as well as for moon. The ozone content in the vertical was calculated both for moon and sun using the same formula and same absorption and scattering coefficients. It must be noted that due to the prevalence of clear skies and insignificant large particle scattering during day, it was assumed that the effect of haze could be neglected both during day and night.

It was found that the slope of the curve of N against μ increased at night for all the three wavelength pairs. But this increase was not the same for all the three pairs of wavelengths. It was maximum for D(λ3176/3398) and minimum for A(3055/3254).

If the effect is due to an increase in ozone, the increase of slope should be the same irrespective of the wavelengths used.

Table 2 gives the summary of the results of moon observations for determining the total ozone amount during night. The ozone values are also determined from the direct sun observations.

Results showed that the apparent increase was different for the three pairs of wavelengths, the mean excess for A being

I

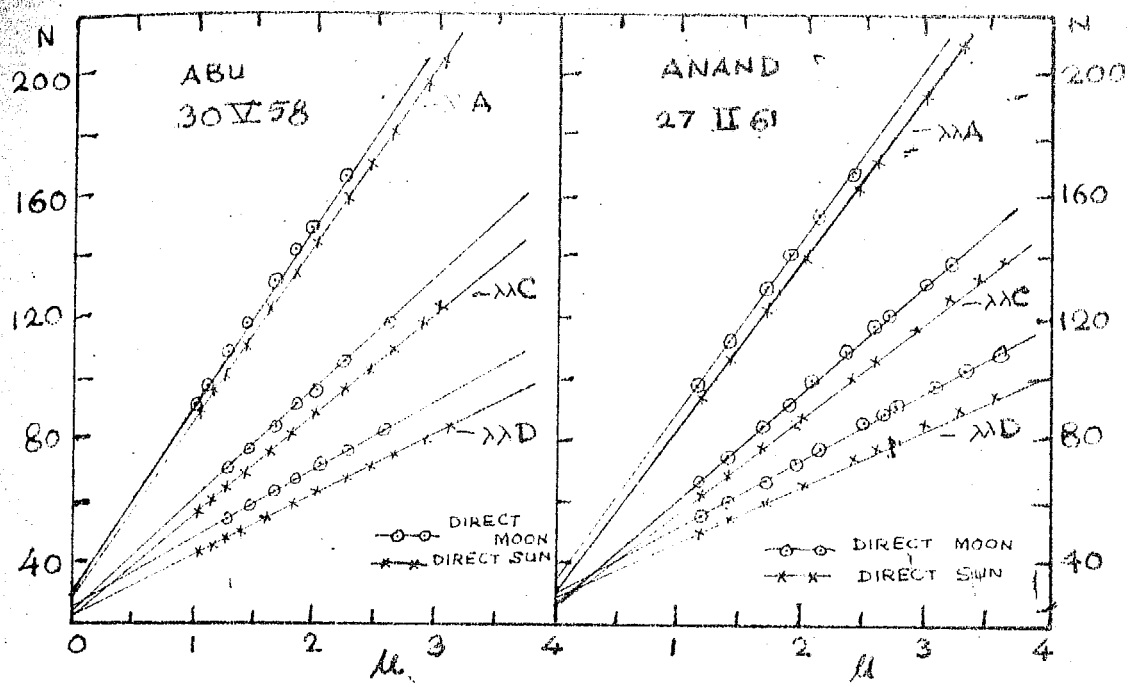
N
ABU
30 V 58
λλA
λλC
λλD
DIRECT MOON
DIRECT SUN
ANAND
27 II 61
μ

FIG. 1

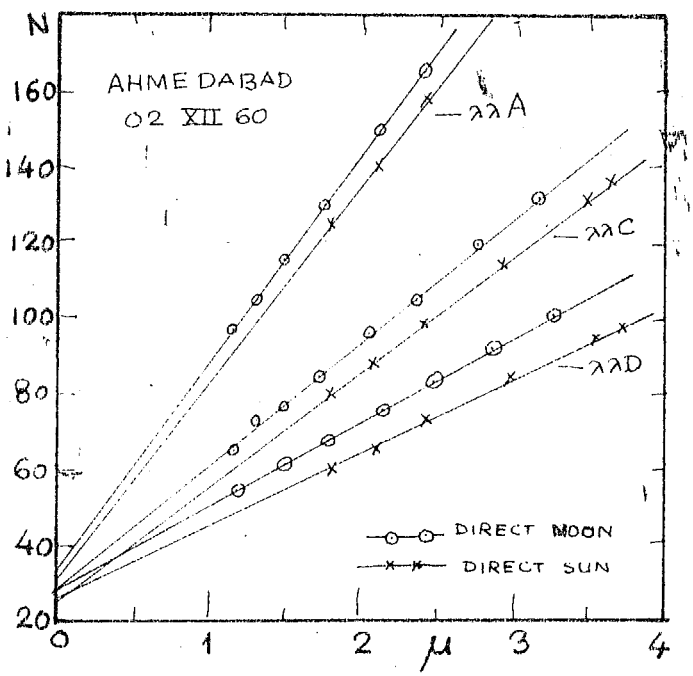
N
AHMEDABAD
02 XII 60
λλA
λλC
λλD
DIRECT MOON
DIRECT SUN
μ

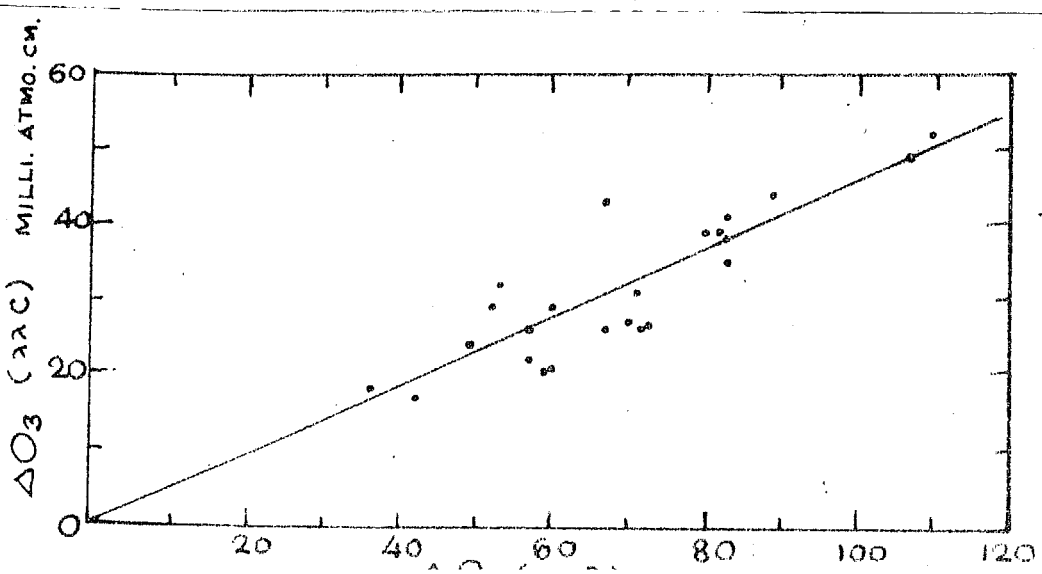
MILLI. ATMO. CM.
(λλC)

FIG. 2

0.015 cm, for C, 0.031 cm and for D 0.069 cm. It should be noted that no correction was made for large particles-scattering either during day or night.

Plotting the values of ΔO_3 (difference in ozone amounts during day and night) obtained with $\lambda\lambda C$ against those with $\lambda\lambda D$ (Fig.2), it was found that the curve was a straight line with a small scatter.

Examination of these apparent ozone increases with $\lambda\lambda A$, $\lambda\lambda C$ and $\lambda\lambda D$ showed that they were roughly in inverse proportion to the values of $\alpha - \alpha'$ (Table 3).

Using the difference method with CD or AD pairs of wavelengths showed that there was no significant systematic increase of ozone during night (Table 2). This means that the apparent increase in ozone during night is not real but the increase is due to increased attenuation of light due to large particle scattering.

Dr.R.N.Kulkarni and Mr.P.D.Angreji collaborated with me in taking the moon observations and Dr.K.R.Ramanathan helped me in interpreting them. A brief summary of this work was presented by Dr.Ramanathan at the International Ozone Symposium held at Arosa in August 1961.

I

Table 2

Observations of ozone with moon-light

Station	Date	O_3 (Sun)			O_3 (Moon-Sun)			O_3 (Moon-Sun)	
		A	C	D	A	C	D	AD	CD
Abu	30-5-58	-	246	245	-	26	57	-	2
"	31-5-58	-	252	245	-	21	60	-	- 8
"	22-2-59	-	219	218	-	43	67	-	8
"	23-2-59	-	240	249	-	18	36	-	3
"	23/24-3-59	-	235	242	-	21	60	+	- 9
"	24-3-59	-	222	215	-	49	107	-	5
"	24/25-3-59	-	232	238	-	32	58	-	13
"	25-3-59	-	216	218	-	44	89	-	10
"	26-3-59	-	220	222	-	29	60	-	5
"	12/13-11-59	-	227	237	-	22	57	-	- 2
"	13-11-59	-	217	219	-	38	83	-	2
"	14-11-59	-	226	235	-	26	67	-	- 5
"	14/15-11-59	-	233	251	-	31	71	-	2
"	15-11-59	-	232	239	-	29	52	-	10
"	16-11-59	-	240	249	-	24	49	-	2
Ahmedabad	30-11-60	230	226	235	24	27	70	6	- 5
"	1-12-60	-	231	231	-	26	72	-	- 8
"	2-12-60	230	225	230	14	26	72	- 2	2
"	31/1- 1-61	-	214	218	-	41	83	-	8
Anand	27-2-61	244	234	234	17	39	82	1	- 1
"	28-2-61	242	235	234	15	39	80	1	8
"	1- 3-61	244	234	238	7	35	83	-13	0
"	1/2-3-61	236	229	235	15	52	110	-13	0
"	3- 3-61	-	222	223	-	17	42	-	- 3
Mean values with No.of days of obvn)		238 (6)	230 (24)	233 (24)	15 (6)	31 (24)	69 (24)	- 3 (6)	1.6 (24)

I

Table 3.

Wavelength pair.	Mean difference of ozone ΔO_3 D.U. (Moon-Sun)	$\alpha - \alpha'$	$(\alpha - \alpha')\ \Delta O_3$
A	15	1.762	26
C	31	0.865	27
D	69	0.374	26

REFERENCES

1. Dobson G.M.B., Observer's Handbook for the Ozone Spectrophotometer, No.54, M/s.R.& J.Beck Ltd., London.
2. Dobson G.M.B., "Adjustment and calibration of ozone spectrophotometer", Annals of IGY, 5, 90 (1957).
3. Fabry C. and Buisson M., J.Phys.Rad.Serie., 5, 3, 196 (1913).
4. Dobson G.M.B. and Harrison D.N., Proc.Roy.Soc.A, 110, 660 (1926).
5. Dobson G.M.B., Harrison D.N. and Lawrence J., Proc.Roy.Soc.A, 114, 521 (1927).
6. Dobson G.M.B., Proc.Roy.Soc.A, 129, 411 (1930).
7. Ramanathan K.R. and Karandikar R.V., Q.J.Roy.Met.Soc., 75, 257 (1949).
8. Dobson G.M.B., Q.J.Roy.Met.Soc.,77, 483 (1951).
9. Ramanathan K.R. and Murthy Bh.V.R., Nature, 172, 633 (1953).
10. Fournier d'Albe E.M., I.U.G.G. 10th Gen.Assembly, Sci.Proc.Int.Ass.Meteor., 1954, p.149, London, Butterworth (1956).
11. Dobson G.M.B., Annals of IGY, 5, 46 (1957).

I

CHAPTER II

RESULTS OF MEASUREMENTS OF TOTAL OZONE AT ABU, DELHI, SRINAGAR AND KODAIKANAL IN THE YEAR 1957-59

CONTENTS

CHAPTER II

RESULTS OF MEASUREMENTS OF TOTAL OZONE AT ABU, DELHI, SRINAGAR AND KODAIKANAL IN THE YEARS 1957-59

1. Introduction

In India during the IGY and IGC, daily ozone measurements were regularly made at Abu (24° N), Srinagar (34° N), Delhi (28°.5 N) and Kodaikanal (10° N), with Dobson spectrophotometers.

The instruments were periodically checked for Q setting and also for wedge calibration so the data were collected under similar conditions at all the four places, and can be expected to give a correct picture of the day to day and seasonal variations of ozone.

Ozone observations at Abu have been regularly made since 1952 and they are available for studying the long term variations. Mr.P.D.Angreji has been responsible for taking ozone observations at Srinagar. Messrs R.N.Kulkarni (1952-53) and S.S.Degaonker (1953-56) have been responsible for taking ozone observations at Abu. Observers of the India Meteorological Department are responsible for ozone observations at Delhi and Kodaikanal. The ozone observations at Abu were made by me from January 1957 to December 1959.

The ozone values presented in this and in the subsequent chapters were calculated from observations made with λλCC' and the absorption coefficients of Vigroux[1]. The earlier observations were calculated with absorption coefficients of Nye and Choong[2] were converted to Vigroux levels by multiplying the ozone amounts observed with λλCC' by 1.33.

2. Day-to-day variations of ozone over Abu

Fig.1 gives the day-to-day values of ozone amount over Abu for the period 1952-59.

The maximum ozone occurred in May-June during 1952-55 and in April-May during the years 1956-59. The ozone starts falling in June, remains constant during the monsoon months and then again decreases and becomes a minimum in Nov-Dec. In January, the ozone amount begins to rise. In 1952 the ozone amount was lower than in other years, the mean value with Vigroux coefficients being 0.190 cm.

3. Day-to-day variations over other Indian Stations

Figs.2, 3 and 4 give the day-to-day ozone amounts for all the four stations during 1957-59.

Over North India, the day-to-day fluctuations in ozone amount are largest in Jan-Mar, when active western disturbances pass across the country.

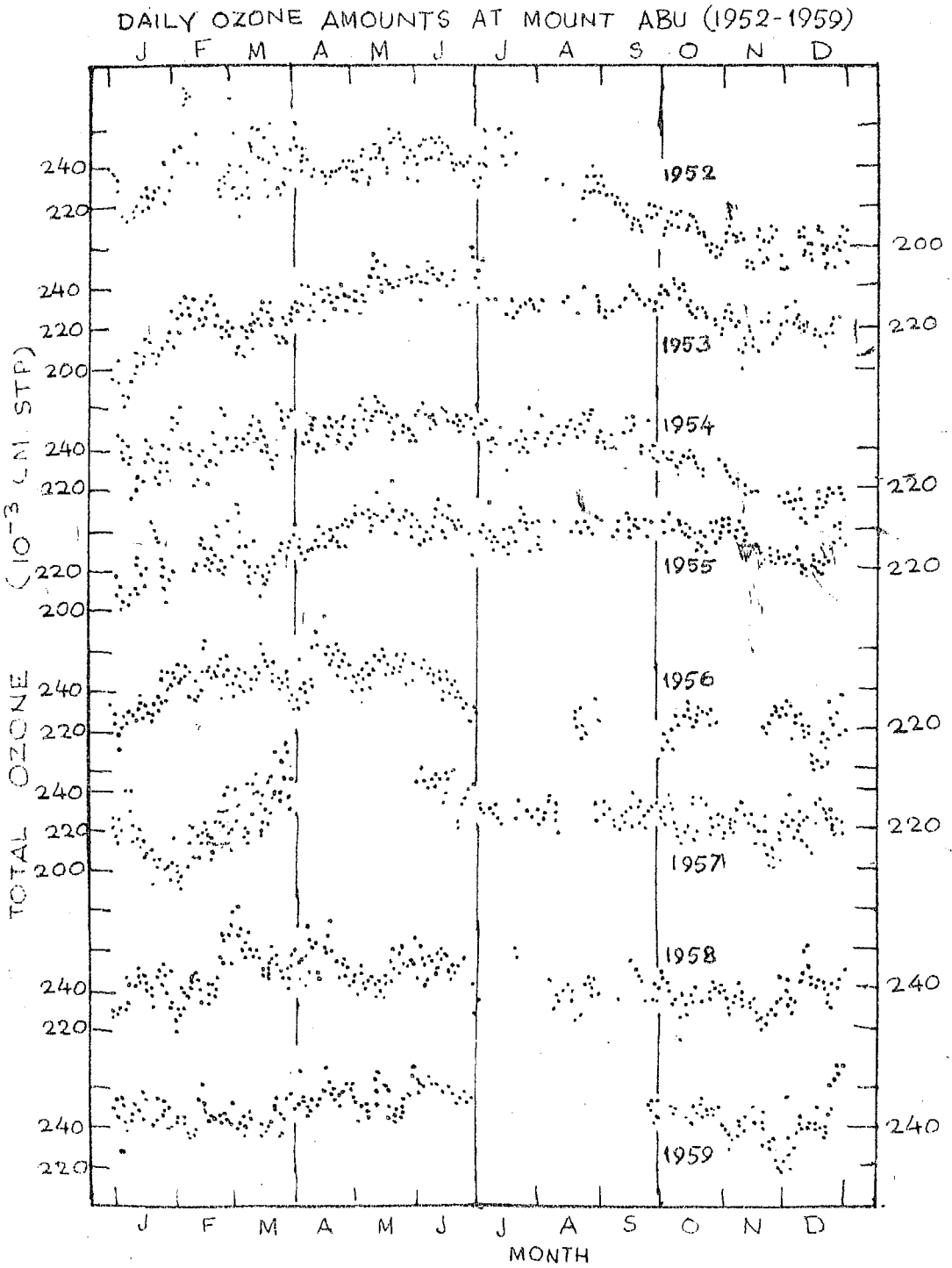
DAILY OZONE AMOUNTS AT MOUNT ABU (1952-1959)
J F M A M J J A S O N D
1952
1953
1954
1955
1956
1957
1958
1959
240
220
200
TOTAL OZONE (10⁻³ CM STP)
MONTH

FIG. 1

II

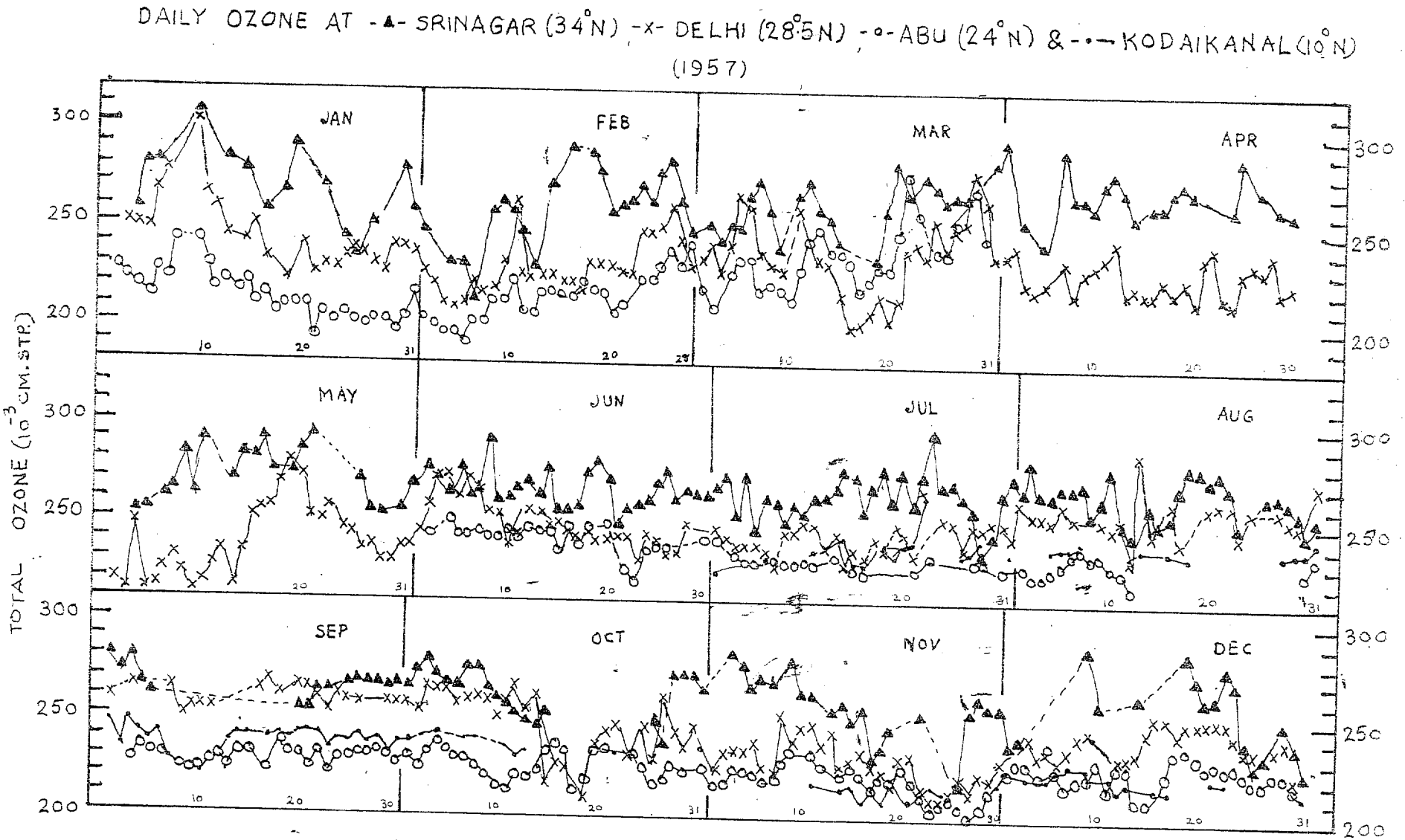
DAILY OZONE AT -▲- SRINAGAR (34°N) -x- DELHI (28·5N) -o- ABU (24°N) & -·- KODAIKANAL (10°N)
(1957)
JAN
FEB
MAR
APR
MAY
JUN
JUL
AUG
SEP
OCT
NOV
DEC
TOTAL OZONE (10^{-3} CM. STP.)
300
250
200

FIG. 2

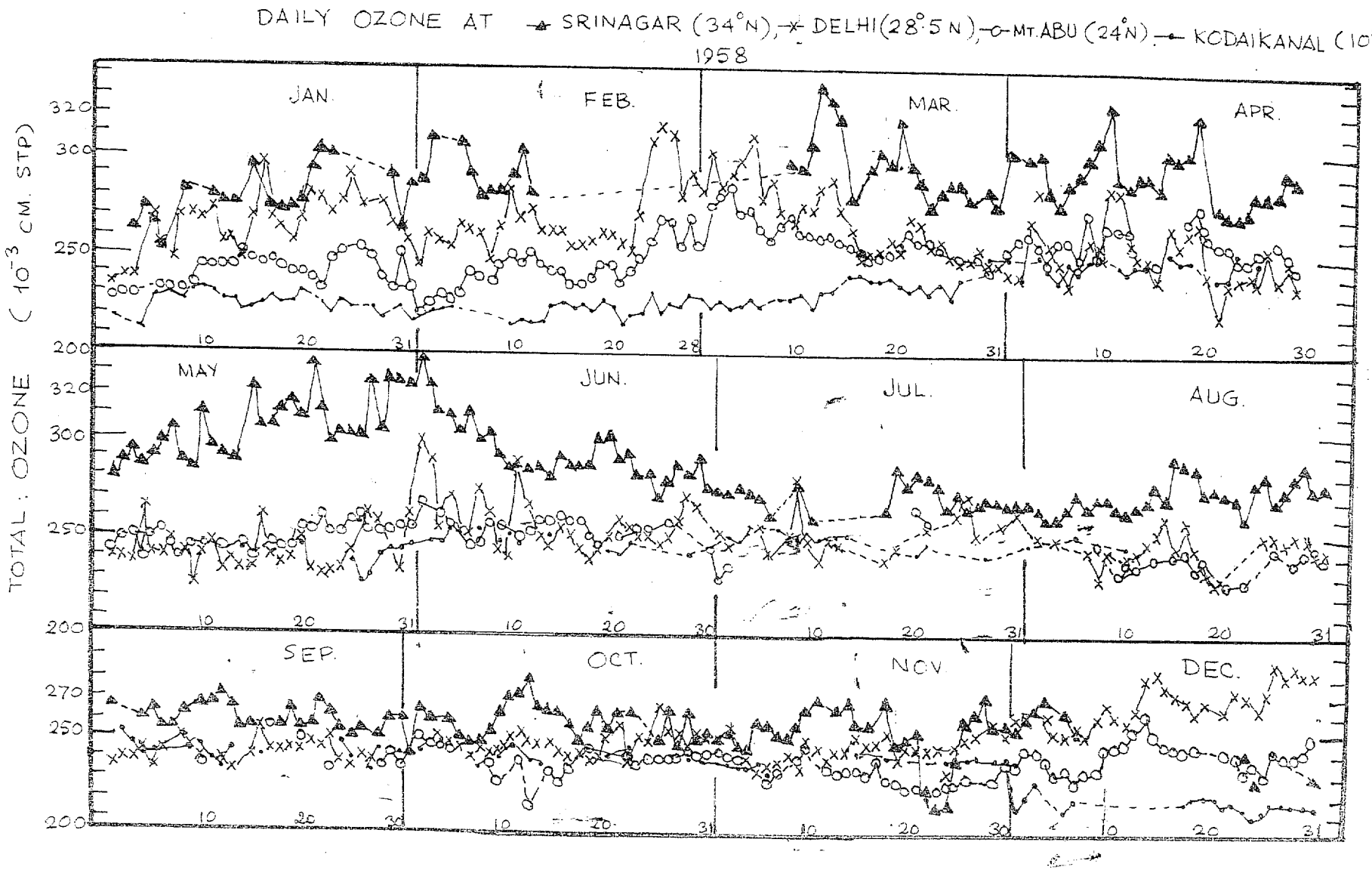
DAILY OZONE AT SRINAGAR (34°N), DELHI (28°5 N), MT. ABU (24°N), KODAIKANAL (10°N)
1958
TOTAL OZONE (10⁻³ CM. STP)
JAN.
FEB.
MAR.
APR.
MAY
JUN.
JUL.
AUG.
SEP.
OCT.
NOV.
DEC.

FIG. 3

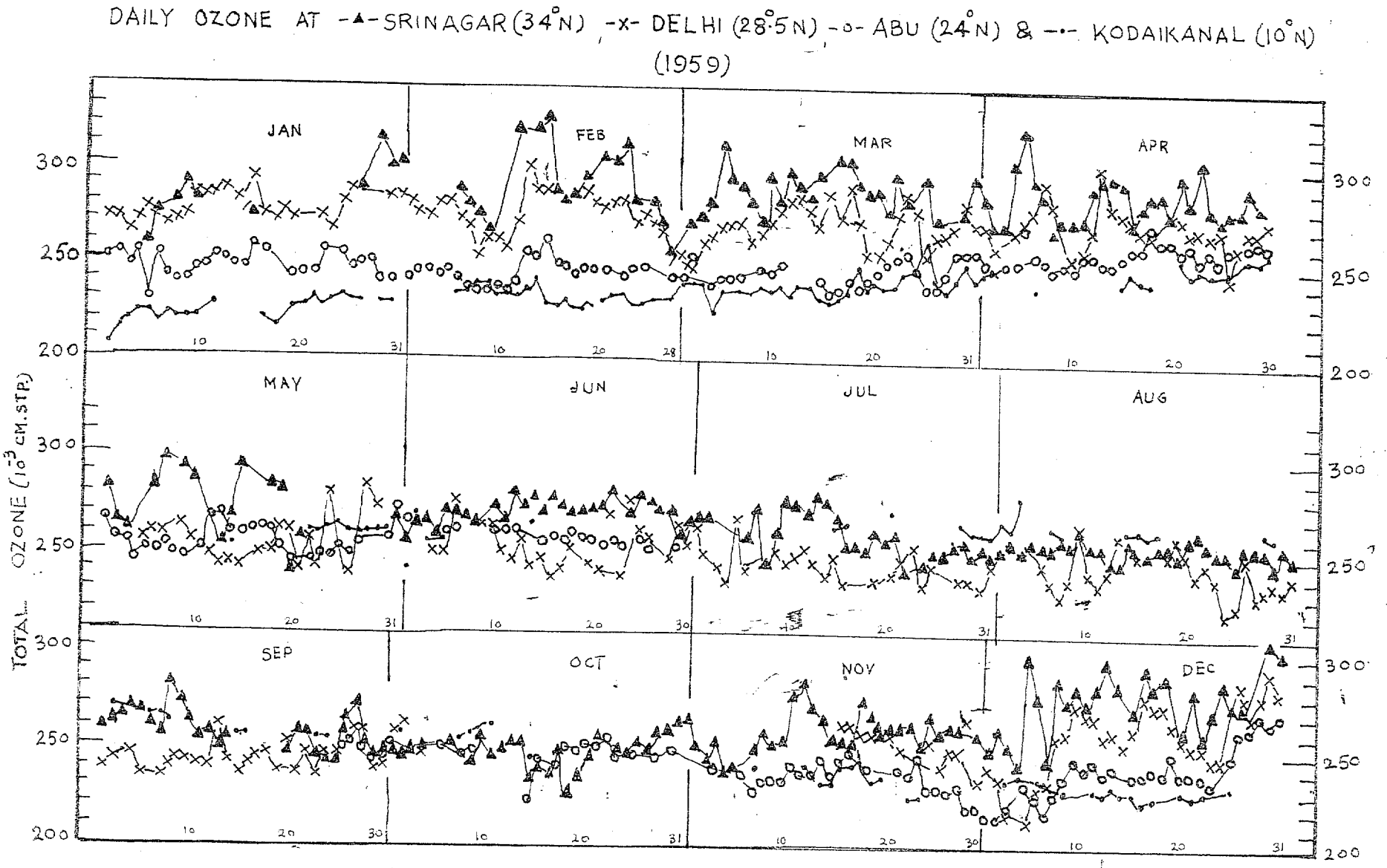
DAILY OZONE AT -▲- SRINAGAR (34°N) -x- DELHI (28·5N) -o- ABU (24°N) & -·- KODAIKANAL (10°N)
(1959)
JAN
FEB
MAR
APR
MAY
JUN
JUL
AUG
SEP
OCT
NOV
DEC
TOTAL OZONE (10^{-3} CM. STP.)
300
250
200
10
20
31
28
30

FIG. 4

The ozone amount over Srinagar and Delhi starts increasing in Nov-Dec, while the amounts over Mt.Abu and Kodaikanal increase later. The gradient of ozone amount between south India and north India is greatest in the months April to May. In the months April to September the ozone values of Delhi, Abu and Kodaikanal become almost identical and the fluctuations subside. The ozone values over Delhi during this period sometimes go below Abu values. From November onward, the Delhi values go on increasing and the difference between the Abu and Delhi values increases. It can also be shown from the figures that when the ozone amount increases from its period of minimum in Nov-Dec. the increase takes place in a series of waves or surges. These surges are generally associated with the passage of troughs of low pressure at 4 to 9 km. Another interesting point is that on many occasions, the maximum at Srinagar occurs one day earlier than at Delhi or Abu.

In 1957-58, the ozone values at Srinagar, Delhi and Abu were going parallel to each other upto the end of May. In June and July, the Delhi values were nearly the same as those at Abu, but in August Delhi separated out and followed Srinagar. Kodaikanal remains higher than Abu from July-October. Abu values were lowest in November 1957 among all the stations in the three years.

Fig.5 gives the ten-day mean ozone amounts at Srinagar, New Delhi and Mt.Abu from 1952-59.

II

TEN-DAY MEAN OZONE VALUES AT SRINAGAR, NEW DELHI & MT. ABU

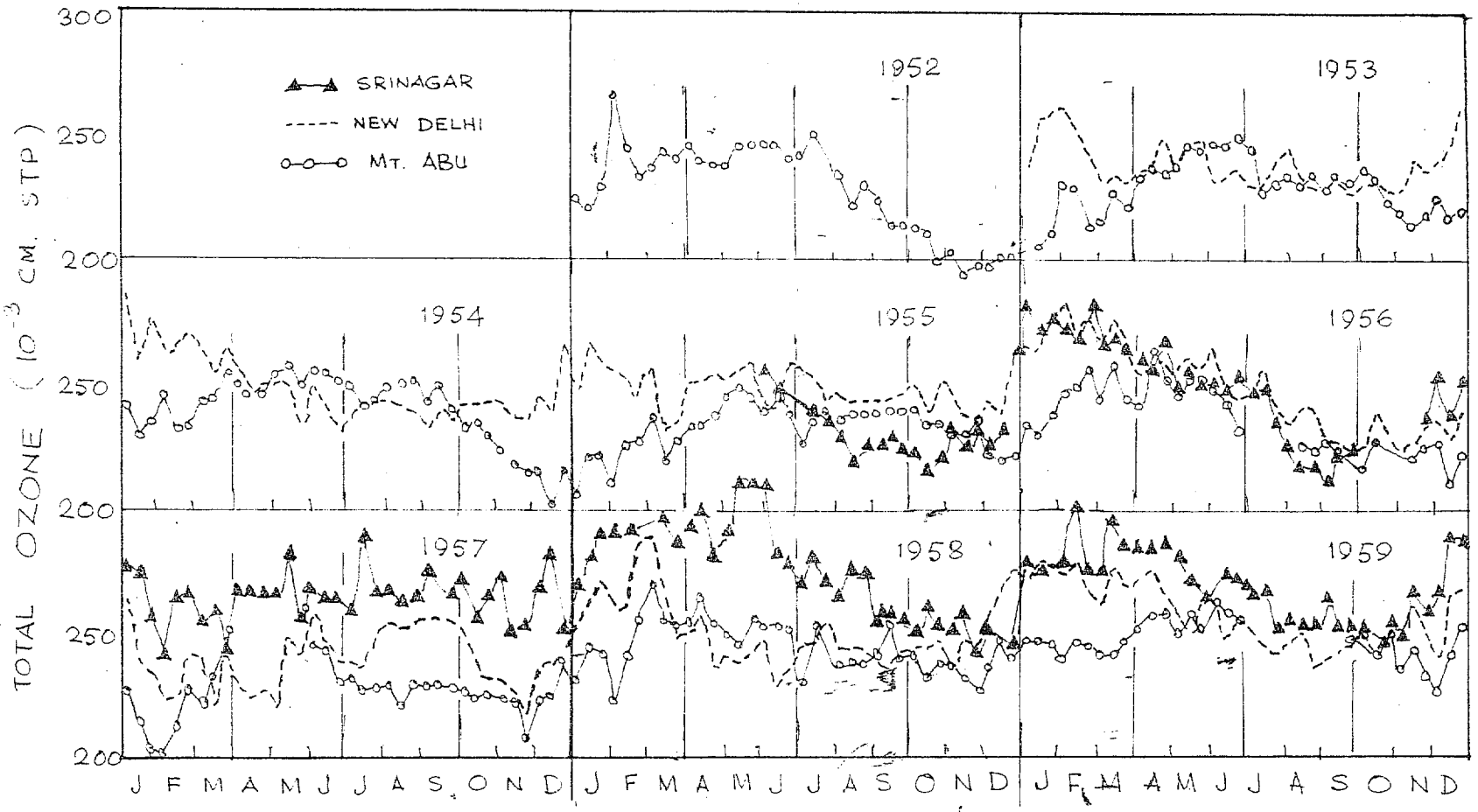

FIG. 5

4. Seasonal variations of ozone over the Indian stations compared with those over Japan

Atmospheric ozone has a well established seasonal variation with a maximum in spring and a minimum in autumn.

In Fig.6, the monthly mean values of ozone amount over Srinagar, Delhi, Abu and Kodaikanal are shown together with those over Tateno.

All the Indian stations fall in one group with low ozone values. Tateno (36°N) is at about the same latitude as Srinagar (34°N), but the ozone values of Tateno are much higher than those at Srinagar. Tateno falls in the group corresponding to higher latitudes where the seasonal variations of ozone amount are markedly larger. At Tateno, the mean ozone amount varies from 0.250 cm to 0.450 cm whereas over Indian stations it varies from 0.200 cm to 0.300 cm.

In summer, however, the ozone content over Tateno is almost equal to that over Indian stations. Occassionally in summer, the Tateno values are even smaller than the values at Srinagar or Delhi. The Tateno ozone starts separating from the Indian group in December and the difference increases rapidly.

The following is a summary of the important points regarding the seasonal variation of ozone over Indian stations:-

(1) At Srinagar and Delhi, the maximum ozone values occur

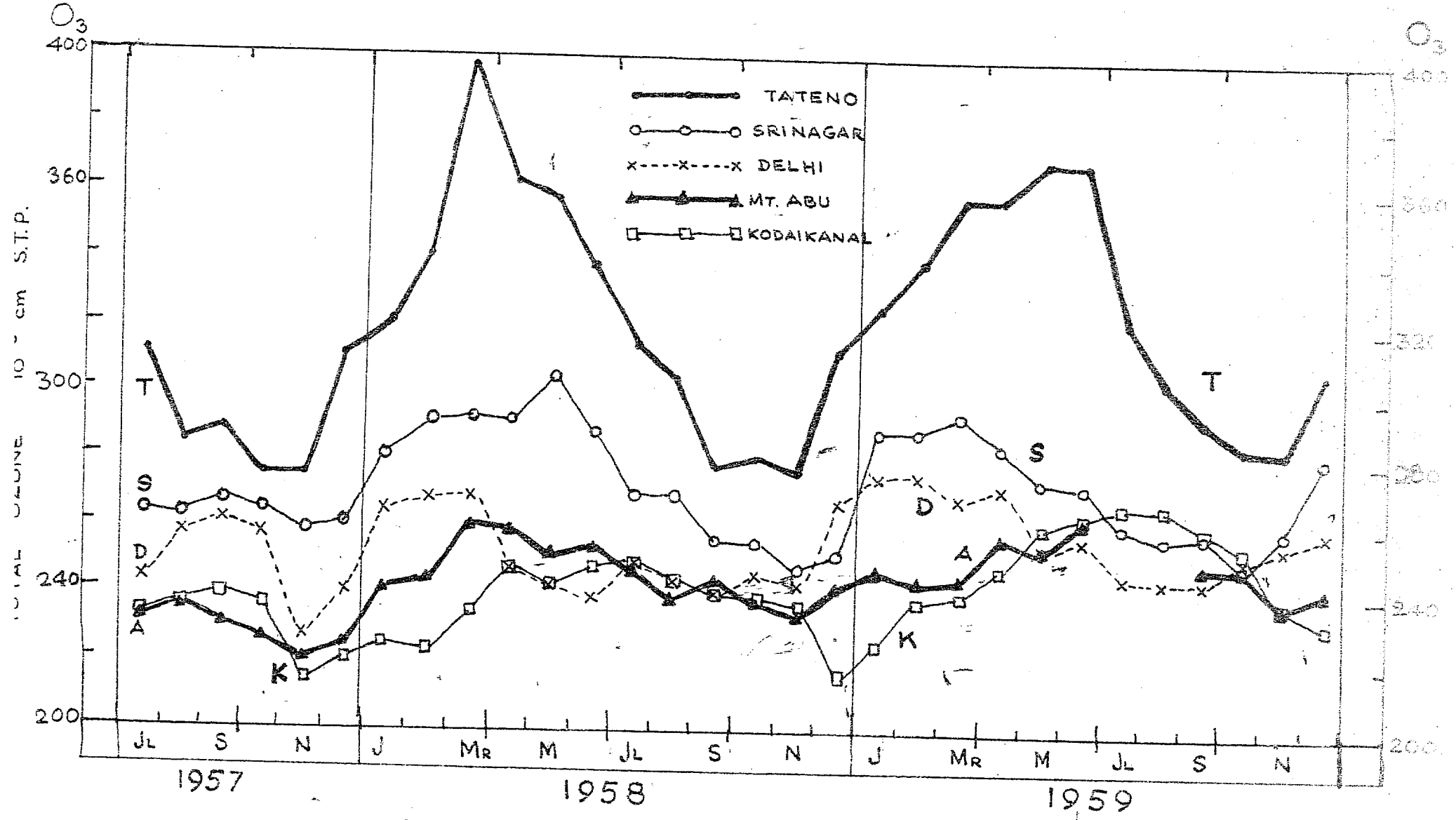

MONTHLY MEAN OZONE AMOUNTS FOR 1957 - 59

FIG. 6

in January and February whereas at Abu it is shifted to April-May and at Kodaikanal to June-July.

(2) The minimum at Abu occurs in autumn. It occurs later both at Delhi and Srinagar. By the end of November the ozone values at Delhi starts increasing, while at Mt.Abu a slow rise takes place in the beginning of December followed by a more rapid rise in the middle of January. In Srinagar, the rise of ozone takes place even earlier than at Delhi. Both at Srinagar and Delhi, the decrease in ozone starts in April and the minimum is reached in October-November.

(3) The maximum values at Srinagar, Delhi and Abu increase with latitude.

Some general remarks

For a better understanding of the seasonal variations of ozone, it is necessary to know the seasonal variation of ozone content in different layers of the atmosphere. We shall discuss in the next chapter the umkehr method of determining the vertical distribution of ozone.

REFERENCES

1. Vigroux, E., Ann.d.Astrophy.X, 17, 399 (1954).

2. Ny.T.Z. and S.P.Choong, Chinese J.Phys., 1, 33 (1933).

3. Tables of ozone values during IGY-IGC, published by W.M.O.

CHAPTER III

THE UMKEHR METHOD FOR DETERMINING THE VERTICAL DISTRIBUTION OF OZONE

CONTENTS

CHAPTER III.

THE UMKEHR METHOD OF DETERMINING THE VERTICAL DISTRIBUTION OF OZONE

1. Umkehr effect and its general explanation

When light from the direct sun is observed on different wave-lengths at increasing zenith distances of the sun, the shorter wave-lengths decrease in intensity much more rapidly than the longer wave-lengths due to increased scattering in the atmosphere and also due to increased absorption by ozone at wave-lengths shorter than 3350 Å. For example, if I and I' are the intensities of direct zenith sunlight in the wave-lengths 3114 Å and 3324 Å; the ratio I/I' continuously decreases with increasing zenith distance of the sun. The behaviour is however different if the spectrum of the clear zenith sky is observed. In this case, I/I' goes on decreasing as the sun goes down upto a certain limit, but beyond a certain zenith distance (Z about 85°) the ratio I/I' begins to increase and shows an inversion (Umkehr).

This observation was first made by Dr.F.W.P.Götz[1] at Spitzbergen in 1929 and he explained it as being due to the fact that the ozone in the atmosphere was mostly located at some height above the surface of the earth. This discovery

has formed the basis of a method of determining the vertical distribution of ozone.

The light from the zenith sky is made up of the light scattered by air at different levels in the atmosphere. In Fig.1, let us suppose that most of the ozone is concentrated in a thin layer at a height h above the ground and let P_1A, P_2B be two representative beams which are scattered by air in the vertical, A being above the ozone layer and B below it.

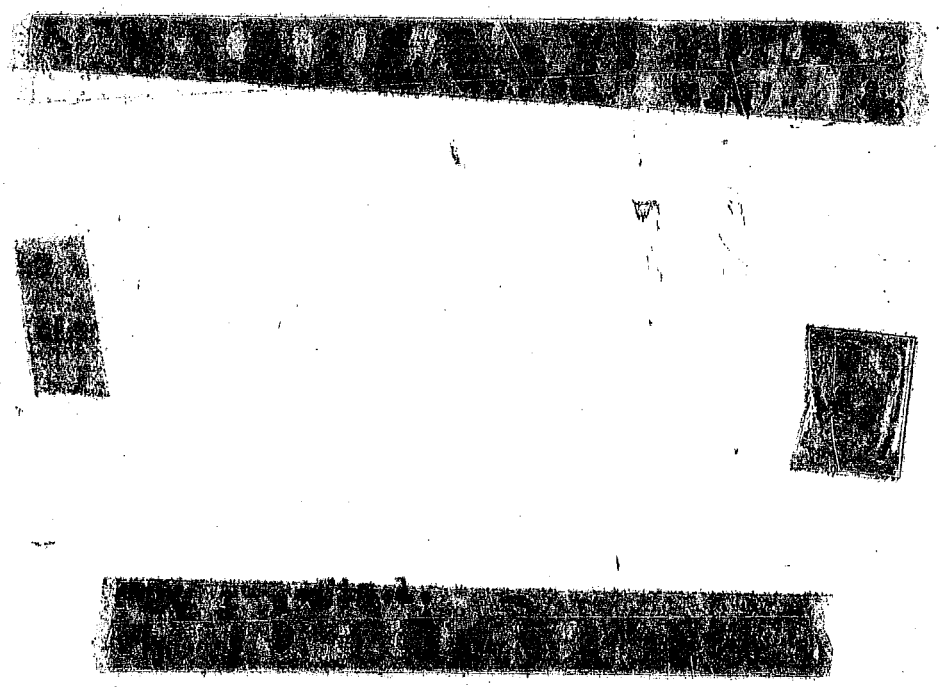

The light received at O in a vertical direction is composed of the light scattered by the atmosphere from below the ozone layer, within the ozone layer and from above the ozone layer. As the zenith distance of the sun increases the attenuation due to ozone in the path P_2B increases and at some stage, the light transmitted into the lower atmosphere and scattered by it becomes negligible compared with that scattered by the air above the ozone layer. This happens first

for the more absorbed wave-length (3114 Å). At that stage, some light of 3324 Å would still be entering the lower part of the atmosphere. When the zenith distance of the sun increases, I' from below B will continue to decrease and I/I' will increase.

A detailed study of the curve of variation of I/I' with the sun's zenith distance can be made the basis for determining the vertical distribution of ozone.

2. Umkehr observations

The decimal absorption coefficient of ozone at 3114 Å is 0.912 while that at 3324 Å is 0.047. The ratio of the intensities of the zenith scattered solar radiation in two narrow bands near these wave-lengths is measured for different zenith distances of the sun by means of the calibrated optical wedge of the Dobson spectrophotometer. The curve representing log I/I' against sec Z or Z^4 shows a reversal and is known as the "Umkehr" curve. It is customary, following Dobson, to plot log I/I' against Z^4 in order to widen the curve near the inversion.

3. Calculation of the vertical distribution of ozone

The method used in India for calculating the ozone distribution in the atmosphere from umkehr measurements is

the method B of Dobson and Götz[2] as modified by Ramanathan and Dave[3].

The intensity I of primary scattered light of wave-length λ received per unit solid angle at the ground from the zenith sky is given by

$$I = K(1+\cos^2 Z) I_0 \int_0^\infty \rho_h \left[10^{-\alpha \int_h^\infty \chi_h \sec \xi_h \, dh - \alpha \int_0^h \chi_h \, dh} \times 10^{-\int_h^\infty \beta_h \sec \xi_h \, dh - \int_0^h \beta_h \, dh} \right] dh$$

$$= K(1+\cos^2 Z) I_0 \int_0^\infty \rho_h \cdot 10^{-\alpha Y - \beta F} \, dh$$

where Z is the zenith distance of the sun, ρ_h is the density of air at a height h, α the absorption coefficient of ozone per unit thickness at S.T.P. and β the coefficient of scattering of air per unit atmosphere, Y represents the total integrated thickness of ozone traversed by sunlight from a point outside the atmosphere to a height h vertically above the observer and from there vertically downward the instrument. Y is a function of the height distribution of ozone. F denotes the integrated air mass traversed along the same path in terms of the mass in a unit standard atmosphere.

A similar equation can be written down for the intensity I' of the longer wavelength λ' with corresponding values α' and β' of ozone absorption and scattering attenuation.

Thus we can obtain log I/I' for any assumed distribution of ozone. The necessary tables for computing log I/I' with a

given distribution of ozone are given in the Annals of the IGY, Vol.5, 1957-58. Knowing the total ozone present in the atmosphere at the time of observation, a number of theoretical Umkehr curves can be calculated assuming different distributions of ozone. The distribution for which the calculated curve fits the observed curve within specified limits is taken to represent the distribution of ozone in the atmosphere. This is the method adopted by Götz, Meetham and Dobson.

Ramanathan and Dave divide the atmosphere from sea level upto 54 km into 9 layers, each of 6 km thickness. They assume that within each layer, the ozone is uniformly distributed.

4. Corrections for multiple scattering

So far, we have considered primary scattering only. Götz, Meetham and Dobson considered that the inclusion of multiply scattered light in the calculation of the theoretical umkehr curve would not alter the curve but would only displace it bodily. It has been shown that this would not be correct. The wave-lengths 3114 Å and 3324 Å are very differently absorbed by ozone and as their scattering coefficients are also different, the contribution of multiple scattering in different layers of the atmosphere to the total scattered light from the zenith would not be in the same proportion when the zenith distance of the sun changes.

If the intensity of light of wave-length λ or λ' which is received from the atmosphere in a vertical direction be decomposed into primary scattered light (P or P') and multiply scattered light (M or M'), what we measure with the Dobson spectrophotometer is log I/I' for different solar zenith distances where

$$\frac{I}{I'} = \frac{P + M}{P' + M'} = \frac{P}{P'} \frac{(1 + M/P)}{(1 + M'/P')}$$

We could correct the I/I' curve to give P/P' if we know the actual values of M/P and M'/P' for different zenith distances of the sun. Since the ozone absorption coefficients for 3114 and 3324 wave-lengths are widely different, the values of M/P and M'/P' for these two wave-lengths behave differently with change in sec Z.

The determination of M/P for a scattering and absorbing atmosphere whose the absorbing component is a function of height, is an important problem in atmospheric optics. This has been recently studied by Sekera and Dave[5] for a plane parallel atmosphere assuming that there is no ozone below a certain level and that above that level, the ozone distribution has a form similar to a Chapman distribution.

As a practical empirical solution, [illegible] Ramanathan[4] suggested that if instead of comparing the intensities of light of two wave-lengths such as λ 3114 Å and λ 3324 Å whose absorption coefficients are very different and hence whose

multiple scattering would also be very different, we compare the intensities of two wave-lengths like λ 3055 Å and λ 3114 Å whose scattering coefficients are near each other and whose absorption coefficients are, though unequal, of the same order of magnitude (1.932 and 0.912), we may expect $\log (I_{3055}/I_{3114})$ curve to be a better approximation to the corresponding $\log (P_{3055}/P_{3114})$ curve than $\log (I_{3114}/I_{3324})$ would be to $\log (P_{3114}/P_{3324})$, where P is the primary scattered light.

Thus the problem could be reduced to that of obtaining the curve of $\log (I_{3055}/I_{3114})$ against Z^4.

It was also suggested that if two other wave-lengths λ 3114 and λ 3176 (α = 0.912 and 0.391) were used, we should, if we make a proper correction for multiple scattering, obtain the same distribution of ozone as with λ 3055 and λ 3114.

In practice, we obtain two umkehr curves on the same day with two pairs of wave-lengths $\log (I_{3114}/I_{3324})$ and $\log (I_{3055}/I_{3254})$ with the Dobson spectrophotometer.

Since ozone absorption is small at both λ 3324 and λ 3254 we can assume that the total zenith scattered light at these wave-lengths would be proportional to the respective primary scattered intensities and that

$$\log (I_{3254}/I_{3324}) = \log (P_{3254}/P_{3324}).$$

$\log (I_{3055}/I_{3114})$ can be obtained by subtracting

$\log (I_{3254}/I_{3324})$ from $\{\log (I_{3055}/I_{3254}) - \log (I_{3114}/I_{3324})\}$

Fig.2(a) gives examples of observed umkehr curves for $\lambda\lambda$ A, $\lambda\lambda$ C and $\lambda\lambda$ D pairs of wave-lengths for ozone amounts 0.223 cm at Mt.Abu on 20-11-58 and 0.292 cm at Srinagar on 12-5-1958 respectively, and the curves (crosses) calculated on the assumption that there was primary scattering only.

Fig.2(b) gives the derived umkehr curves for $\log (I_{3055}/I_{3114})$ and for $\log (I_{3114}/I_{3176})$.

The derived umkehr curve of $\log (I_{3055}/I_{3114})$ will be a better approximation to $\log (P_{3055}/P_{3114})$ although it is realised that it is not strictly correct to assume that the ratio M/P for λ 3055 and λ 3114 are equal. The derived umkehr curve of $\log (I_{3055}/I_{3114})$ can be used to determine the vertical distribution of ozone by the usual method of trial and error.

The distribution thus obtained was used to compute an umkehr curve for $\log (I_{3114}/I_{3324})$ taking into account primary scattering only. It is found that the points of the umkehr curve thus calculated differ from the points on the observed curve of $\log (I_{3114}/I_{3324})$ by amounts which vary with the zenith distance of the sun.

Corrections were obtained by subtracting corresponding

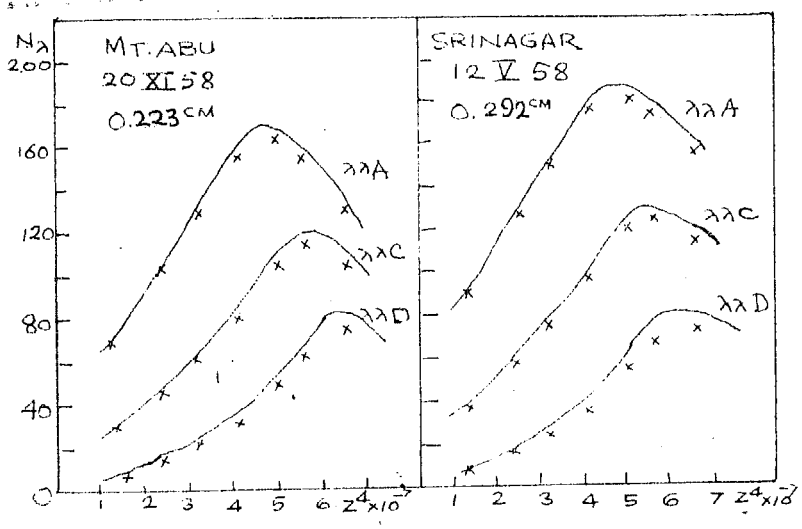
MT. ABU
20 XI 58
0.223 CM
SRINAGAR
12 V 58
0.292 CM
λλA
λλC
λλD
N_λ
$Z^4 \times 10^{-7}$

(a)

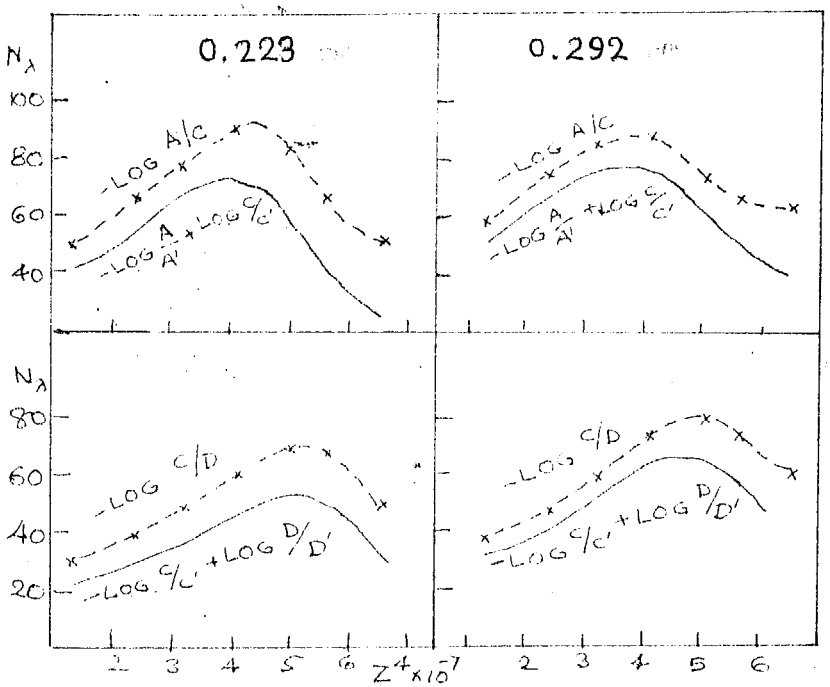
0.223
0.292
N_λ
-LOG A/C
-LOG A/A' + LOG C/C'
-LOG C/D
-LOG C/C' + LOG D/D'
$Z^4 \times 10^{-7}$

(b)

FIG. 2

points in the two curves for different zenith distances and for different ozone amounts. Table 1 below gives the corrections thus found for different wave-lengths and for different ozone amounts. Thus one can derive umkehr curve of primery scattered light by applying appropriate corrections at different zenith distances of the sun to the observed umkehr curves with different pairs of wave-lengths.

Table 1.

Mean multiple scattering corrections calculated from $\lambda\lambda$(A-C) distribution of ozone, for different ozone amounts.

(To be subtracted from N_s)

$\lambda\lambda$	Ozone amount D.U.	Corrections Z = 60°	70°	75°	80°	84°	86°.5	88°	90°
A/A'	295	0	1.0	2.0	4.0	4.5	4.7	5.0	5.0
	475	-	0.0	1.2	2.7	2.3	2.3	-	3.3
C/C'	295	0	0.7	2.0	4.0	5.0	5.0	4.7	4.6
	475	-	0.0	1.2	3.1	2.5	2.5	-	2.5
D/D'	295	0	1.0	2.0	4.0	5.0	6.0	6.0	6.0
	475	-	0.0	1.0	2.0	2.3	3.7	-	3.7
Corrections according to Sekera & Dave relative to point at 60°.									
C/C'	250	0	2.5	4.5	10.5	13.0	11.5	10.0	-
Corrections given in IGY Manual									
C/C'	240	0	1.0	2.0	4.5	6.0	6.0	6.0	6.0

The following interesting points may be noted :-

(1) For the same ozone amount, corrections for A & C pairs

of wave-lengths are nearly the same, but for D pair of wave-length the corrections are slightly higher than those for A or C.

(2) The corrections obtained for high ozone amount (475) at Resolute are smaller than the corrections for low ozone amounts (< 295 D.U.) obtained over India.

(3) In India for ozone < 295 D.U. the corrections now obtained for angles greater than 34° are slightly smaller than those used by Ramanathan and Dave.

The following general statements may be made regarding the multiple scattering corrections.

(1) For the same ozone amounts there does not seem to be significant difference in the correction to be applied to observations with A or C pairs of wave-lengths but high corrections are required for longer wave-lengths i.e. the effect of multiple scattering increases with increasing wave-length or decreasing ozone absorption.

(2) The correction becomes smaller with increase in ozone amount i.e. the effect of multiple scattering decreases with increasing ozone amounts.

Sekera and Dave[5] have recently discussed theoretically the corrections to be applied to the umkehr curve for multiple scattering. They assume a plane parallel atmosphere, divided into two layers an upper layer in which ozone is distributed

according to photochemical theory and a lower-layer in which there is no ozone. The scattering optical thickness of the upper layer is assumed to be small and only primary scattering is taken into consideration in this layer. The scattering optical thickness of the lower layer is large and all orders of scattering are considered in this layer.

In Table 1, the corrections for multiple scattering on the umkehr curves according to Sekera and Dave are also given, along with the secondary scattering correction given according to IGY manual.

Table 2 gives the vertical distribution of ozone over few selected stations calculated from umkehr measurements by differential method using $\lambda\lambda$(A-C) and also with corrections applied to the observed umkehr curves according to (1) IGY manual and (2) Sekera and Dave.

If one compares these distributions, one finds that there is not much difference in distributions, the agreement between them is rather good. It may be mentioned that the same multiple scattering corrections given by Sekera and Dave for ozone 250 D.U. have been used for higher values of ozone also.

5. <u>Summary of some vertical distributions of ozone obtained by the "Umkehr" method over Abu</u>

Fig.3 represents three typical umkehr curves with $\lambda\lambda$ C

TYPICAL UMKEHR CURVES FOR DIFF. OZONE AMOUNTS OVER ABU

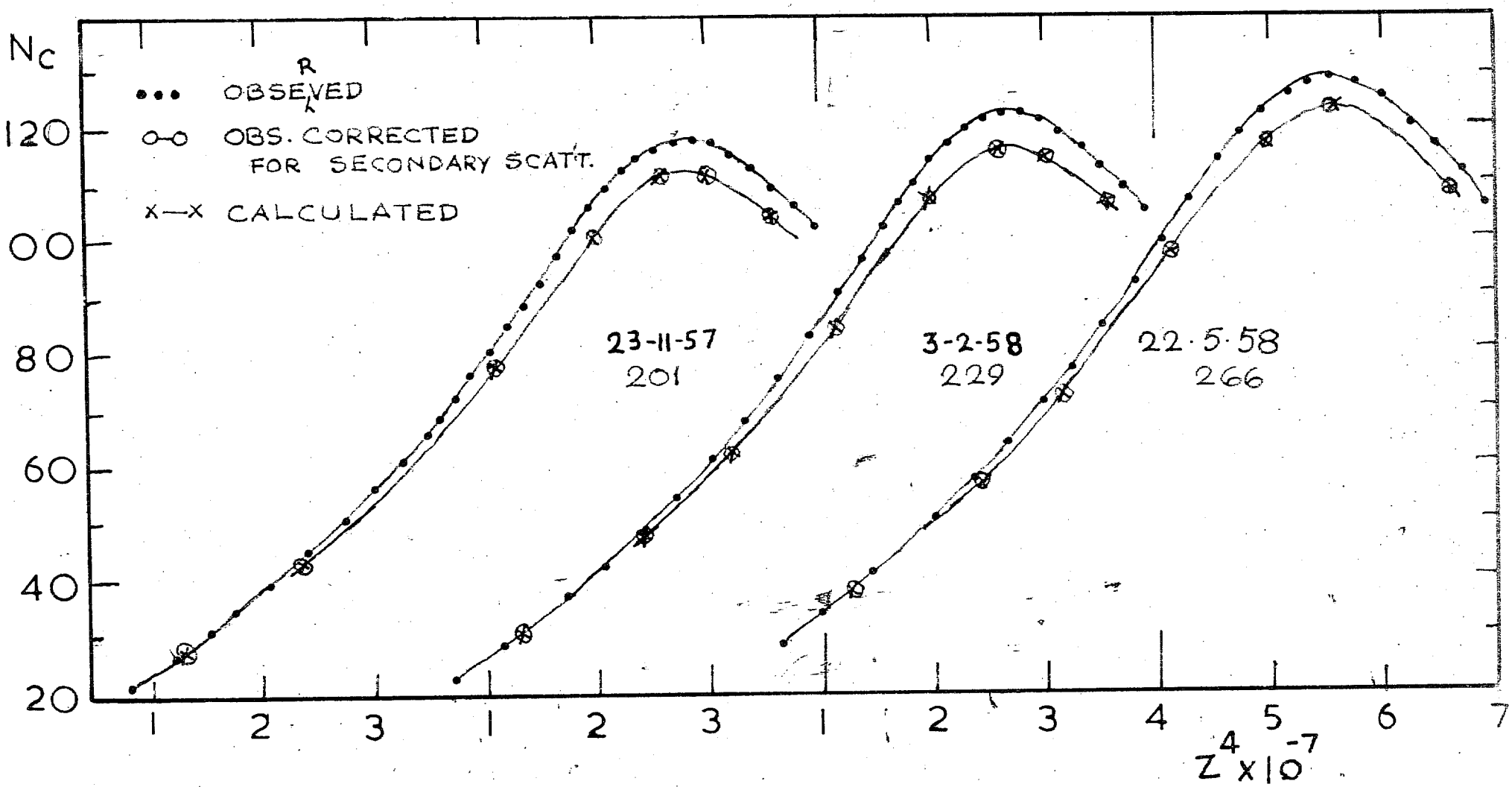

FIG.3

Table 2.

Vertical distributions of ozone for few selected stations calculated by method B applying the corrections according to (1) IGY manual, (2) Sekera and Dave and (3) calculated by differential method (ozone amount calculated by Vigroux' α).

Place	Date	Ozone amount D.U.	Corrections used.	Ozone amounts in D.U./KM in different layers								
				0-6	6-12	12-18	18-24	24-30	30-36	36-42	42-48	48-54
Abu	23-2-53	250	A-C	1.3	2.7	3.2	5.3	15.4	8.8	3.1	1.1	0.7
			Acc.to IGY	1.3	2.7	3.6	5.3	15.4	8.8	2.6	1.1	0.8
			Acc.to S&D	2.0	3.3	4.2	5.6	15.8	6.8	2.0	1.1	0.8
"	7-2-53	230	A-C	2.0	2.0	2.0	5.1	14.6	7.4	3.4	0.9	0.9
			Acc.to IGY	2.0	2.0	2.7	5.1	15.6	7.4	2.7	0.9	0.9
			Acc.to S&D	0.7	1.9	2.7	6.0	14.6	7.4	3.1	1.1	0.9
Srinagar	12-5-53	231	A-C	1.7	4.7	6.0	7.3	15.3	8.0	3.4	1.2	0.8
			Acc.to IGY	1.7	4.7	6.0	7.3	15.7	8.0	2.9	1.2	0.9
			Acc.to S&D	3.0	5.3	6.6	8.0	14.4	6.6	2.4	1.2	0.9
Tateno	3-3-53	432	Acc.to IGY	4.6	10.6	14.7	15.2	15.3	7.0	4.0	1.1	0.5
			Acc.to S&D	4.6	10.2	13.7	19.2	13.7	5.7	3.6	1.1	0.5
Sapporo	8-10-53	313	Acc.to IGY	2.0	3.3	6.6	10.2	16.1	6.2	4.4	2.0	1.2
			Acc.to S&D	3.3	4.0	6.0	10.0	16.9	5.6	4.0	1.3	1.1

for different values of ozone over Mt.Abu. The values of ozone were 266 D.U., 229 D.U. and 201 D.U. respectively. The vertical distributions were calculated by IGY method B applying secondary scattering corrections at different zenith angles. The necessary tables of log $\Delta m_n = \beta F$ and $\Delta S = \Delta h$ given by Ramanathan and Dave in their paper in Annals of IGY were used with proper values of β , β'. The tables of log $\Delta m_n = \beta F$ have been corrected for the altitudes of stations above sea level.

Fig.4 illustrates the block diagram of vertical distribution of ozone on those three days calculated by IGY method B.

Table 3 represents the vertical distributions of ozone for few days over Mt.Abu, calculated by IGY method applying secondary scattering corrections. It is seen that when ozone changes take place, the major changes occur in 12-24 km. Some ozone is found even at ground level which agrees well with the surface ozone measurements. Ozone above 36 km does not vary much with the total ozone. The changes of ozone in different layers with total ozone changes is shown in Fig.5.

Fig.5 represents the scatter diagram of fractional ozone in various layers in the atmosphere. It is based on the ozone amounts at different heights calculated from 39 sets of umkehr curves, calculated by IGY method B with secondary scattering corrections. The atmosphere is divided into 4 layers

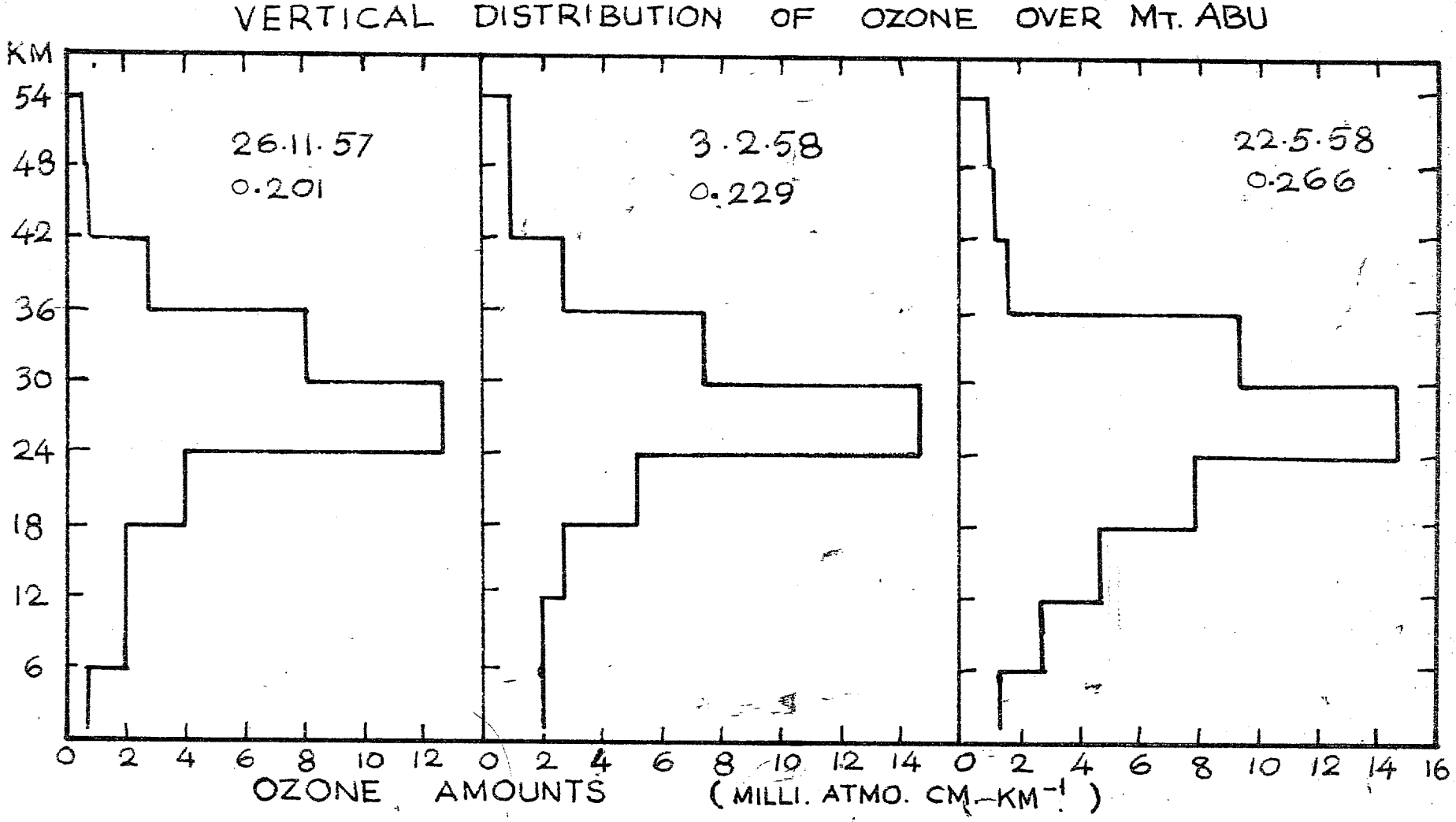
VERTICAL DISTRIBUTION OF OZONE OVER MT. ABU
KM
54
48
42
36
30
24
18
12
6
26.11.57
0.201
3.2.58
0.229
22.5.58
0.266
0 2 4 6 8 10 12
0 2 4 6 8 10 12 14
0 2 4 6 8 10 12 14 16
OZONE AMOUNTS (MILLI. ATMO. CM.-KM^{-1})

FIG. 4

III

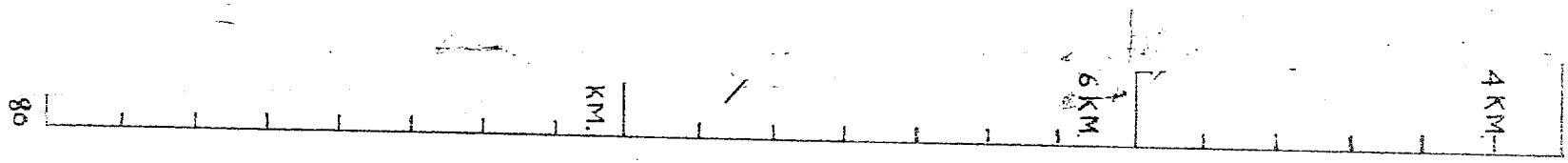
80
KM.
6 KM.
4 KM.

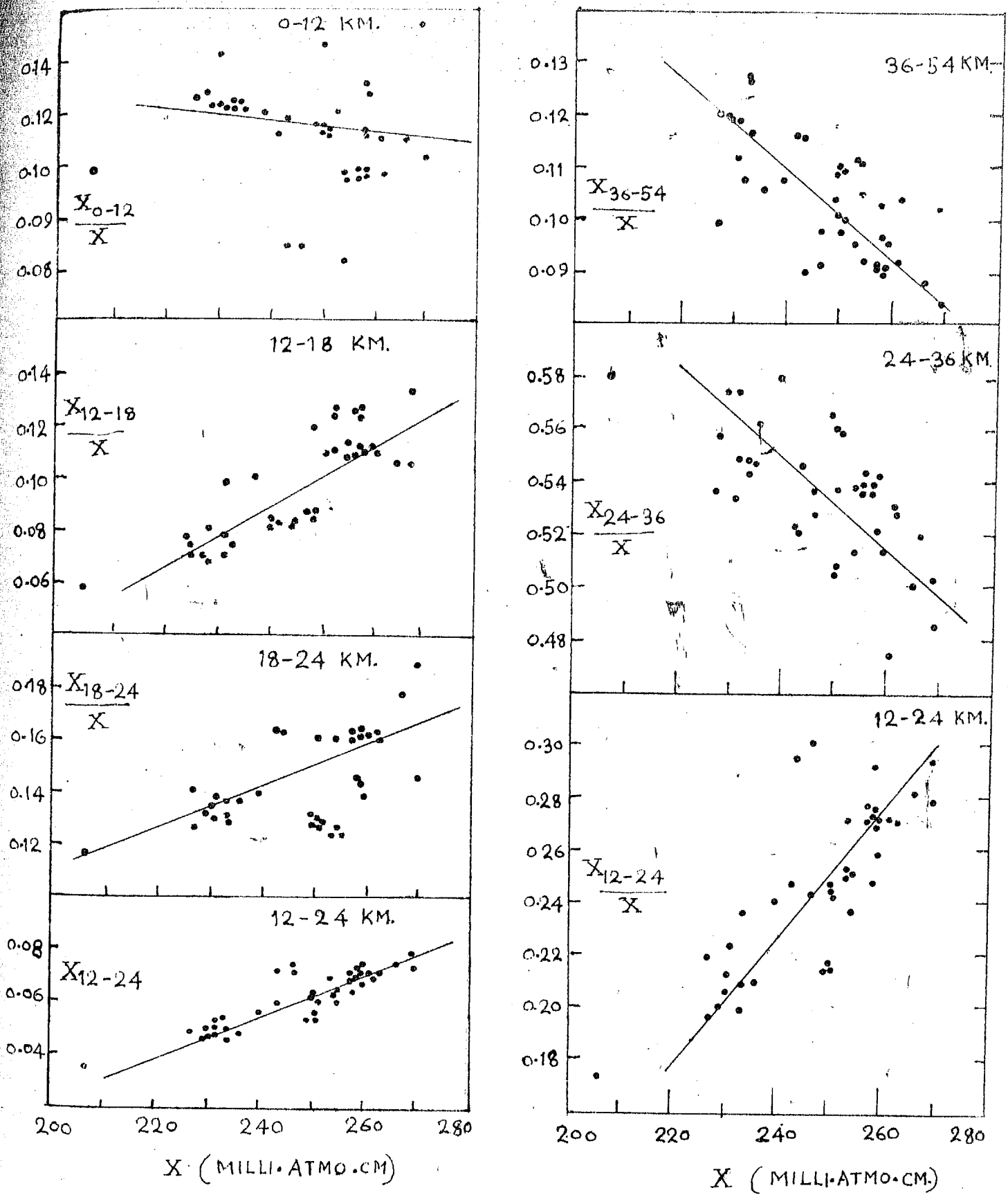

SCATTER DIAGRAMS OF FRACTIONAL OZONE AMOUNTS AT VARIOUS LEVELS AND OF OZONE BETWEEN 12-24 KM. OVER MT. ABU, CALCULATED FROM 38 SETS OF UMKEHR MEASUREMENTS MADE DURING 1957-59

Table 3.

Vertical ozone distribution over Mt.Abu, calculated by method B, from umkehr observations with λλC.

Date	Total Ozone D.U.	Ozone amounts in D.U/KM in different layers								
		0-6	6-12	12-18	18-24	24-30	30-36	36-42	42-48	48-54 Km
18-6-57	239	1.3	2.7	4.9	5.6	15.3	8.6	2.7	0.8	0.8
23-11-57	207	1.3	2.0	2.9	4.9	13.3	6.0	2.7	0.8	0.7
26-11-57	207	0.7	2.0	2.0	4.0	12.6	8.0	2.8	0.8	0.7
27-11-57	202	1.3	2.0	2.7	3.8	11.7	8.0	2.7	0.9	0.7
6- 1-58	233	2.0	2.0	2.7	5.1	14.6	7.5	2.9	1.1	0.9
8- 1-58	229	1.3	2.7	2.9	4.6	13.3	8.6	2.9	1.1	0.5
26- 1-58	249	1.3	2.7	3.6	5.3	15.3	9.0	2.7	0.8	0.5
30- 1-58	254	0.7	1.3	4.6	5.3	16.0	10.5	2.4	0.3	0.7
3- 2-58	229	2.0	2.0	2.7	5.1	14.6	7.3	2.7	0.9	0.9
7- 2-58	230	2.0	2.0	2.7	5.1	14.6	7.4	2.7	0.9	0.9
10- 2-58	254	0.5	2.7	5.3	5.3	14.6	9.3	2.7	1.3	0.4
11- 2-58	244	0.7	2.0	4.0	7.7	14.6	7.3	2.4	1.2	0.9
13- 2-58	250	1.3	2.7	3.6	6.7	15.4	7.8	2.7	1.1	0.4
22- 2-58	243	2.0	2.0	3.3	6.7	14.6	7.3	2.9	1.3	0.4
23- 2-58	250	1.3	2.7	3.6	5.3	15.4	8.3	2.7	1.1	0.3
25-2-58	269	1.3	2.4	4.6	8.5	15.4	7.8	2.9	0.5	0.7
23- 4-58	257	0.9	2.7	4.3	7.1	14.6	8.5	2.4	1.2	0.8
25- 4-58	250	1.3	2.7	3.6	5.3	15.4	8.8	2.8	1.1	0.7

Table 3 (contd.)

Date	Total Ozone D.U.	Ozone amounts in D.U/KM in different layers 0-6	6-12	12-18	18-24	24-30	30-36	36-42	42-48	48-54 Km
18- 5-58	243	0.7	1.3	3.3	8.7	14.6	8.4	2.0	0.9	0.7
19- 5-58	246	0.7	1.3	3.3	9.1	14.6	8.3	2.0	0.9	0.8
21- 5-58	257	0.7	2.7	4.7	6.9	14.6	9.3	1.6	1.2	1.1
22- 5-58	266	1.3	2.7	4.6	7.8	14.6	9.3	1.6	1.2	1.1
24- 5-58	253	0.7	2.7	4.8	7.0	14.6	9.3	1.7	1.2	0.9
27- 5-58	258	0.7	2.7	4.8	6.9	14.6	9.8	1.6	1.2	1.1
30-10-58	242	1.3	2.0	3.3	6.7	14.6	7.3	3.1	1.3	0.3
19-11-58	227	2.0	2.0	2.7	4.8	14.6	7.3	2.7	0.9	0.9
22-11-58	223	2.0	2.4	3.3	4.4	13.3	7.3	2.9	0.9	0.7
24-11-58	229	2.0	2.7	4.0	4.4	13.3	7.3	2.9	0.9	0.7
24-12-58	233	2.0	2.0	3.1	5.1	14.6	7.4	2.9	0.9	0.7
7- 4-59	250	2.0	2.3	4.9	5.3	14.1	7.3	2.7	1.1	0.4
8- 4-59	250	2.0	3.3	4.6	5.6	14.1	7.3	2.7	1.1	0.4
13- 4-59	254	0.5	2.7	5.3	5.3	14.6	9.1	2.7	1.3	0.7
15- 4-59	254	0.5	2.7	5.0	5.6	14.6	9.0	2.8	1.3	0.7
17- 4-59	259	1.3	3.3	5.4	5.7	14.0	9.2	1.6	1.3	0.9
22- 4-59	262	0.7	2.7	4.8	7.5	14.6	9.3	2.4	1.2	0.9
1- 5-59	269	2.7	3.3	6.0	6.5	13.3	9.3	1.6	1.2	0.9
7- 5-59	253	1.3	4.0	7.0	9.6	10.6	5.3	2.7	0.7	0.5
14- 5-59	261	1.2	2.7	4.8	7.5	14.6	9.3	1.6	1.2	1.0

0-12 Km, 12-24 Km, 24-36 Km and 36-54 Km. In Fig.5 the ozone amount in 12-24 Km is also plotted against the total ozone. Vigroux'[6] absorption coefficients were used.

The 12-24 Km level is subdivided into 12-18 and 18-24 Km and the fractional ozone amounts plotted against the total ozone.

The following points are of interest :-

(1) When the ozone amount increases, the percentage ozone amount decreases above 36 Km.

(2) Ozone amount in 24-36 Km increases as total ozone amount increases but the percentage ozone amount decreases with ozone amount.

(3) The ozone amount in 12-24 Km increases with the total ozone. The percentage of the total ozone also increases when the total ozone increases. The percentage increase is pronounced in 12-18 Km.

(4) The ozone amount between 0-12 Km does not change much with total ozone.

It is seen from Fig.5 that when the total amount of ozone is 220 D.U., 11 % of it is found in 0-12 Km, 18 % in 12-24 Km, 6 % between 12-18 Km and 12 % between 18-24 Km; 58 % in 24-36 Km and 13 % in 36-54 Km. But when the ozone amount changes to 270 D.U., 9 % is found in 0-12 Km, 23 %

between 12-24 Km, (12 % in 12-18 Km and 16 % in 18-24 Km), 54 % in 24-36 Km while 9 % is in 36-54 Km layer.

6. Comparison of vertical distributions of ozone at stations in different latitudes and seasons

To obtain comparable vertical distributions of ozone at different places it would be of great help if the same method could be used at all the places. If the observations could be synoptic, they would be of even greater value.

Vertical distributions have been calculated from umkehr observations made at the following places with the Dobson spectrophotometer following an identical procedure of computation. Kodaikanal ($10^{\circ}N$), Abu ($24^{\circ}N$), Torishima ($31^{\circ}N$), Srinagar ($34^{\circ}N$), Tateno ($36^{\circ}N$), Sapporo ($43^{\circ}N$), Arosa ($47^{\circ}N$), Moosonee ($51^{\circ}N$), Eskdalemuir ($55^{\circ}N$), Alaska ($65^{\circ}N$), Tromsø ($70^{\circ}N$) and Resolute ($75^{\circ}N$).

In computing the vertical distributions of ozone from the observed umkehr curves, tables prepared by K.R.Ramanathan and J.V.Dave for a 6 Km division of the atmosphere in the IGY Instruction Manual have been used. The corrections to be applied to the umkehr curves for the secondary scattering given by them in the same manual have been used uniformly throughout whenever the ozone amount was smaller than 300 D.U. The tables of $\log \Delta m_n - \beta F$ for λ 3114 and λ' 3324 have been corrected for the altitudes

of the stations above sea level. The secondary scattering corrections to be applied to the umkehr curves are not the same when ozone amounts are high. The corrections for ozone amounts between 300 D.U. to 475 D.U. have been used as given in Table 1.

Table 4 gives the summary of the vertical distributions of ozone computed for the places mentioned above.

The following points are of interest :-

(1) Throughout the year, there is more ozone in the troposphere in latitudes higher than 30°N than in lower latitudes.

(2) When the total ozone increases, the major part of the increase takes place at levels below 24 Km at middle and high latitudes. Significant amounts are brought down to 12-13 Km in sub-tropical latitudes.

(3) The ozone above 36 Km is not changed appreciably when the total ozone amount is changed.

Fig.6 gives the position of the centre of mass of ozone at different places in summer (when ozone amount is generally low) and in winter-spring (when the ozone amount is often high).

The centre of mass of ozone is higher over the equator (above 26 Km) than at higher latitudes (about 20 Km). During winter there is a sharp fall of the center of mass of ozone at 30°N, whereas the decrease is more gradual during summer.

III

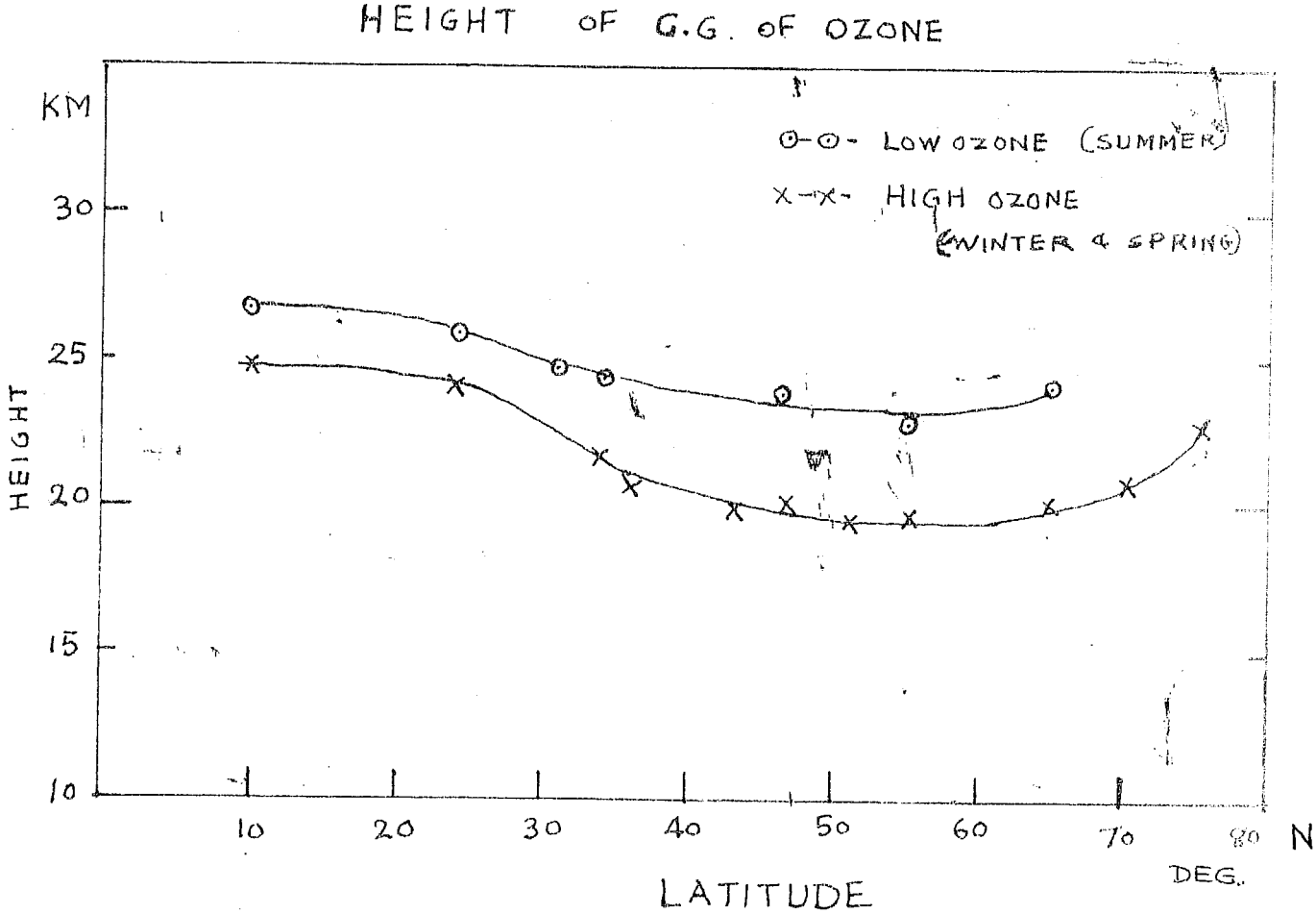
HEIGHT OF G.G. OF OZONE
KM
30
25
20
15
10
HEIGHT
O-O- LOW OZONE (SUMMER)
X-X- HIGH OZONE
(WINTER & SPRING)
10
20
30
40
50
60
70
80
N
DEG.
LATITUDE

FIG. 6

III

Table 4.

Vertical distributions of ozone over stations at different latitudes calculated from umkehr measurements with λλC by method B (corrections used as given in table 1; ozone calculated with Vigroux' ∝).

Place	Date	Ozone amount D.U.	Ozone amounts in D.U/KM in different layers 0-6	6-12	12-18	18-24	24-30	30-36	36-42	42-48	48-54 Km
Kodaikanal	20- 1-58	231	2.0	2.3	2.7	5.1	14.6	7.2	2.5	1.3	0.7
(10°N)	30- 5-58	243	2.0	2.0	3.3	6.6	14.6	7.3	2.7	1.3	0.7
"	29-11-58	238	1.3	3.3	4.6	5.3	13.3	6.8	2.8	1.2	0.8
"	29-12-58	217	0.7	0.9	3.0	7.3	13.3	6.0	3.3	2.0	0.4
Torishima (31°N)	10- 4-58	312	2.0	3.3	6.6	8.0	17.7	6.9	4.4	2.0	1.2
Srinagar	12- 5-58	291	1.7	4.7	6.0	7.3	15.7	8.0	2.9	1.2	0.9
(34°N)	5- 8-57	269	2.0	2.7	4.6	5.6	17.3	8.6	2.7	0.7	0.5
Tateno	28- 2-58	376	2.7	5.3	10.6	12.9	16.6	7.3	5.0	0.7	0.4
(36°N)	3- 3-58	432	4.6	10.6	14.7	15.2	15.3	7.0	4.0	1.1	0.5
"	4- 3-58	441	4.6	9.3	13.3	16.3	16.6	6.6	4.2	1.2	1.2
"	5- 3-58	407	4.0	8.6	11.8	13.7	16.6	7.2	5.2	0.5	0.1
Sapporo	11- 9-58	315	2.0	3.3	6.6	10.6	16.1	6.2	4.5	2.0	1.1
(43°N)	2-12-58	315	3.3	4.6	9.3	7.6	16.3	6.6	2.4	1.3	0.9
"	3-10-58	313	2.0	3.3	6.6	10.3	16.1	6.3	4.4	2.0	1.2

Table 4 (contd.)

Place	Date	Ozone amount D.U.	Ozone amounts in D.U/KM in different layers 0-6	6-12	12-18	18-24	24-30	30-36	36-42	42-48	48-54 Km
Sapporo	16-10-58	319	2.7	4.0	6.6	10.6	16.1	6.2	3.7	2.0	1.2
"	13- 4-58	475	5.3	10.0	13.6	14.9	17.9	9.6	3.7	1.1	0.9
Moosonee	20- 7-57	300	4.6	6.5	5.4	8.2	10.9	8.5	3.6	1.3	0.5
(51°N)	15- 2-58	496	4.1	10.9	21.8	18.3	15.0	6.8	3.4	1.4	0.7
Eskdalemuir	3- 5-59	444	6.0	11.2	12.0	17.7	15.3	6.8	3.1	1.2	0.9
(55°N)	27- 3-59	257	2.0	4.6	5.4	7.7	13.3	5.3	2.4	1.2	0.9
Alaska	24- 3-54	437	5.3	10.8	12.0	16.6	17.3	5.6	3.1	1.2	1.1
(65°N)	13-10-53	295	2.3	4.6	6.0	7.3	26.6	8.0	3.1	1.3	1.2
Tromsø (70°N)	Mar.1941	443	4.0	9.3	11.2	20.1	13.4	5.1	3.3	1.3	1.2
Arosa	30- 3-58	408	4.4	8.0	11.4	16.3	16.2	6.0	3.2	1.3	1.2
(47°N)	9- 3-56	263	2.0	3.3	4.9	8.0	14.0	6.7	2.7	1.2	1.1
Resolute (75°N)	21- 9-58	314	1.4	2.1	13.6	13.6	9.0	4.8	4.5	2.4	0.9

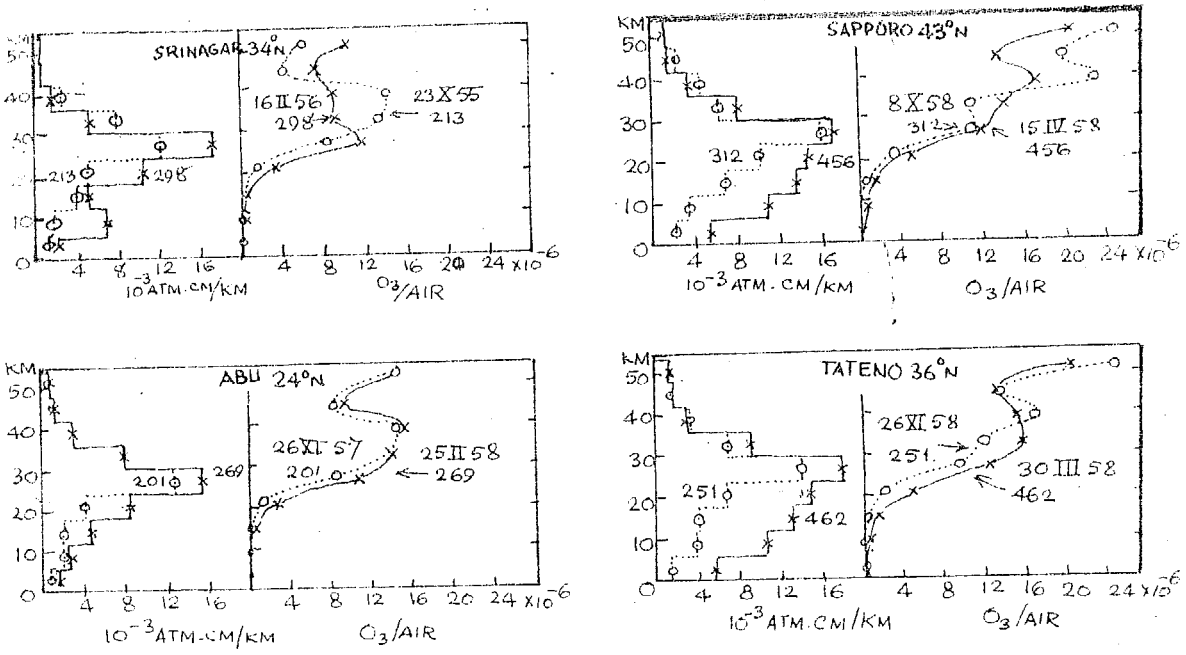

FIG. 7 (a)

FIG. 7 (b)

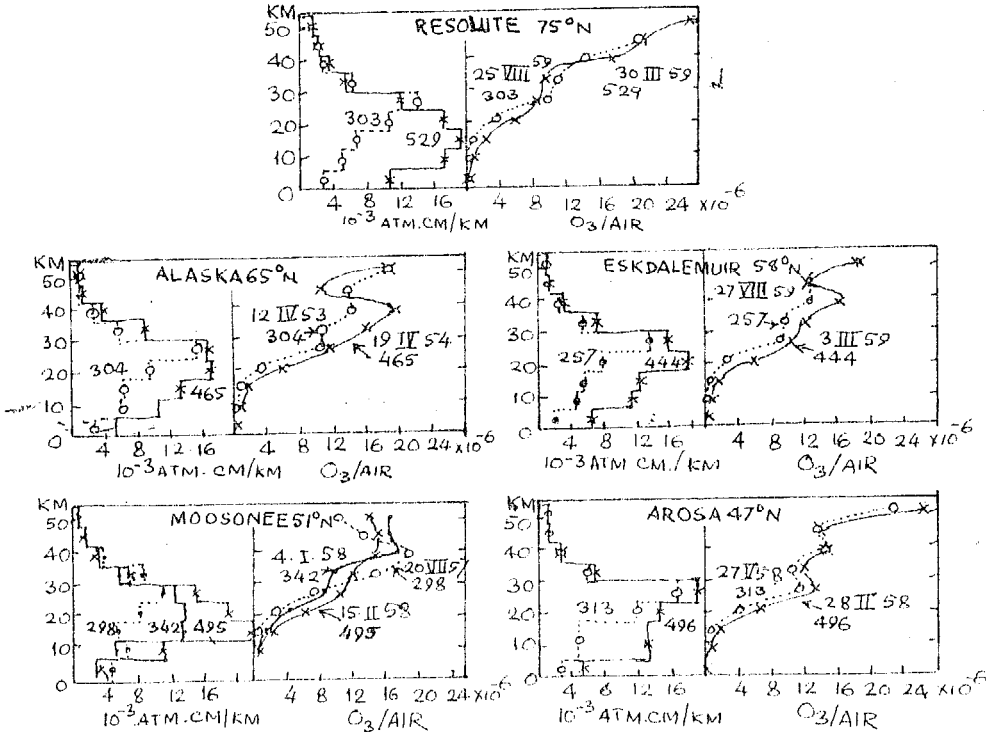

VERTICAL DISTRIBUTION OF OZONE IN WINTER AND SUMMER

EXPRESSED AS (1) O_3 IN 10^{-3} ATM. CM/KM (2) MIXING RATIO (BY WEIGHT)

7. Second umkehr at very low sun*

Umkehr measurements with Dobson spectrophotometer were made at Ahmedabad and were continued for sometimes even after sunset with all the three wavelength pairs $\lambda\lambda A$, $\lambda\lambda C$ and $\lambda\lambda D$. The values of Log I'/I, for different zenith distances of sun were plotted against Z^4. The curves showed the same usual trend, but when sun was 2^0 or 3^0 below horizon the reversal in the trend of Log I'/I was observed in all the three curves, the reversal in the longer wavelengths occuring latter than in $\lambda\lambda A$. The third reversal in Log I'/I, was also observed on some days.

The similar phenomenon was observed by Dr.Dutsch[7] at Arosa. These were seen by him on $\lambda\lambda C$ when sun was $3\frac{1}{2}^0$ and on $\lambda\lambda D$ when sun was 4^0 below horizon.

Fig.3 shows the typical umkehr curve illustrating the second and third reversal in Log I'/I in all the three wavelengths pairs.

In the next chapter, other methods of determining the vertical distribution of ozone will be described.

---

* A brief summary of this work was presented by Dr.Ramanathan at the International Ozone Symposium held at Arosa in August 1961.

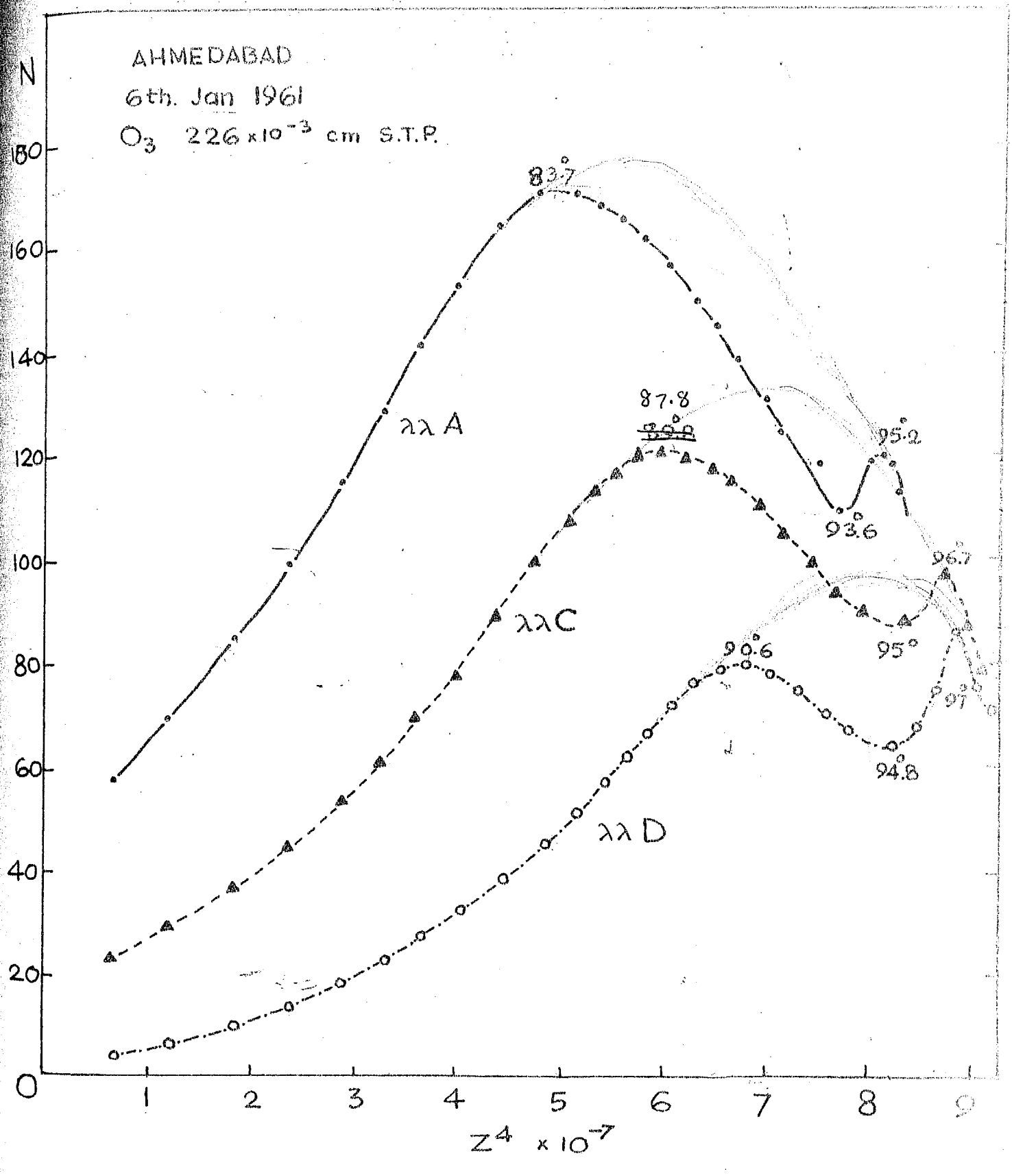

SECOND UMKEHR AT VERY LOW SUN

FIG. 8

REFERENCES

1. Gotz F.W.P., Compendium of Meteorology, p.275 (1951), American Meteorological Society, Boston, Massachusetts.
2. Gotz F.W.P., Meetham A.R. and Dobson G.M.B., Proc. Roy.Soc.A, 145, 416 (1934).
3. Ramanathan K.R. and Dave J.V., Annals of IGY, 5, 23 (1957).
4. Ramanathan K.R., Murthy Bh.V.R. and Kulkarni R.N., Q.J.Roy.Met.Soc., 78, 625 (1952).
5. Sekera Z. and Dave J.V., Astrophys.J.(U.S.A.), 133,1, 210 (1961).
6. Vigroux E., Ann.d.Astrophys., 17, 399 (1954).
7. Dutsch H.U., Final report on ozone and general circulation in the stratosphere, Geophy.Res., Directorate of Air Force of Cambridge and U.S.

CHAPTER IV

OTHER METHODS OF DETERMINING THE VERTICAL DISTRIBUTION OF OZONE IN THE ATMOSPHERE

CONTENTS

CHAPTER IV

OTHER METHODS OF DETERMINING THE VERTICAL DISTRIBUTION OF OZONE IN THE ATMOSPHERE

The methods of determining the vertical distribution of ozone can be divided broadly into two groups:

(1) Indirect methods: (a) Umkehr, (b) Infra-red and (c) Lunar Eclipse or satellite, and

(2) Direct methods : (a) Chemical, and (b) Optical.

I. Indirect methods

I(a) The umkehr method of determining ozone distribution in the vertical has been described in the last chapter.

I(b) Infra-red method

Strong[1] in 1941 suggested a method of determining the ozone distribution from simultaneous measurements of the intensity of solar radiation in the ultra-violet and the infra-red. Ozone has a strong absorption band at 9.6 μ in the infra-red regions.

Absorption in the ultraviolet depends only on the total amount of ozone in the path traversed by the beam, while

in the infra-red it depends also on the pressure at the levels in which ozone is present. It is possible to combine simultaneous measurements of the intensity in the ultra-violet and infra-red so as to yield a mean effective pressure for the centre of gravity of atmospheric ozone.

The manner in which the intensity of the 9.6 μ absorption band depends on the amount of ozone and the pressure of air with which it is associated has been determined by laboratory experiments by Summerfeld, and by Walshaw & Goody[2,3]. The method of Walshaw and Goody is briefly described below.

A double monochromator having two 30° rock salt prisms in Littrow mounting was so arranged that the dispersions reinforced one another. The detector was a Golay pneumatic cell. The radiation was chopped at 12 cps and the output signal from the detector operated a pen recorder after being amplified. Care was taken to stop any stray radiation from reaching the detector. The spectrometer was sealed in a vacuum tight chamber and dried with silica gel. Radiation was allowed to enter through a window and the scanning mechanism and slit width control were operated electrically from outside.

Method of evaluation of mean height of ozone

The principle of the method is that the area of the

9.6 μ absorption band depends on the total ozone and on its mean pressure. If one knows the law of variation of the area of the whole band with ozone amount and with pressure, one can find the effective mean pressure at which the whole ozone in the atmosphere may be supposed to be concentrated. An approximate solution to the problem of absorption along a pressure gradient is given by regarding all the absorbing gases to be concentrated at a mean pressure given by the formula

$$\bar{p} = \frac{\int_0^a p \rho \, dh}{\int_0^a \rho \, dh}$$

ρ is the density of ozone between h and h+dh. The total ozone amount can be obtained by the ultraviolet absorption method with a Dobson's spectrophotometer.

The area of the band can be determined by planimetering the area enclosed below the curve of background intensity and the width of the band and then multiplying the area by a constant determined from the frequency calibration of the spectrometer. The complete description of the band apart from the ozone effect is however very complicated due to such problems as the combined effect of Doppler and collision broadening etc.

An empirical relation between the total ozone amount and the effective mean pressure at which it is situated and

the band area was found by laboratory experiments. A number of spectra were taken in the 9.6 μ band with mixtures of air and ozone, by keeping the ozone amount constant and varying the pressure from 0.1 to 760 mm of mercury, and another set was obtained by varying the ozone amount from 0.001 to 1.5 cm at STP and keeping the pressure constant. The band area was found to be proportional to $p^{0.20}$ approximately.

Thus by knowing the absorption band area and the total ozone amount, the mean pressure at which the ozone is situated can be found. The effective pressures were then converted into heights in I.C.A.N. standard atmosphere (i.e. a pressure of 170 mm of Hg at 11 Km and a constant temperature of 216°.5 K above).

This method has an advantage that the effect of molecular scattering is unimportant, but dust and haze have a significant influence on the 9.6 μ band.

In a later paper Epstein, Osterberg and Adel[4] (1955) and R.M.Goody and W.T.Roach[5] have given a method using both absorption on the 9.6 μ band and emission on the same band.

The emission measurements are made in the sky at a number of zenith angles; it is also made from liquid air, and from a black cavity kept at a constant temperature near the room temperature.

The following expression for the emission area of the 9.6 μ band was derived from the theory of radiation :-

$$\frac{A}{\mathcal{T}(b)} = \int B \, dx \qquad (1)$$

where B is the Planck black body radiation in the 9.6 μ band and $\mathcal{T}(b)$ is the mean background radiation transmitted to the ground and $A/\mathcal{T}(b)$ is the emission area of the 9.6 μ band just above the emitting layer responsible for the background and which can be calculated from the equation. Ozone distribution is determined by adjusting the ozone in different layers by trial and error to give the best fit to the ozone emission area.

Goody and Roach divided the atmosphere into three layers and assumed the following distribution of ozone in each layer.

	Layer	O_3 in cm STP per mb.
1.	Ground to tropopause	$a(p_1/p)$
2.	Tropopause to 30 mb	$b(p_1/p)^2$
3.	$<$ 30 mb	$c(p_1/p)^{-1}$

where p_1 and p are the pressures at the bottom and top of each layer and a, b, c are the constants to be adjusted to give the best fit for the ozone emission area.

The integral in equation (1) is evaluated by summing the contributions from these three layers, treating each layer as if it had a unique average value of $B(\bar{B})$. For an optically thin layer $\bar{B}$ is given by

$$\bar{B} = \frac{\int_{p_2}^{p_1} B \rho \, dp}{\int_{p_2}^{p_1} \rho \, dp}$$

and for an optically thick layer $\bar{B}$ corresponds to a level near to the bottom of the layer and this expression is used to evaluate $\bar{B}$ for all the three layers.

For each day of observations $\bar{B}$ is determined. A value of 'a' is selected and 'b', 'c' are then calculated from the known m(0) and $\bar{p}(0)$ where m(0) is the mean ozone amount obtained from Dobson spectrophotometer and $\bar{p}(0)$ is the mean pressure of ozone determined by the absorption of ozone in 9.6 μ band. The integral in the equation (1) is then determined for a range of zenith angles. The calculation is repeated for different values of 'a' untill the best fit to the corrected ozone emission is found.

Epstein, Osterberg and Adel[4,6] in their work on the vertical distribution of ozone from the infra-red and ultra-violet observations divided the atmosphere into 13 layers 1.75 to 5 Km thick, between 2 Km and 47.5 Km. They assumed that ozone was distributed uniformly in each layer and that each layer was isothermal and isobaric. In the computation of the ozone distributions they made use of (1) the effective radiation temperature of ozone layer called ERTOR, (2) A_o, the fractional absorption by atmospheric ozone

over the 9.6 μ band in the direction of observation, (3) w, the precipitable water vapour in a vertical column of the atmosphere and (4) u, the total ozone amount in a vertical column.

The radiation from the ozone was compared with that of a black body radiator corrected for the observed greyness of ozone. This corrected radiation intensity was converted to a temperature ERTOR, by the Planck black body relationship. A_o, for the entire band was determined from the area of the band obtained by planimetering after allowing for the absorption by water vapour w. The total ozone amount u, was determined by Dobson spectrophotometer.

From A_o, the fractional absorption over the central 0.14 μ band (e_o) was determined. Summerfeld has given a relation from laboratory experiments, between the transmissivity, the effective thickness of ozone u_r, the actual ozone amount u, and the pressure. The relation between emissivity and u_r was determined to fit the data where u_r was equal to $u(p/p_o)^{0.295}$.

Thus from A_o, the emissivity $(1-e_o)$ was obtained and substituting this in Summerfeld's relationship between u_r and emissivity, u_r was calculated in the direction of observation. To determine the effective thickness of the ozone in the vertical column, u_r is divided by μ, the cosine of the zenith angle.

The infra-red radiation temperature ERTOR is maximum from the lowest layers of the atmosphere (troposphere). So the method would be insensitive to changes of ozone in the stratosphere. In spite of this, Epstein, Osterberg and Adel have observed marked seasonal variations in the vertical distribution of ozone and an indication of annual variation of ozone in phases with season above 30 Km.

Dust and haze are likely to contribute substantially to 9.6 μ radiation. Hence use of this method in the presence of haze and dust are likely to lead to confusing results.

I(c) Lunar Eclipse method

Barbier, Chalonge and Vigroux[7] in 1942 suggested the use of spectrophotometric measurements of the earth's shadow on the moon's disc for studying the absorption of sunlight in the earth's high atmosphere. In 1950 H.K.Paetzold[8,9,10] in Weissenau used this method for determining the ozone distribution in the atmosphere. An important feature of this method is that the ozone distribution over a range of geographic latitudes can be determined simultaneously from measurements made at one place.

The spectral intensity of the light in the Chappuis band is measured at the edge of the umbra on the moon perpendicular to the boundary of the shadow. Photographs are taken of the darkened moon using interference filters at 6000 Å, at 5000 Å and at 4000 Å in various phases of the eclipse.

From measurements taken at 4000 Å and 5000 Å one can determine the atmospheric extinction outside the ozone absorption band due to scattering in the form $A.\lambda^{B}$ and from the additional measurements taken within the Chappius band, the ozone distribution can be calculated. Vigroux, in one case, has given the plot of relative spectral intensity distribution of the shadowed portion on the moon's surface for various shadow points and for a wavelength range from 4500 Å to 6500 Å. One can calculate how the intensity in the Chappius band would vary for different ozone distributions.

Evaluation:-

Let $P(\gamma)$ be a point on the darkened moon near the boundary of the earth's shadow, where γ is the angle between the line joining P with the centre of the earth, and the line joining the centres of the sun and the earth. Let $O_3(\gamma)$ be the mean ozone mass in the earth's atmosphere traversed by a beam of light arriving at P. $O_3(\gamma)$ is determined from the intensity measurements made at the shadow point P. Let us consider a ray of light from the sun at a height h from the surface of the earth and let $O_3(h)$ be the mean ozone mass traversed by that ray in the earth's atmosphere. Now assuming the sun as a point source, the height h can be calculated when $O_3(h)$ equals $O_3(\gamma)$, using the data of atmospheric refraction given by Link. By knowing $O_3(h)$ for different shadow points on the moon the distribution of ozone in the vertical can be calculated.

The results obtained of the ozone distribution by this method were compared with the distribution obtained by other methods. The method is however of limited use, being applicable only when there is a lunar eclipse and the sky is clear.

2. Direct methods

2(a) Chemical methods

The determination of ozone by the chemical method depends on the well known chemical reaction, the oxidation of KI in neutral solution.

$$2KI + O_3 + H_2O \longrightarrow O_2 + 2KOH + I_2 \qquad (1)$$

Chemical methods for determining ozone in the atmosphere from observations on aircraft were first developed by Regener[11] and Ehmert[12]. Recording methods were constructed by Gluekauf and others[13] and by Bowen and Regener[14].

Ehmert's [12,15,16] method is briefly described below:-

A 2 % solution of potassium iodide is made in double distilled water with a few μgm of sodium thiosulphate. A few c.c. of this solution are taken in a small bottle which is fitted to a bubbling apparatus. A known volume of air is drawn through sintered glass diaphragm and the KI solution. The ozone in the air reacts with the potassium iodide liberating

iodine. The presence of $Na_2S_2O_3$ removes the free iodine. The excess $Na_2S_2O_3$ remains in the solution. The sodium thiosulphate in the solution through which air has been passed is determined by electrochemical titration. The difference between the amounts of $Na_2S_2O_3$ contained (1) in bubbled solution and (2) in the original unbubbled solution, is the iodine equivalent of the ozone contained in the volume of air that has been passed through the solution.

Bowen and Regener's apparatus for measuring the ozone concentration at different heights using air craft, consists of a pair of electrodes immersed in a solution of potassium iodide and $Na_2S_2O_3$ through which air is bubbled. Iodine is liberated continuously by the action of the ozone in the air. The liberated iodine is neutralised by $Na_2S_2O_3$ and when all the $Na_2S_2O_3$ is consumed, the free iodine depolarises the cathode and a current begins to flow in the circuit. This current is amplified and triggers a relay when it reaches a set value. The solution then gets discarded automatically and a fresh solution is injected into the reaction chamber and the above process is repeated. The volume of air necessary to pass through the solution to create a current, sufficient to trigger the relay is measured by the number of pump strokes. The flow of air for each stroke of the pump is known. From this the amount of ozone per unit volume of air is calculated.

J.Carbonay and A.Vassy[17] built an apparatus using the same principle as Regener. In this device, the reaction

bowl is washed out after each measurement. This removes the traces of iodine and other products.

Chemical method for measuring the ozone distribution in the troposphere and the lower stratosphere

In England, A.W.Brewer, R.H.Kay and Dobson G.M.B.[13] developed a chemical "radio sonde" which can be carried in air craft for measuring the ozone amount at different levels.

The equipment consists of two parts : (1) the Kew radio-sonde transmitter and (2) the ozone element with the detector. This equipment is kept in a Dewar flask and is carried in balloon or air craft.

In a later compact version of the instrument developed by Brewer[19], the electrodes are parallel wires wound round an insulating tube and the KI solution is allowed to drop on the tube at the rate of one drop per minute, so that a steady supply of KI is obtained. The tube with its electrodes is kept inside an outer enclosure and air is allowed to pass over the wired tube at a steady rate and let out through an outlet. By increasing the length of the electrodes and reducing the gap between them, the evaporation of free iodine could be reduced to a minimum. The electrolysis is carried out by applying a voltage of 0.1 to 0.2 volt between the electrodes. The small current that has developed depends on the free iodine present in the solution and is amplified by a transistor

amplifier and put on the radio-sonde. With O_3 of the order of 0.002 cm/km the current was about 2-3 μA and this could be magnified to 100 μA by the use of the amplifier. The accuracy of the instrument was good, the estimated error being about 2 %. It can measure concentrations of ozone of one part in 10^9 in about 20 seconds. During the IGY the Brewer ozone equipment has been used in England, at Malta and at Halley Bay in the Antarctica to measure ozone upto a height of about 20 Km.

In an alternative method, Brewer and Milford[20] used an anode of silver or mercury to prevent the reformed iodine from circulating. Silver iodide or mercury iodide are formed at the anode which is so insoluble that they effectively remove the reformed iodine from solution.

V.H.Regener[21] has recently developed a new method for the quick determination of ozone in an instrument which can be carried in sounding balloons.

Air is aspirated from outside and is made to flow over a disc on which there is a thin layer of a chemi-luminescent organic substance "luminol". When ozonised air passes over it, the disc emits light whose intensity is proportional to the concentration of ozone in the air. This light can be measured indirectly with a photo-multiplier. In Regener's instrument, the output of the photo-multiplier was of the order of 0.5 μA at a potential difference of 110 volts between dynodes, when

air containing 50 μgm of O_3 per c.c. was drawn past the disc at the rate of 500 c.c./min. Using a small electrometer tube as amplifier, the output from it was used to control the audio frequency of a blocking oscillator, and this audio signal modulated the standard U.S.A. Weather Bureau radio-sonde transmitter.

Regener's instrument showed a considerable amount of detail in the vertical distribution of ozone. Near the tropopause, the ozone density showed a definite more or less sharp rise and the maximum in the stratosphere was quite clear.

2(b). Measurements of the vertical distribution of ozone by optical methods

Measurements with spectrographs sent up in balloons:

The original spectrographic method of determining ozone in the atmosphere due to E. and V.H.Regener[22,23] has been used with modified instruments by Regener[24] in New Mexico and by Paetzold[25,26,27] in Germany.

A light weight quartz spectrograph is used and successive exposures of the ultra-violet end of the solar spectrum are made at regular intervals during the flight with the spectrograph continuously directed at a quartz surface covered with magnesium oxide, and mounted below the vertical collimator tube. From the slope of the intensity of the ultra-violet end of the solar spectrum and the known coefficients of absorption of ozone,

the thickness of atmospheric ozone between the spectrograph and the sun could be made at different heights.

In Paetzold's flights in Germany, the spectrograph was made robust needing no readjustment even after rough landings. The spectrographs were also standardised. The optics, the barograph and the thermograph were fitted in a closed metal case. A magnesium oxide plate irradiated by the sun served as the source of light. A ring diaphragm was used to reduce the scattered light of the sky. The height of the balloon equipment was determined by the barometer and also by a theodolite.

Optical 'radio-sonde' methods:

Paetzold and his co-workers[28,29] in Weissenau and Madame Vassy in Paris have developed optical ozone sondes which have been extensively used in many parts of the world. In Paetzold's instrument, filters transmitting in the ultraviolet region optimum at 3100 Å and in the blue at 3700 Å are used. A selenium photoelement is used for the measurement of intensity. Above the photoelement, there is a hollow quartz sphere, the inside of which is covered with a magnesium oxide layer, to render the illumination of the cell independent of the sun's angle of incidence. The photocurrents are amplified by a three stage amplifier and their intensities are transmitted to the receiving ground station indicating the positions of the needle of an ammeter over a rotating Morse cylinder.

The light falling on the photoelement is periodically

extinguished by a rotating dial at a frequency of 50 sec^{-1}. Photocurrents are amplified 10^3 times by the three stage RC Amplifier. For checking the amplifier a direct voltage impulse (600 sec^{-1}) is amplified at the same time. The filters are mounted on a disc which rotates and closes step by step the electric circuits required for the various measurements.

The ozone amount is obtained as a function of the quotient ultraviolet/blue light. The sequence of the automatic measurements of the sonde is :

(1) Intensity of ultraviolet light influenced by ozone,
(2) Intensity of blue light not influenced by ozone,
(3) Pressure,
(4) Control voltage for checking the amplifier and
(5) Temperature.

As one cycle lasts 20 sec, ozone measurements take place every 200 meters. The sonde weighs 4 Kg and reaches an altitude of 28 to 30 Km with a 2 Kg neoprene balloon. Balloon ascents with the Paetzold instruments have shown :

(1) the meridional variation of ozone,
(2) seasonal fluctuations of the ozone content at various heights and
(3) a summer maximum above 30 Km.

Determination of ozone concentration at levels above 30 Km

Spectrographs carried in V2 rockets have been used

in U.S.A. to determine the vertical distribution of ozone at still higher levels. A series of solar ultraviolet spectra were photographed by E.S.Johnson et al[30,31] near sunset from two spectrographs carried in rockets fired at White Sands. There have been a number of successful ascents since 1946.

As the rocket ascends the amount of ozone above it decreases and the spectra extend towards shorter wavelengths. The amount of ozone above the spectrograph is determined by comparing each spectrum with a spectrum obtained when the rocket is above the level of detectable ozone.

The comparisons of the spectra are made by photographic photometry. The data are obtained with a low sun so as to increase the optical path through ozone. The ozone distribution curves obtained by rocket firings support the curves obtained by Gotz, Meetham and Dobson[32] and by Karandikar and Ramanathan[33] by the umkehr method, for the same amount of ozone. However, the distribution obtained on the same day by the umkehr method and by the rocket borne spectrographs showed some disagreement in the height of maximum concentration. This is now known to be due to the neglect of second order and higher order of scattering in the calculation of ozone distribution from umkehr observations. The observed curves have also been compared with the curves calculated photochemically by Craig[34] (1950), by Bates and Nicolet[35] and by Johnson et al.

Conclusion

Each of the methods used for determining the vertical distribution of ozone in the atmosphere has its own advantages and disadvantages. A spectrograph carried in a rocket is the only satisfactory method available for determining the ozone at the highest levels of the atmosphere. The balloon method is useful for levels up to 35 Km. The chemical method allows measurements of the details of ozone distribution in the troposphere and lower stratosphere with fair accuracy. Both the chemical and optical ozone-sonde methods have a promising future for synoptic studies of ozone distribution in the vertical over a large area.

The infra-red method appears promising but needs further work. Most of the existing knowledge of the distribution of ozone in the upper troposphere and stratosphere at different latitudes has come from the Götz Umkehr method. The Götz method is simple and inexpensive and many measurements can easily be obtained provided atmospheric conditions are favourable. Uncertainties in the calculation of the distribution from the observations are being overcome, but the method is rather insensitive to changes in ozone concentration in the lower atmosphere.

For synoptic purposes, the chemical or optical ozone-sonde method is likely to prove the most valuable. They can be used in all kinds of weather.

The next chapter deals with the distribution of ozone over the earth from measurements made during IGY-IGC.

REFERENCES

1. Strong J., Jour.Franklin Inst., 231, 121 (1941).
2. Goody R.M. and Walshaw C.D., Q.J.Roy.Met.Soc., 82, 177 (1956).
3. Walshaw C.D. and Goody R.M., Proc.Toronto Conf. 1953 49 (1954).
4. Epstein E.S., Osterberg C. and Adel A., J.Met., 13, 319 (1956).
5. Goody R.M. and Roach W.T., Q.J.Roy.Met.Soc., 82, 217 (1956).
6. Epstein E.S., Osterberg C. and Adel A., J.Atmos.Terr. Phy., 8, 347 (1956).
7. Barbier D., Chalonge E. and Vigroux E., Ann.Astrophys., 5, 1 (1942).
8. Paetzold H.K., J.Atm.Terr.Phy., 3, 125 (1953).
9. Paetzold H.K., Zeit.Fur Naturf., 12, 661 (1950).
10. Paetzold H.K., Zeit.Fur Naturf., 29, 325 (1952).
11. Regener V.H., Met.Zeit., 55, 459 (1938).
12. Ehmert A., Zs.Naturf., 46, 321 (1949).
13. Glueckauf E., Hal H.I., Martin G.R. and Paneth F.A., J.Chem.Soc., 1, (1944).
14. Bowen J.G. and Regener V.H., J.Geoph.Res., 56, 307 (1951).

15. Ehmert A., J.Atmos.Terres.Phy., 2, 133 (1952).

16. Ehmert A., Advances in Chemistry, Series No.21, 133-132, Amer.Chem.Soc.(1959).

17. Carbenay J. and Vassy A., Annales de Geophysique, 9, 300 (1953).

18. Brewer A.W., Kay R.H. and Dobson G.M.B., Rocket exploration of upper atmosphere, 139, Pergamon Press, (1954).

19. Brewer A.W., Q.J.Roy.Met.Soc., 83, 356 (1957).

20. Brewer A.W. and Milford J.R., Proc.Roy.Soc.,A, 256, 470 (1960).

21. Regener V.H., XII General Assembly of I.U.G.G., Helsinki, Finland (1960).

22. Regener E. and Regener V.H., Phys.Z., 35, 788 (1934).

23. Regener E. and Regener V.H., Nature, 134, 330 (1934).

24. Regener V.H., Nature, 167, 276 (1951).

25. Paetzold H.K., J.Geoph.Res., 56, 365 (1954).

26. Paetzold H.K., Sci.Proc.Int.Assoc.Meteorology, I.U.G.G., Rome, 201 (1954).

27. Paetzold H.K., Uber die Photochemie der End atmosphere Unter besonder Berucksichtigung der ozonschicht Hab Dissertationschrift (1954).

28. Paetzold H.K. and Kulcke, Weissenau Ozone Symposium, (1956).

29. Paetzold H.K., Advances in Chemistry, No.21, 201, American Chemical Society (1959).

30. Johnson F.S., Purcell J.D., Tousey R. and Watanabe K., Rocket exploration of the high atmosphere, 193, Pergamon Press (1954).

31. Johnson F.S. and Purcell J.D., J.Geophy.Res., 57, 157 (1952).

32. Götz F.W.P., Meetham A.C. and Dobson G.M.B., Proc. Roy.Soc.A., 145, 416 (1934).

33. Karandikar R.V. and Ramanathan K.R., Proc.Ind.Acad.Sc. A., 29, 330 (1949).

34. Cragg R.A., Met.Monographs, 2, 1 (1950).

35. Bates D.R. and Nicolet M., J.Geophy.Res., 55, 301 (1950).

CHAPTER V

DISTRIBUTION OF OZONE OVER THE EARTH FROM MEASUREMENTS MADE DURING IGY-IGC PERIOD

CONTENTS

CHAPTER V

DISTRIBUTION OF OZONE OVER THE EARTH FROM MEASUREMENTS MADE DURING IGY-IGC PERIOD

1. Introduction

The ozone observations made during IGY-IGC period at about 30 stations in the northern hemisphere and at a few stations in the southern hemisphere were collected together and examined to study the geographic distribution of ozone over the earth.

Conspicuous departures from regular latitudinal variation of ozone were observed. Sudden changes in ozone amounts observed in winter in high latitudes shortly before or after the end of the polar night are briefly discussed with reference to the sudden stratospheric warmings of the polar and sub-polar atmosphere.

2. Regional differences

Dobson[1] first gave a diagram of ozone distribution with latitude from his world-wide survey of ozone observations. He established that the mean ozone amount generally increases with latitude at least upto 63°N. Götz[2] in 1944 made a significant remark that the distribution of ozone was not entirely latitudinal but also depended on the geographical situation of the place.

Some ozone observations made even before the IGY period brought out some conspicuous examples showing that the mean ozone amount at a station was not a function of latitude alone.

Fig.1 represents the monthly mean ozone amounts during the IGY-IGC period at Marcus Island (24°N) in Japan and at Mt.Abu (24°N) in India. Both are at the same latitude but the ozone values at Marcus Island are much larger than those at Mt.Abu.

The ozone values at Aarhus (56°N) are significantly higher than those at Eskdalemuir (55°N), eventhough both are approximately at the same latitudes in Europe. The ozone values at Tateno (36°N) in Japan were found to be very large compared to those at Srinagar (34°N) in India.

The same anomaly was observed by Kulkarni, Angreji and Ramanathan[3] in case of Tateno and Srinagar. They suggested that the cold Siberian anticyclones with their periodic cold waves tended to increase the ozone amounts over Tateno and the Indian summer monsoon and the Himalayas likewise exerted a strong depressing influence on the ozone amounts south of the Himalayas.

Marcus Island in the Pacific shows larger amounts of ozone than Mt.Abu. This can also be explained on the same basis. Besides, one can expect downward motion over the cooler sea, and winds in the upper troposphere and lower stratosphere at Marcus Island would have a component from the north. On both counts, larger values of ozone may be expected.

V

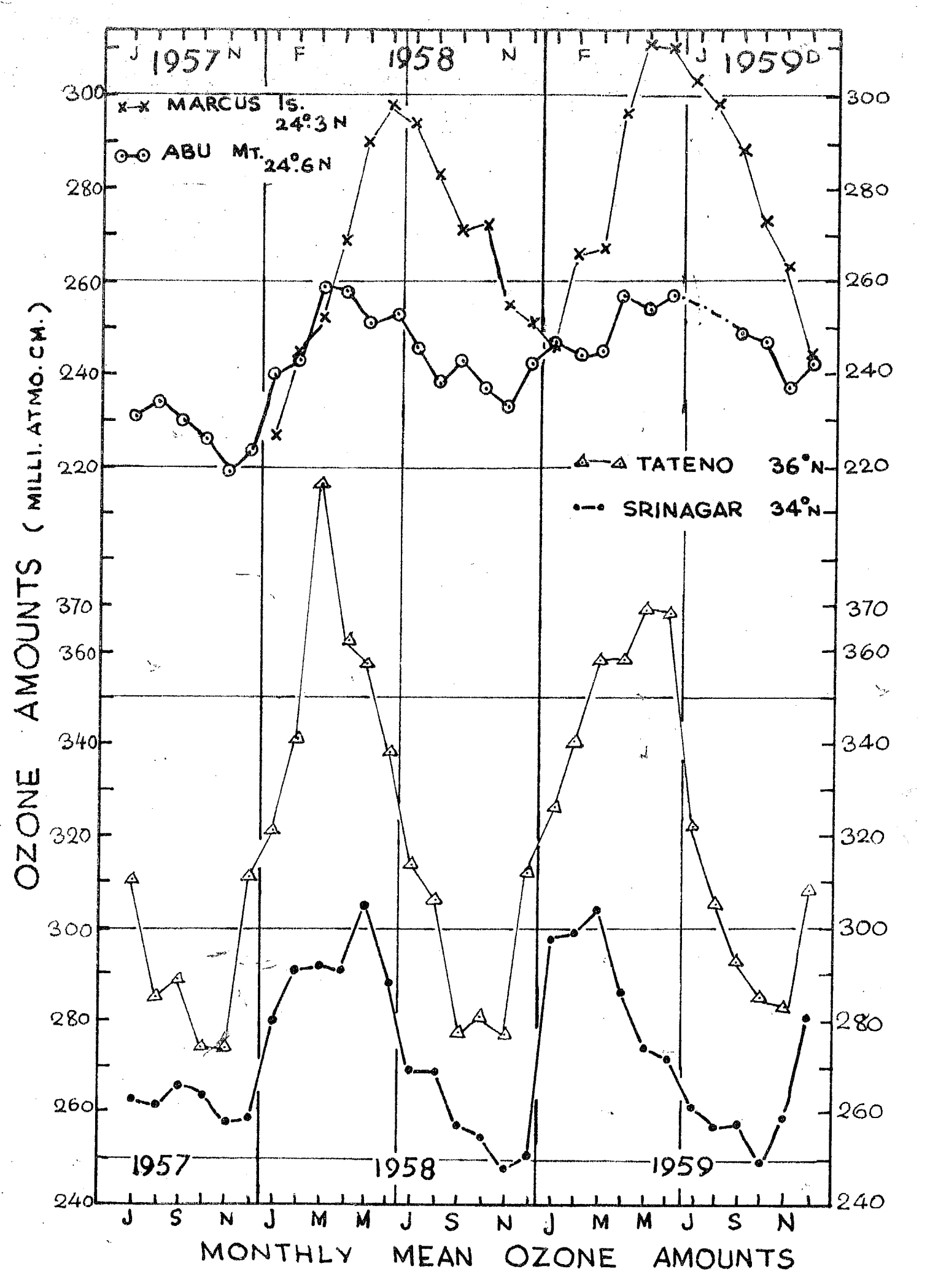
J 1957 N
F 1958 N
F 1959 D
MARCUS Is. 24°3 N
ABU Mt. 24°6 N
TATENO 36°N
SRINAGAR 34°N
OZONE AMOUNTS (MILLI. ATMO. CM.)
300
280
260
240
220
370
360
340
320
300
280
260
240
1957
1958
1959
J S N J M M J S N J M M J S N
MONTHLY MEAN OZONE AMOUNTS

High values of ozone at Aarhus than at Eskdalemuir are, no doubt, due to regional differences. But the cause for this large difference in ozone amounts requires further investigations in a synoptic way of the vertical distribution of ozone at different altitudes, of mixing ratio of ozone/air and of the general circulation.

3. Seasonal and latitudinal variation of total amount of ozone

Fig.2 represents the mean monthly ozone amounts at a few selected stations at different latitudes. They are Tromsø ($70^{\circ}N$) Lerwick ($60^{\circ}N$), Aarhus ($56^{\circ}N$), Eskdalemuir ($55^{\circ}N$), Oxford ($52^{\circ}N$) and Arosa ($47^{\circ}N$) in Europe and Tateno ($36^{\circ}N$), Srinagar ($34^{\circ}N$), Delhi ($23^{\circ}.5N$), Abu ($24^{\circ}.6N$), Marcus Island ($24^{\circ}.3N$) and Kodaikanal ($10^{\circ}N$) in Asia.

It has already been mentioned that the Japanese station Tateno shows markedly higher values than Srinagar particularly in the period March to June, although the latitude of Tateno differs from that of Srinagar by only 2°. The mean ozone amounts at Aarhus are significantly higher than those at Eskdalemuir in the months of January-May. In general, in the same latitude zone, the ozone amounts in winter and spring are larger on the eastern side of the North American and European continents than on the western side.

We can form a useful picture of the latitudinal distribution of total ozone over the earth.

V

Fig.3 represents the average variation of total ozone amount with month and latitude. The isophlets give the total ozone in 10^{-3} cm STP on Vigroux scale. The diagram is based on the ozone data of about 35 stations from both the hemispheres collected during IGY and IGC periods.

In winter and spring, the total ozone is minimum at the equator and maximum at very high latitudes.

It will be noticed that on the average January-February represents the period of the greatest range of change of total ozone in high latitudes of the northern hemisphere. In the southern hemisphere, there appear two distinct zones of maximum ozone, one in spring near the latitude of Macquarie Island ($54^{o}.6S$) and another in early summer in the Antarctic. The two maxima merge into one in the northern hemisphere.

In early spring, the amount of ozone in the northern hemisphere increases rapidly with latitude at 25^{o} to 40^{o} and again near about $65^{o}N$. In the southern hemisphere spring, on the other hand, the maximum is found at about $50^{o}S$ and there is a decrease of ozone at high latitudes.

Fig.4 shows the ozone variation at two stations in the two hemispheres, one at Halley Bay ($75^{o}S$) and the other at Resolute ($75^{o}N$). The delay in the time of onset of ozone increase in the southern hemisphere after the end of the polar winter must have associated with it a significant difference in the lower stratospheric circulations in the two hemispheres.

V

OZONE DISTRIBUTION IN DIFFERENT MONTHS FROM 1957 TO 1959

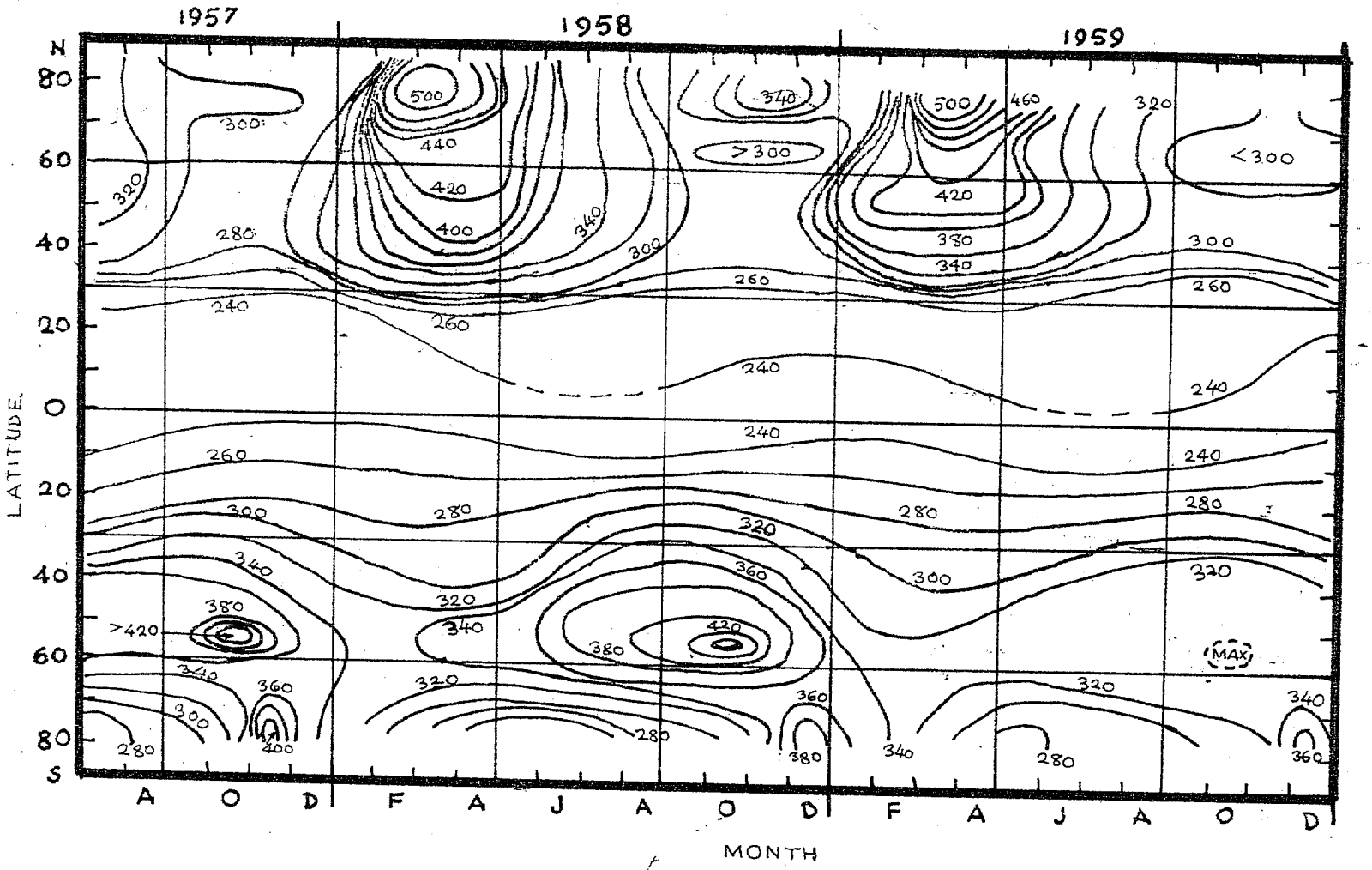

FIG.3

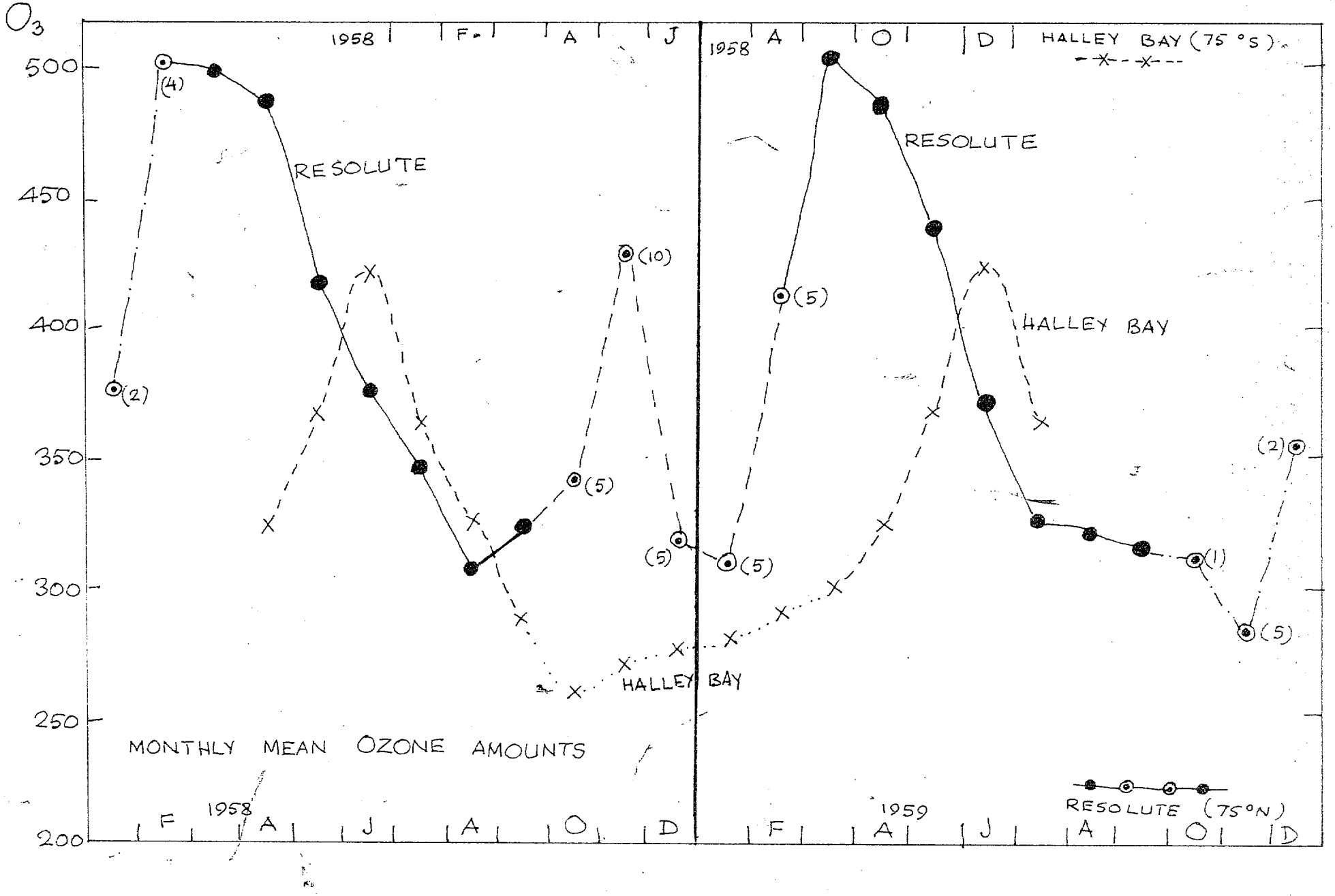
O_3
500
450
400
350
300
250
200
1958
F
A
J
A
O
D
1959
RESOLUTE
HALLEY BAY
HALLEY BAY (75 °S)
RESOLUTE (75°N)
(4)
(2)
(10)
(5)
(5)
(5)
(5)
(1)
(2)
(5)
MONTHLY MEAN OZONE AMOUNTS

FIG. 4

4. Polar warming and associated ozone changes

The ozone amounts at very high northern latitudes are found to increase very rapidly in the months of January and February, compared to other moderately high and low latitudes. These increases are very large and abrupt. Such changes were found at Tromsø, a few years ago and they were suspected to be due to insufficient accuracy of measurements of ozone amounts during the polar night. But afterwards, it was found that large increase of ozone near about the end of the polar night at Tromsø was genuine, and was connected with the break up of the polar stratospheric vortex. This phenomenon was discovered by Scherhag from observations in middle latitudes as early as 1952.

Fig.5 represents the polar stratosphere warming and associated ozone changes in both hemispheres. Daily ozone values at Halley Bay (75°S) and upper air temperatures in centigrade (10-day average) at 20 mb, 50 mb and 150 mb over South pole (90°S) are plotted. Similar plot is made of daily ozone values at Tromsø (69°.7N) and upper air temperatures at 10 mb, 50 mb and 100 mb over the drifting Ice station Alpha (82°-85°N). Upper air temperatures are according to H.Wexler[4].

The Arctic and Antarctic curves are displaced by six months so as to bring the same seasons together. Vertical lines are drawn to indicate period of absence of sun.

V

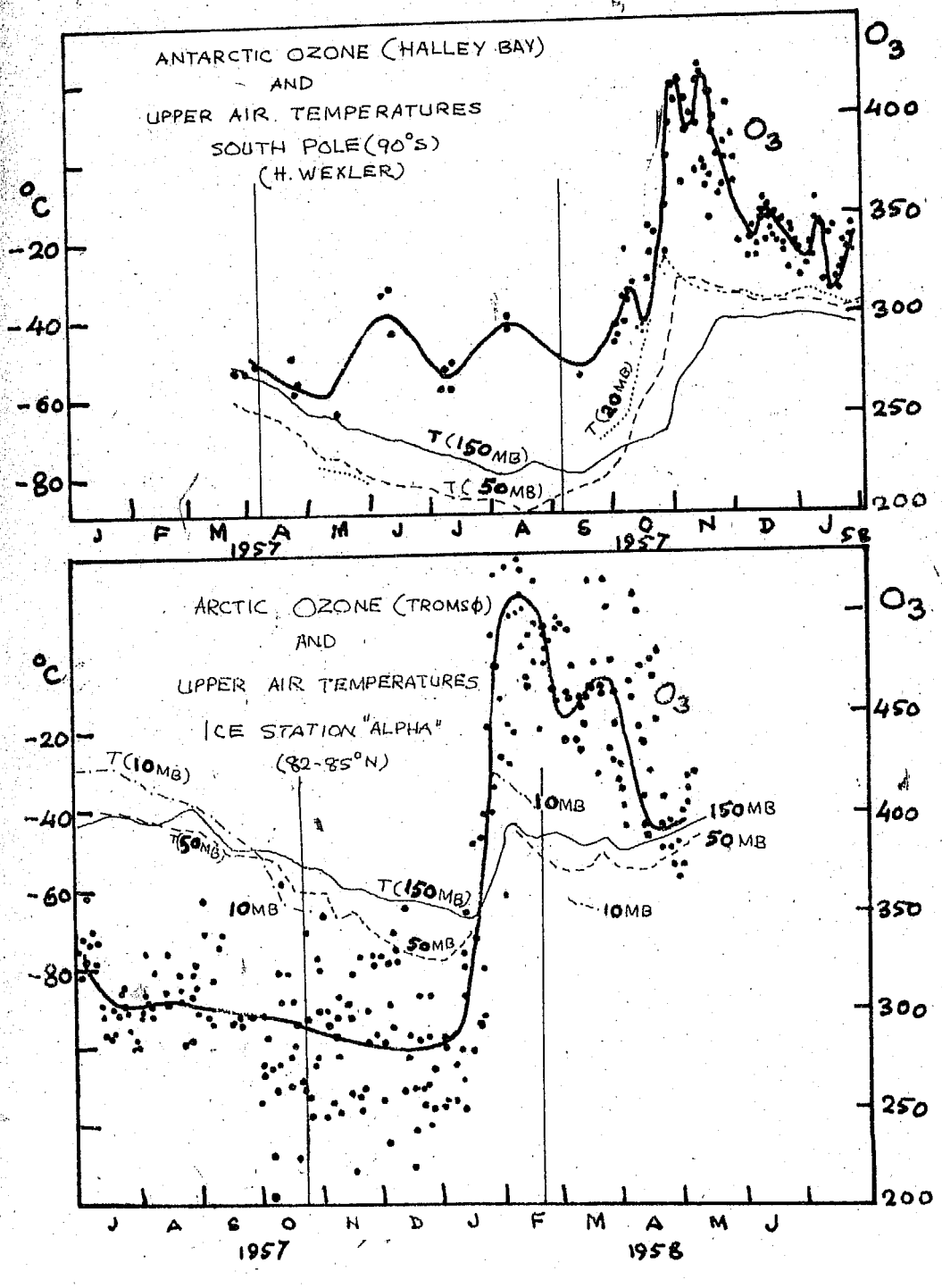
ANTARCTIC OZONE (HALLEY BAY)
AND
UPPER AIR TEMPERATURES
SOUTH POLE (90°S)
(H. WEXLER)
°C
-20
-40
-60
-80
O3
400
350
300
250
200
T(150MB)
T(50MB)
T(30MB)
J F M A M J J A S O N D J
1957
58
ARCTIC OZONE (TROMSØ)
AND
UPPER AIR TEMPERATURES
ICE STATION "ALPHA"
(82-85°N)
°C
-20
-40
-60
-80
O3
450
400
350
300
250
200
T(10MB)
T(50MB)
T(150MB)
10MB
50MB
150MB
J A S O N D J F M A M J
1957
1958

FIG. 5

V

From the figure, it will be seen that strong temperature increases at 20 mb, 30 mb and 50 mb at the South pole were observed only after the sun's return in October. The ozone amounts at Halley Bay also showed rapid increases from 0.300 cm to about 0.450 cm during the same period.

In the case of Ice station Alpha, the marked temperature rise at 10 mb, 50 mb and 150 mb took place before the returns of the sun. The temperature increased upto about -30°C at 30 km in the first week of February. The ozone values at Tromso shot up from 0.300 cm to 0.500 cm during that period.

Fig.6 gives another example of explosive stratospheric warming and associated ozone changes. In Fig.6, daily values of total ozone and temperatures at 10-15 mb level over Reykjavik for the period January-February 1953 are plotted. The ozone amounts started increasing from 22nd January 1953 and became maximum (300 D.U. to 550 D.U.) on 29th January 1953 which further fell to about 350 D.U. on 5th February 1953. It again started increasing and became maximum (600 D.U.) on about 10th February 1953. It then decreased and recovered to its normal value. The temperature at 10-15 mb level also showed similar trends during that period. On 22nd January 1953, the temperature was about -70°C and then it shot up. Unfortunately temperature data during 25th January 1953 - 10th February 1953 were not available. But the temperatures at 10-15 mb level on 10th February 1953 was found to be about -30°C. This suggests that the temperatures also shot up from about -70°C to -30°C during that period.

V

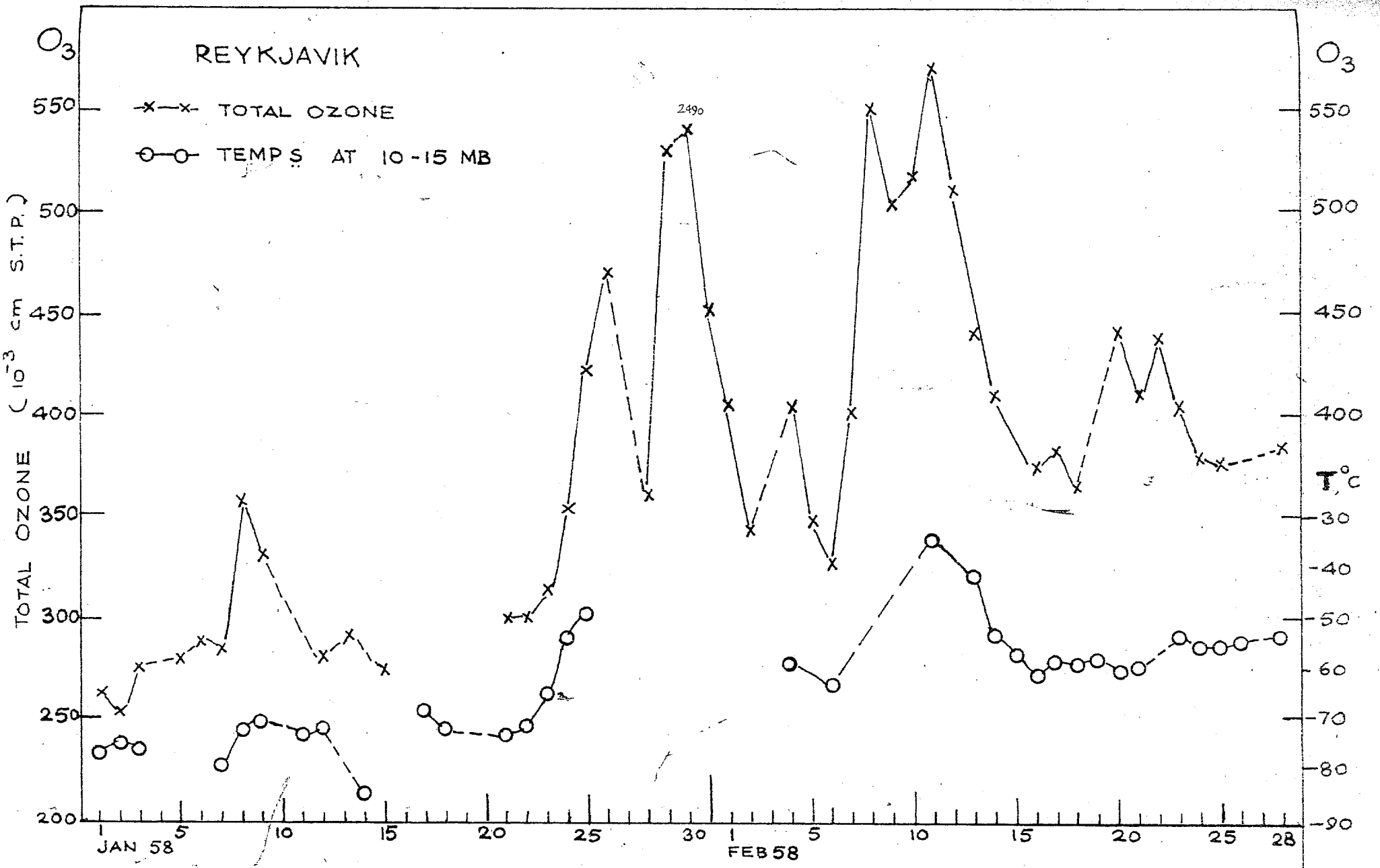

TOTAL OZONE AMOUNTS & 10-15 MB. TEMPS AT REYKJAVIK FOR THE PERIOD JAN - FEB 1958

V

FIG. 6

This rapid increase in the total ozone content of the atmosphere in high and middle latitudes in the second half of winter and early spring cannot be due to an increase in production rate[5], because the largest increase takes place in regions where there is little ozone-producing radiation. As pointed out many years ago by Dütsch[6], the phenomenon requires a northward transport of ozone at ozone creating levels from middle to high latitudes and a downward transport at the higher latitudes. It should be emphasised that over regions of polar night, ozone can be accumulated in excess of the amounts corresponding to photo-chemical equilibrium at the same levels in the sunlit part of the atmosphere owing to the absence of de-ozonising radiations.

A large scale mixing scheme between middle and high latitudes at levels above 25-30 km in which air ozonised to its equilibrium value in middle latitudes flows northward into the dark atmosphere, and in its place under-ozonised air from the polar night region flows into the sunlit area coupled with a gradual sinking of the air in higher latitudes can explain the rise of ozone in late winter and spring. The amplitude of the meridional oscillation and the rate of sinking have however to be sufficiently large. When large scale sinkings of air associated with sudden stratospheric warmings take place, we may expect abnormally high ozone amounts in the middle stratosphere over polar regions and also large rises of ozone.

Upper air observations in the Arctic and Antarctic

before and during the IGY have demonstrated the existence of cold stratospheric lows near the poles during winter with rings of circumpolar strong winds. This zone of strong winds has probably a much larger amplitude in the northern hemisphere than in the southern, due, no doubt to the distribution of continents and oceans. The vortex breaks down earlier in the Arctic. These break-downs are associated with explosive warmings of the stratosphere and the warming extends from above downwards.

REFERENCES

1. Dobson G.M.B., Harrison D.N. & Lawrence J., Proc.Roy. Soc., 114, 521 (1927).
2. Götz F.W.P., Vjschr.naturf.Ges.Zurich, 89, 250-264 (Ref.in Gotz's article compendium of meteorology, 1951) (1944).
3. Kulkarni R.N., Angreji P.D. & Ramanathan K.R., Meteorology and Geophy., Tokyo, Japan, V.10, No.2, p.85 (1959).
4. M.Wexler H., Q.J.Roy.Met.Soc., 85, 196 (1959).
5. Ramanathan K.R., Symposium on Atmospheric Ozone at Helsinki of I.U.G.G. - Int.Ass.Met. (1960).
6. Dütsch H.U., Symposium on Atmospheric Ozone, Rome Assembly of I.U.G.G. - Int.Ass.Met. (1964).

V

SECTION II

DETECTION OF DUST LAYERS IN THE ATMOSPHERE BY TWILIGHT SCATTERING

CHAPTER I

SUMMARY OF PREVIOUS WORK

CHAPTER I

SUMMARY OF PREVIOUS WORK

Introduction

1. As the sun goes down below the horizon, the lower part of the earth's atmosphere comes successively into the shadow of the earth while the upper part continues to be directly illuminated. With the decrease in the fraction of the atmosphere illuminated by the direct rays of the sun, the scattering of light by the molecules and other particles composing the atmosphere, gradually decreases. This period of decreasing sky brightness from sunset to night and the corresponding period of increasing brightness from night to sunrise, known respectively as evening twilight and morning twilight, are of great interest to physicists from the point of view of studying the physics of the atmosphere.

The period of twilight is some what arbitrarily divided by astronomers into three parts, viz. (1) Civil Twilight - extending from the time when the centre of the sun's disc is $0^{\circ}50'$ below horizon to the time when the centre of the sun's disc is 6° below horizon, (2) Nautical Twilight - extending from the time when the centre of the sun is 6° below horizon to the time when the centre of the sun is 12° below horizon, and (3) Astronomical Twilight - the time interval when the

sun's depression is 12° to 18° below horizon. Night conditions are assumed to set in when the sun's depression is above 18°.

2. Neglecting the effect of dust and cloud, the intensity of illumination of the zenith sky during twilight is made up of (1) primary scattering along the vertical by the molecules in those layers of the atmosphere which are directly illuminated by the sun's rays, (2) secondary and multiple scattering by the molecules in the different layers of the atmosphere, (3) radiation from molecules or atoms in the upper atmosphere which have been raised to an excited state by absorption of solar radiation or by collisions with ionised or excited molecules and (4) scattering by large particles of terrestrial and extra-terrestrial origin.

In addition to the loss of intensity due to molecular scattering, the intensity of the light from the sky suffers attenuation in the lower atmosphere due to absorption by water-vapour and haze, scattering by large particles and by ozone in the upper atmosphere.

3. The brightness of the sky during twilight has been the subject of investigation by many workers and measurements of the intensity of the twilight sky in the zenith and in different parts of the sky have been made with visual photometers and with photoelectric photometers during the interval when the sun is 0° to 20° below the horizon.

A good summary of the work done previous to 1933 has

been given by P. Gruner[1] in his article on "Neueste Dammerungsforschungen" in Ergebnisse der Kosmischen Physik III.

M.W.Chiplonkar[2] studied the brightness of the twilight sky at the zenith with a visual photometer using both green (VG_1) (Schott and Genossen) and red (27A) (Wratten) filters, first at Bombay and then at Poona and at Mt.Sinhagad.

An excellent summary of all the important previous observations in the field together with a full account of the author's own work has been given by Arvid Ljunghall[3] in his dissertation on "The intensity of twilight and its connection with the density of the atmosphere".

Ljunghall used a IP22 phototube in conjunction with three light filters transmitting wavelengths in blue, green and red for measurements of sky intensity. From measurements of zenith sky intensity, he made an attempt to derive the atmospheric density at different levels and compared his results with those of other workers.

4. Since Ljunghall published his thesis, there has been a great increase in our knowledge of the upper atmosphere from a number of sources such as radio-sondes carried in balloons and rockets, from measurements of sound propagation and from the study of the emission of light from the sky during twilight. The Physical Research Laboratory, Ahmedabad, has been engaged on a programme of work involving the correlation of data relating to the upper atmosphere from various sources. The

study of brightness of the atmosphere during twilight has been one of the lines of work. J.V.Dave[4] made extensive measurements of the sky brightness at zenith during twilight at Mt.Abu, as part of this programme in 1951. He studied the variation of the intensity and polarisation of the light from the twilight sky in defined regions of the spectrum.

Dave used an R.C.A. 931 A photomultiplier in conjunction with filters transmitting wavelengths in different spectral regions from the ultra-violet to red. He used a telescope which covered a circular field of sky of 9° diameter. He extended his observations from the time of sun-set to about -20° sun's depression below horizon, and recorded the readings of the amplified photo-current I at intervals of 1/2 a minute. He plotted the intensity I (in arbitrary units) of the zenith sky during twilight in defined spectral regions against the sun's depression θ, below horizon.

5. The following is a summary of the important results of Dave's observations of I against θ :

(1) There is a change in the slope of the curves when the sun's depression is 3° below horizon. It is more pronounced in the ultra-violet and violet and becomes progressively less conspicuous as one goes towards the red.

(2) The intensities in the green, yellow and red regions flatten out at 13° to 14°, while in the violet and blue, the flattening occurs at about 16°.

(3) In the green and the red and perhaps also in the yellow in zenith-scattered light, there are indications of an additional decrease in the rate of fall of intensity with increasing depression at about 12°. This means that there are some additions to brightness which are of the same order of magnitude as the scattered light from the sun's rays at these angles.

Polarisation measurements were also made by [illegible] Dave on a number of clear days both morning and evening in a wide spectral band 4000-5700 Å and also in the spectral region 4350-4850 Å.

The percentage polarisation of the zenith scattered light was calculated from the two components I_l and I_r according to the equation

$$P = \frac{100\ (I_l - I_r)}{(I_l + I_r)}$$

The following interesting results were obtained :-

(1) For small depressions of the sun, the observed values of the polarisation were smaller than those that might be expected from primary scattering by air molecules alone.

(2) There was a further pronounced fall in polarisation between 5°.5 and 8°.5 depression.

(3) The polarisation remained more or less steady at a value of 45 % to 50 % between 3°.5 and 12° of the sun's depression and then decreased rapidly.

Measurements of intensities and polarisation of sky light were also made in the sun's meridian at an angle of 30° on either side of the zenith, using the blue filter for the measurements.

It was found that the changes in the polarisation were sharper on the sun side than on the anti-sun side.

The usual twilight scattering theory assumes that the scattering of sky light is caused only by air molecules. There are however larger particles of dust which are present in the atmosphere which cause some additional brightness in the twilight sky.

Particles of linear dimensions much larger than the wave-length of light scatter light much more in the forward direction and it may be expected that the intensity of the twilight glow will depend on the size, nature and distribution of dust and water particles present in the atmosphere. The dust will also reduce the intensity of the incident primary light illuminating the upper atmosphere. Besides a more or less permanent haze layer decreasing in intensity from the ground upward, there may also be other layers at higher levels. The discontinuities in slope observed in the intensity curves of zenith-sky twilight might be the effect of such dust layers.

6. E.K.Bigg[5,6,7] in Australia carried out some measurements to detect the presence of dust layers in the upper atmosphere by studying the intensity of the sky during twilight with a photo-electric photometer with a small aperture. He carried out measurements of the intensity of the twilight sky at a distance of 70° from the zenith for solar elevations 0° to about 14° below the horizon, and plotted values of 1/I(dI/dt) against h, where h is the lowest height in the atmosphere which the direct sun's rays illuminate when the sky is observed in the particular direction. He assumed that the lowest height corresponded to rays grazing the earth's surface. Refraction through the earth's atmosphere was allowed for.

Brief description of Bigg's experiment

Bigg constructed a telescope with a large waterfilled perspex-lens which had a field of view of about 1° diameter. The light gathered by the telescope was chopped at 350 cycles/sec and then made to fall on an RCA IP22 photomultiplier provided with light filters transmitting wave-lengths in the range 6200-3000 Å. An auxiliary lead sulphide photocell measured light in the region 10,000 to 30,000 Å.

The amplification of the current from the photomultiplier could be adjusted. The illumination I falling on the photo-multiplier could also be regulated by suitable stops. The amplifier gain-control was adjusted in such a way as to keep the output voltage within a defined small range from 6.9 to 7.0 volts. A voltmeter having a full scale deflection of 0.1 volt

I

was placed between this varying output and the steady potential of 7.0 volts. The readings and time constituted the raw data.

Bigg plotted the values of $1/V(dV/dt)$ which were equal to $1/I(dI/dt)$ against h, where h is earth's geometrical shadow height. Refraction of the sun's grazing ray was allowed for. Bigg considered that when we use long wave-lengths and light is scattered at a small angle to the incident beam, there would be observable intensity of light even in the direction of the ray grazing the earth's surface. It was expected that there would be a discontinuous jump in intensity when the lower boundary of the illuminated portion of the atmosphere crosses an aerosol layer followed by a slow continuous change above. The change from clear air to hazy air will obviously contribute far more to the rate of change of intensity then the variation due to the slowly changing intensity in a clear atmosphere. Bigg observed in a direction making 70° with the zenith and took the calculated height of the grazing ray at a discontinuity in rate of change of intensity to correspond to the true height of the scattering layers. This assumption is questionable, because the extinction of the grazing ray will not be negligible and some correction Δh will have to be made to the lowest height in order to get the effective height of the scattering layers.

Bigg also took simultaneous measurements of twilight intensity in the same direction, with a light filter transmitting wave-lengths in the range 10,000-30,000 Å and a selenium

photocells sensitive to infrared region. He concluded that the use of longer wave-length produced sharper discontinuities in the curve, but that the height of the discontinuity was unchanged.

Bigg concluded from the study of his curves that there was dust accumulation at about 15-20 km height and also at 30 km. He also correlated low level temperature inversions taken from radio-sonde data and maxima on the twilight intensity curves of $1/I(dI/dt)$ against h, and concluded that inversions were detectable though it could not be ascertained whether the discontinuities represented the boundaries between regions of different dust content or rapid changes in atmospheric density.

7. Magrelishvili[8] (1958) studied the discontinuity on his twilight curves of $1/I(dI/dh)$ against h_s. He assumed that due to extinction of grazing rays during sunset, the least height accessible to investigation would be about 20 km. so that the effective height of the scattering layers would be h + 20 km. This seems to be an overestimate. The correction to h to be applied will also depend on (a) the wave-length of light used, (b) the solid angle from which light reaches the photocell and (c) the sharpness of the boundaries of the aerosol layers.

For obtaining good resolving power for a given set of dust layers one should use (a) the longest convenient wave-length in order to reduce scattering contribution by air and

(b) the smallest possible beamwidth in the light-gathering equipment in order that the position of the discontinuity may be clearly defined.

Magrolishvili found from his twilight curves, the first maximum at about 45-50 km and a second at about 100 km. The heights of these maxima in curves of Bigg and Magrolishvili differ only due to the correction in the shadow height. Magrolishvili attributed the upper maximum to fluorescence for the following reasons. He made his twilight observations on two different wave-lengths, one on 9400 Å and the other on 5270 Å. He did not find any discontinuities on the curves with 5270 Å but observed two maxima on the curve with 9400 Å, one at about 47 km and second at about 100 km. He argued that if these maxima were due to dust layers they should be observable with 5270 Å also. So it may be due to fluorescence and not due to dust layers. He did not, however, completely reject the possibility of the existence of dust layers in the atmosphere.

With the hope of detecting the presence of dust layers and their day to day changes in the upper atmosphere by the method of twilight scattering, the author made twilight measurements from 1957-59 at Mt.Abu (24°N) which is a station 4000 ft. above sea-level.

In the next chapter, the experimental technique and method of observation will be described.

I

REFERENCES

1. Gruner F., "Neueste Dammerungsforschungen" Ergebnisse der Kosmischen Physik, III.
2. Chiplonkar M.W. and Rande J.D., Proc.Ind.Acad.Sci., 18A, 121 (1943).
3. Ljunghall Arvid, The Intensity of the Twilight and its connection with the Density of the Atmosphere, Meddelande Fran Lunds Astronomiska Observatorium Ser II, Nr.125 (1949).
4. Dave J.V., M.Sc. Thesis submitted to Bombay University, (1952).
5. Bigg E.K., Nature, 177, 77 (1956).
6. Bigg E.K., J.Met., 13, 3, 262 (1956).
7. Bigg E.K., Ind.J.Met. & Geophy., 10, 2, 185 (1959).
8. Megrelishvili T.G., Ind.J.Met. & Geophy., 9, 3, 271 (1958).

I

CHAPTER II

DESCRIPTION OF APPARATUS USED AND METHOD OF OBSERVATION

CONTENTS

CHAPTER II

DESCRIPTION OF APPARATUS USED AND METHOD OF OBSERVATION

1. Introduction

During the twilight period, the light received from any part of the sky is due (1) to light primarily scattered by molecules illuminated by direct sunlight, (2) to light scattered by large particles also illuminated by direct sunlight and (3) to light multiply scattered by molecules and by large particles. Both (1) and (3) are likely to change gradually, but (2) may change rapidly. Therefore, any rapid change in the intensity observed at the ground when the earth's shadow traverses different levels is likely to be due to a discontinuity in vertical distribution of large particles. The problem is to study this change in twilight scattering instrumentally.

2. Experimental technique

Fig.1 is a block diagram of the experimental arrangement used at Abu for twilight observations. It consists of a telescope with a converging lens (f = 30 cm) fitted at one end of the collimating tube. The lower end was fitted with the sliding cover of a photomultiplier box. The central part

of the photocathode of the photomultiplier was at the axis of the collimating tube. The length of the tube and the aperture window near the photocathode are such that the circular field covered by the telescope was 1^{0} in diameter. The telescope was capable of resolving two layers 5 km apart.

A photomultiplier RCA IP22 was used as a light detector in conjunction with the telescope. The photomultiplier was selected for very small dark current and good sensitiveness to near red region. The choice fell on IP22 because no other photomultiplier sensitive to near red region was available at the time. The photomultiplier was mounted inside an aluminium box within a wooden box. Fluctuations in photomultiplier current due to temperature fluctuations could thus be reduced. There was provision in the cover of the wooden box to fix a light filter centrally on the axis of the collimating tube.

A chance filter ORl which had an integrated visible transmission of 5 % and which transmitted the spectral range 6400 Å - 7000 Å was used in conjunction with the photomultiplier. The transmission curve of the filter, the response curve of the photomultiplier and the effective response of the photometer with the filter are shown in Fig.2(a).

3. Choice of filter

As the aim of this work was to study the scattering in a forward direction by large particles larger than molecules,

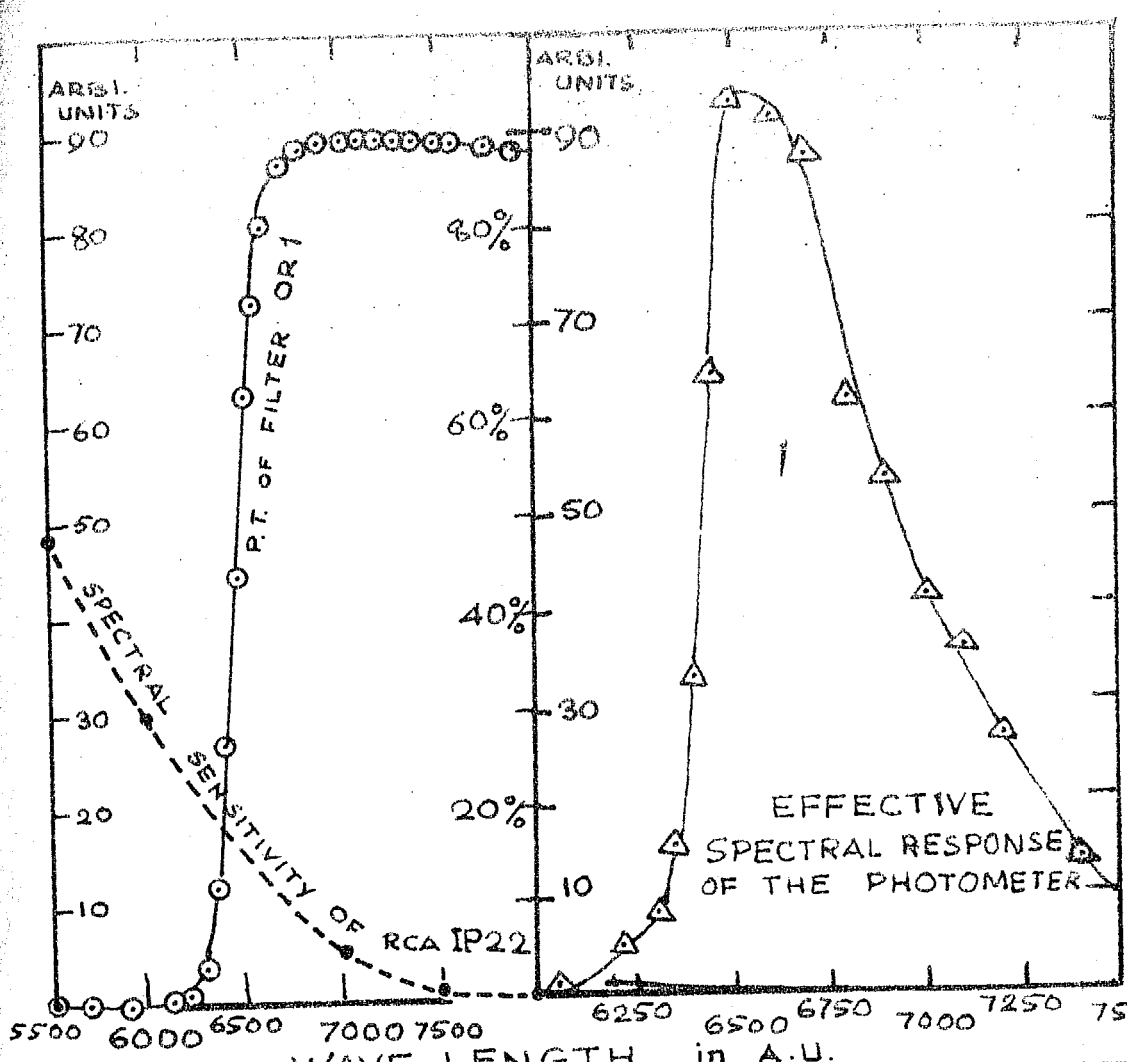

FIG. 2(a)

FIG. 2 (b)

L COLLECTING LENS
C COLLIMATING TUBE WITH
W WOODEN BOX
F FILTER OR 1
S SHUTTER
SK SHUTTER KNOB
B BLEEDER BOX
M METAL HOUSING OF THE PHOTOMULTIPLIER

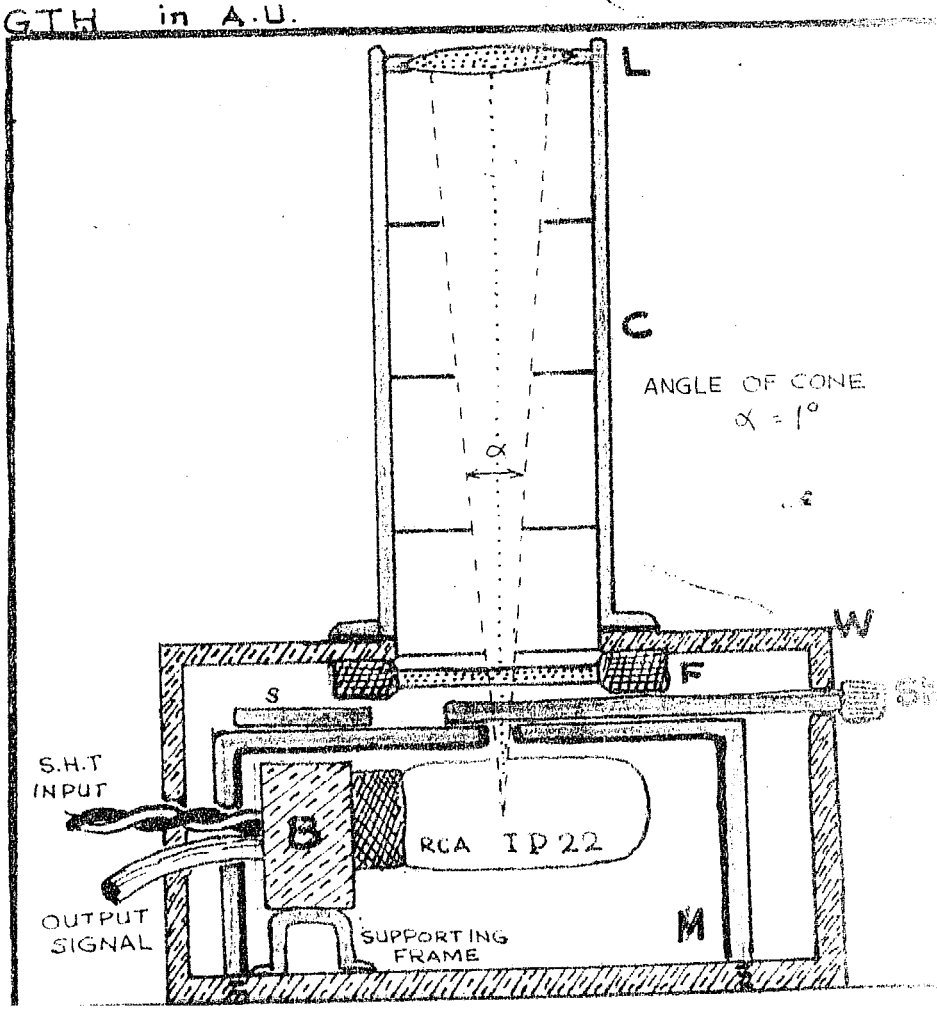

TWILIGHT PHOTOMETER

it would be best to use the longest possible wave-lengths keeping in mind the photomultiplier response, so as to reduce the effect of the molecularly scattered light. Secondly as the sun goes down below the horizon, multiple scattering will be more prominent in the shorter wave-length region. In order to avoid this multiple scattering effect as much as possible, the use of longer wave-lengths was preferred.

As observed by Link (1953) and others, the ratio of secondary to primary scattering at about 100 km of earth shadow height is much smaller for longer wave-lengths than for shorter wave-lengths.

M/P for λ 5300 Å = 0.23

and M/P for λ 9000 Å = 0.06.

Fig.2(b) shows a schematic diagram of the twilight photometer that was used at Abu.

4. Direction of observation

As is well known from the theory of large particle scattering, there will be a great preponderance of light in the forward direction in light scattered by particles whose linear dimensions are large in comparison with λ. It is therefore advisable to observe at a small angle above the horizon. However, the increasing attenuation of light with

increasing zenith distances has also to be considered in deciding on the direction of observation. The photometer unit along with the telescope was mounted on a stand so that the telescope could be directed in any direction.

5. Amplifier and power supplies

The output of the photomultiplier was amplified by a balanced bridge type D.C. amplifier which was both sensitive and stable. The sensitivity could be changed successively by a factor of about 10 at a time, by changing the input grid-leak resistances. The scaling ratios were determined at intervals to check the constancy of the amplifier, by illuminating the photocathode of the photomultiplier by a source of constant intensity and measuring the output current with an AVO model 8 current meter with a range of 50 μA.

The linearity of the amplifier was also checked and found to be good in the range -50 to + 50 μA. Fig.3 shows the plot of input grid voltage against the output current of the amplifier. The H.T of 150 volts for the plate voltage of the amplifier was taken from a V.R regulated power supply. Each dynode of the photomultiplier was given 90 volts from a super-high tension, highly regulated and stabilised power supply. The circuitry of the amplifier and power supplies are shown in Fig.4.

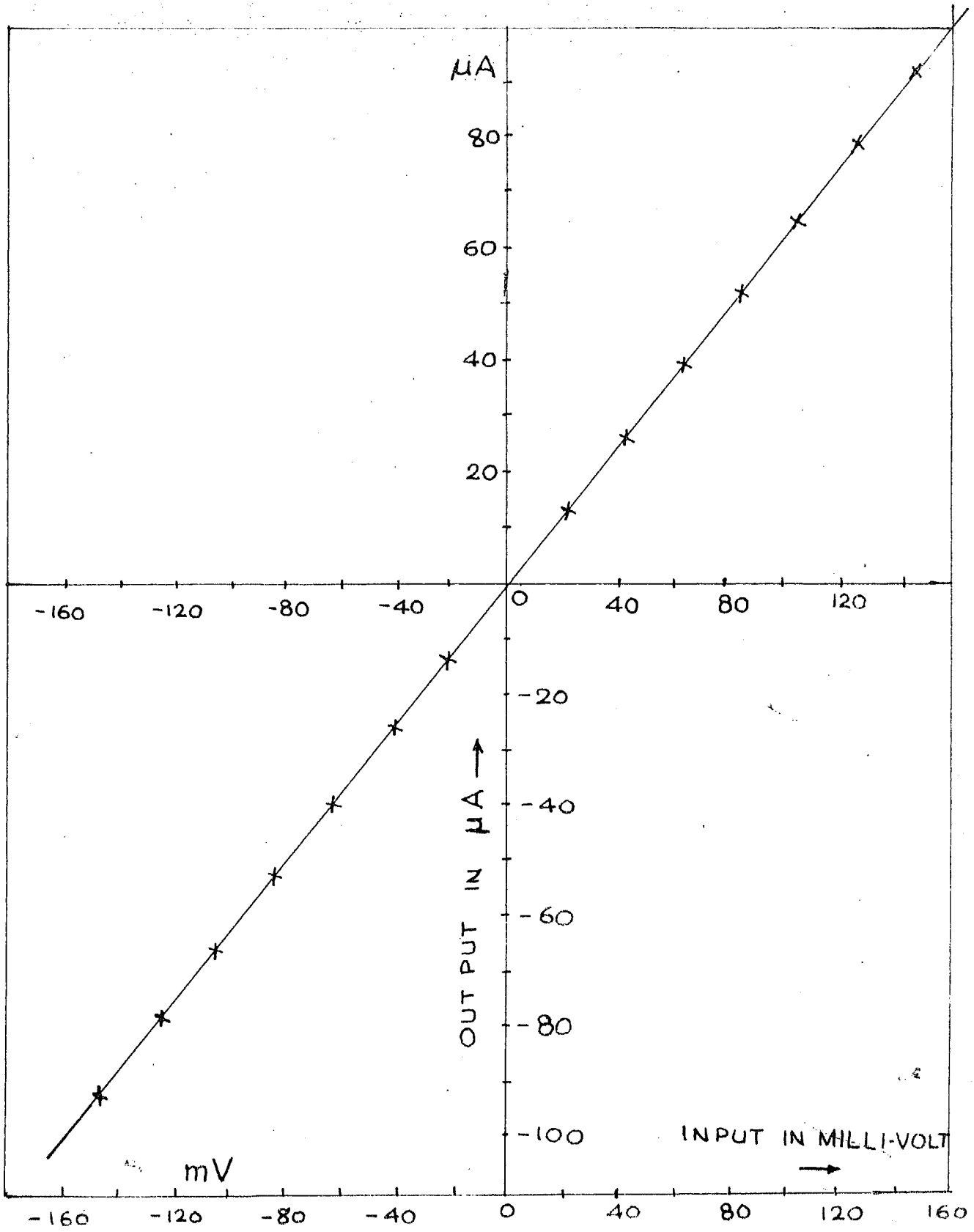

OUT PUT CURRENT OF THE D.C. AMPLIFIER AGAINST IN PUT SIGNAL VOLTAGE.

FIG. 3

II

CIRCUIT DIAGRAM OF THE D.C. AMPLIFIER

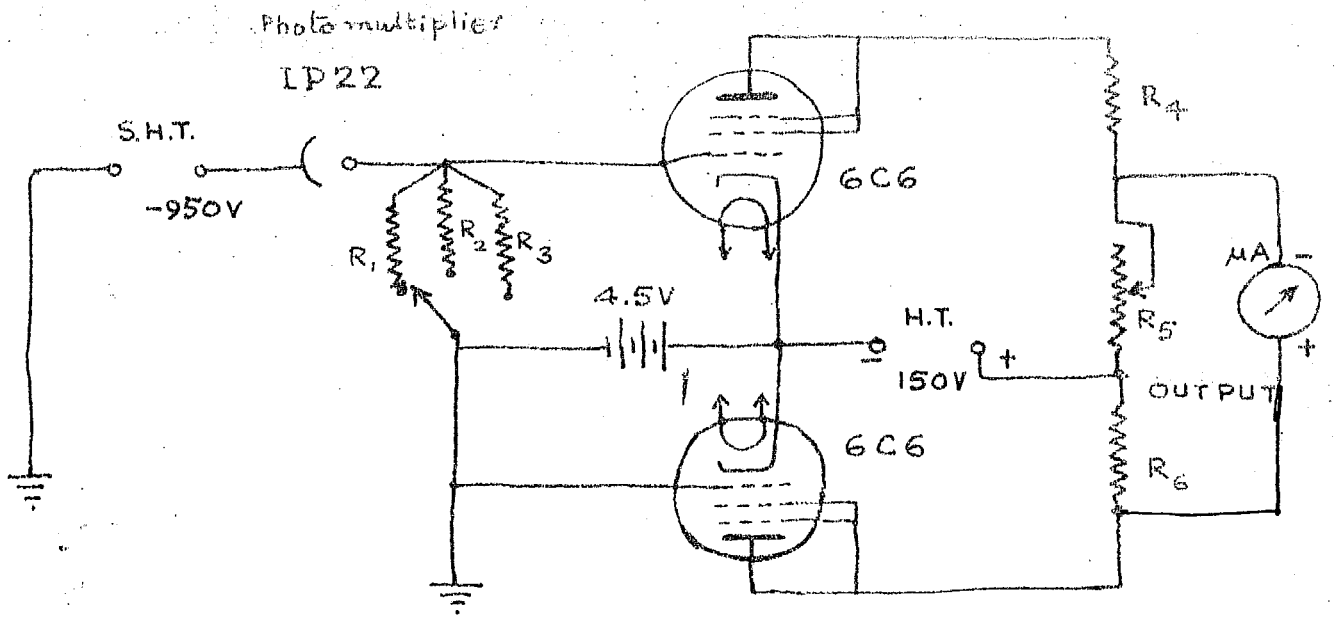

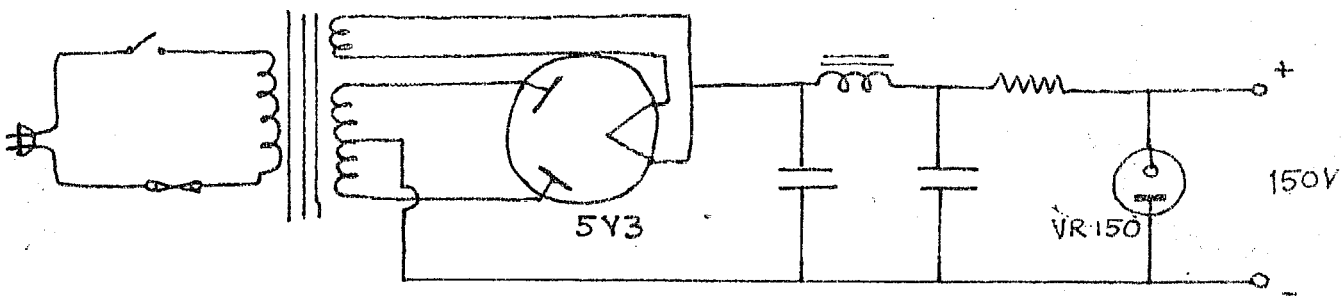

CIRCUIT DIAGRAM OF H.T. POWER SUPPLY

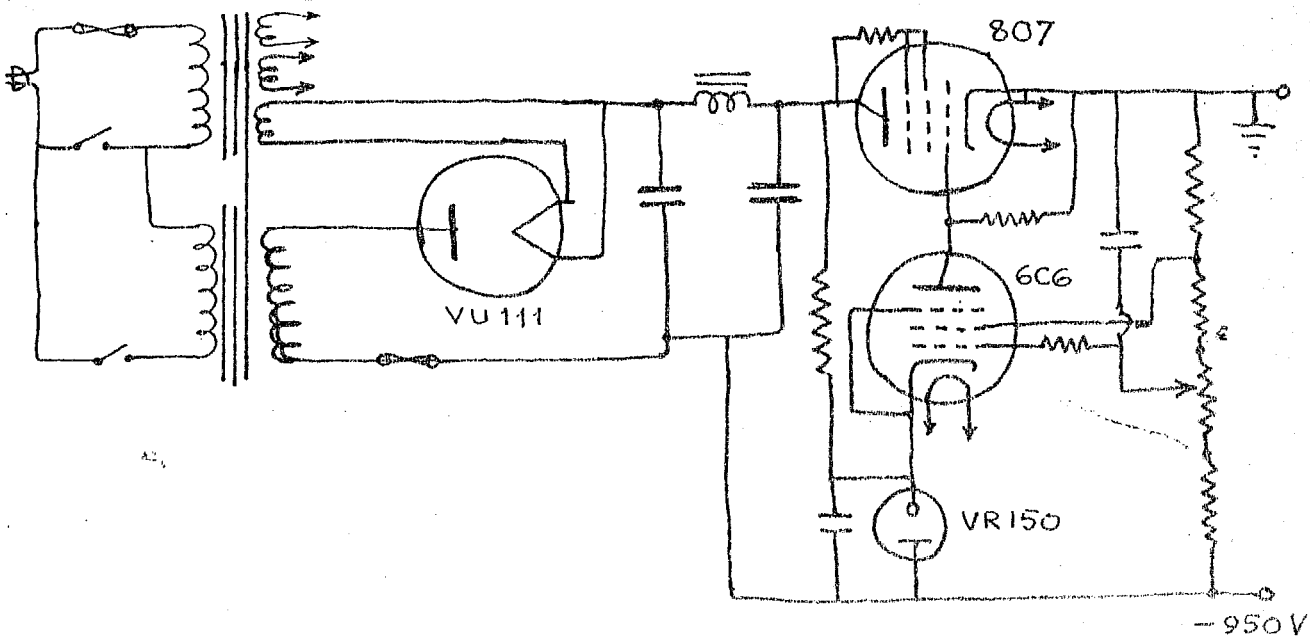

CIRCUIT DIAGRAM OF S.H.T. POWER SUPPLY

FIG. 4

6. Method of observation

The telescope of the photometer was directed towards the sun at an angle of 70° from the zenith. The intensity was measured at intervals of 30 sec starting from the time when the centre of the sun was $0^{\circ}50'$ below horizon to the time when it was 14°-15° below the horizon. The readings of the meter were multiplied by the respective scaling ratios to bring them all to the same scale. The intensity I and the time "t" of observation constitute the raw data.

From the time "t", the depression of the sun θ below the horizon, or the zenith distance of the sun $90^{\circ} + \theta$ could be calculated. The Nautical Almanac gives the Local Mean time, when the centre of the sun is (1) $0^{\circ}\ 50'$, (2) 6°, (3) 12° and (4) 18° below the horizon for different latitudes. From the plots of the sun's depression below horizon and the corresponding times, the sun's depression for each time of observation could be calculated. In the Appendix the values of $\Delta I/I$ corresponding to different values of θ, the sun's depression below horizon, are given for a few days.

In the next chapter the results of the observations and their discussion will be presented.

REFERENCES

1. Link F., Bull.Astr.Insts.Csl., 6 (1953).

CHAPTER III

TWILIGHT INTENSITY MEASUREMENTS AT ABU AND THEIR DISCUSSION

CONTENTS

CHAPTER III

TWILIGHT INTENSITY MEASUREMENTS AT ABU AND THEIR DISCUSSION

1. Introduction

On a clear day when the sun is above the horizon, the whole atmosphere above the observer is directly illuminated by solar radiations. When the sun goes down below the horizon, the lower portion of the earth's atmosphere is gradually cut off from the direct solar rays, first by haze in the lower atmosphere and then by the solid earth itself. Directly scattered light continues to come from the upper atmosphere for some time.

Though the portion of the earth's atmosphere that lies in the earth's shadow is cut off from the direct solar rays, it will be illuminated by scattered light from molecules and from any larger particles that may be present. The amount of secondary and multiply scattered light by molecules decreases rapidly with increase in wavelength.

2. Primary scattered radiations from layers at different heights above the observer when zenith distance of the sun is 90°

The primary scattered radiation from different

heights above the observer when the zenith distance of the sun is 90°, have been computed for λ 4500 Å and for 6600 Å respectively of the solar spectrum according to the method suggested by Ramanathan and Dave[1]. The extinction of primary scattered rays due to molecular scattering, β, has been calculated using the formula of Rayleigh and Cabannes[2], taking into account the depolarisation caused by molecular anisotropy. The values of β, the decimal attenuation coefficients due to scattering by unit thickness of pure atmosphere are 0.020 and 0.100 for red (λ = 6600 Å) and blue (λ = 4500 Å) respectively.

It is known that suspended water and dust particles exist in the lower layers of the atmosphere (particularly in 0-6 Km) and that they would attenuate the grazing rays. The decimal extinction coefficients due to these particles found by Ljunghall[3] from his observations at Helwan have been used for Abu. They are assumed to be independent of wavelengths. The values of extinction by haze used are 0.035, 0.052 and 0.021 for the layers at 1-2, 2-4 and 4-6 Km. Above 6 Km the extinction due to haze is assumed to be negligible.

Fig.1 represents the primary scattered radiation from different heights in the zenith when the sun is on the horizon or, the zenith distance of the sun is 90°. Curve-R relates to red light and curve-B to blue light.

III

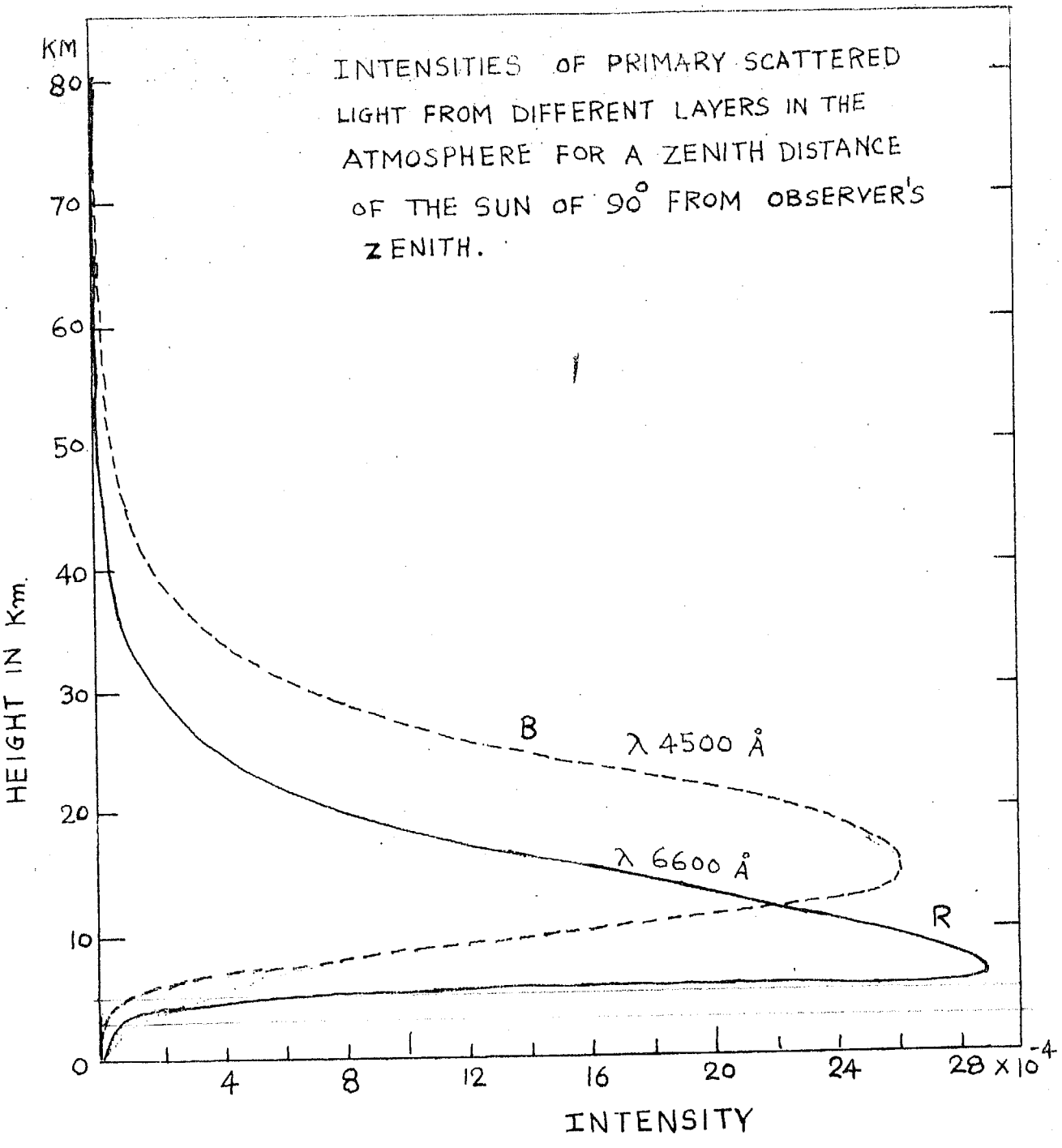

NO ALLOWANCE MADE FOR REFRACTION IN CALCULATING HEIGHTS OF SCATTERING LAYERS.

ATTENUATION DUE TO HAZE FOR RED LIGHT

h KM	δ
1 - 2	0.085
2 - 4	0.052
4 - 6	0.021
> 6	0.000

FIG. 1

It is seen from the figure that the maximum scattered light in blue comes from about 15 Km above the earth's surface. The level of half-maximum of the scattered light is at about 10 Km. Hence the screening height for grazing radiation for blue light in a pure atmosphere may be considered to be about 10 Km.

Examining the curve for red, it is seen that the maximum of the primary scattered light comes from a height of about 6 Km above the surface of the earth and that little light comes from the first 5 Km. Only 2 % of the maximum scattered light comes from near 3 Km.

The observations of twilight intensity were made at Abu looking in the direction of the sun at 70° from the zenith. So, the primary scattered intensity calculated for $Z = 90^{\circ}$ should be corrected for the angle of scattering. The screening height for red light is assumed to be 6 Km.

Khwostikov and Megrelishvili[4] (1960) calculated theoretically the intensity of primary scattered light as a function of the height (no allowance being made for refraction in computing height) for various zenith distances Z of the sun, and with different wavelengths, λ (FIG.1A). The direction of observation was 70° from zenith in the sun's meridian plane. It is seen from their tables that the maximum intensity of scattered light comes from the ray at a height of 9-14 Km above the earth's surface for the region 0.6 - 0.8 μ . Neither

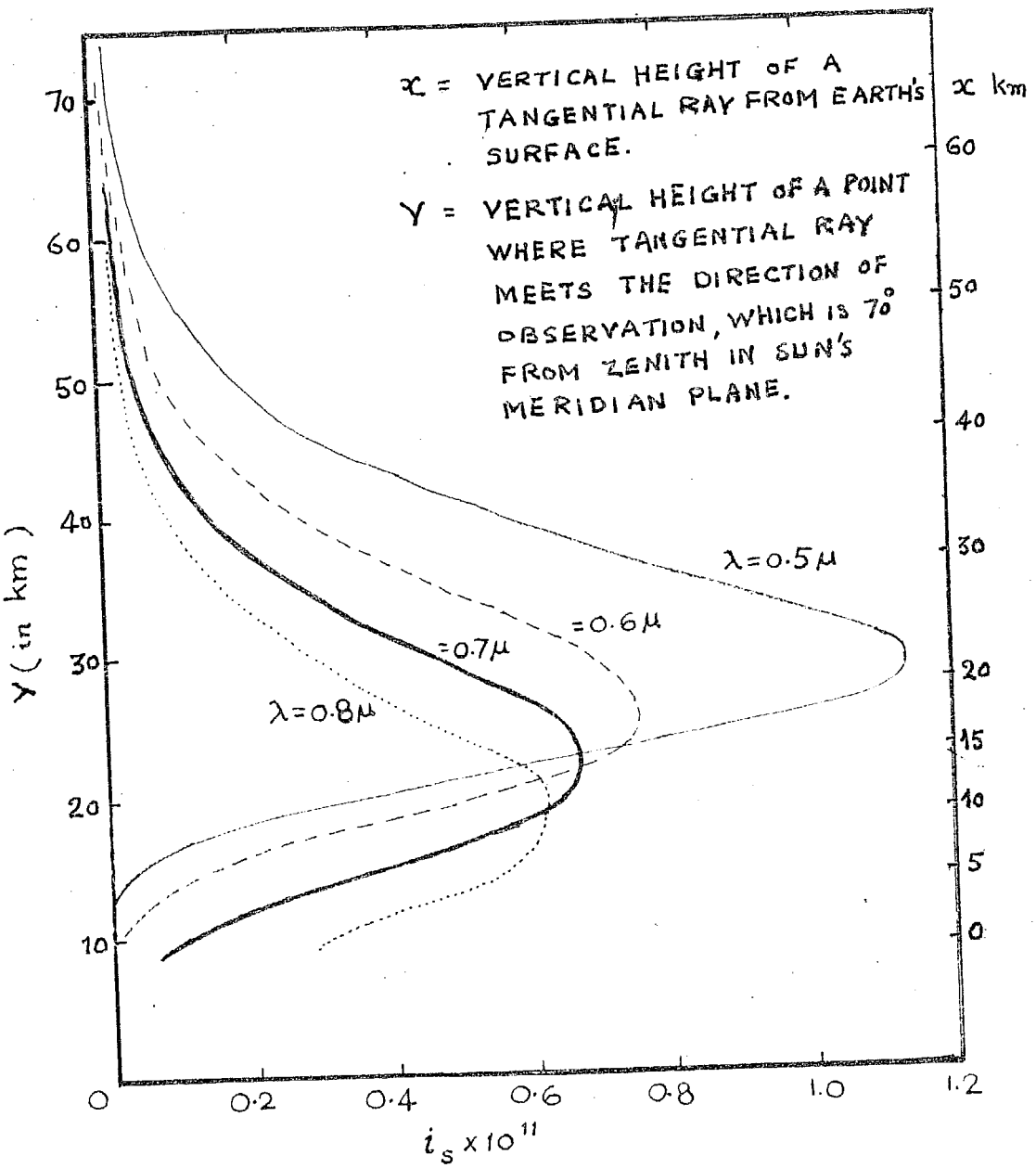

INTENSITY OF SCATTERED LIGHT FROM LAYERS AT DIFFERENT HEIGHTS (Y), FOR DIFFERENT WAVELENGTHS AT $Z = 93.4^\circ$

(after KHWOSTIKOV & MEGRELISHVILI)

FIG. 1A

attenuation of scattered light by water particles in the lower layers of the atmosphere nor refraction was taken into account.

3. The height of base of the directly illuminated region in the atmosphere for different depressions of the sun

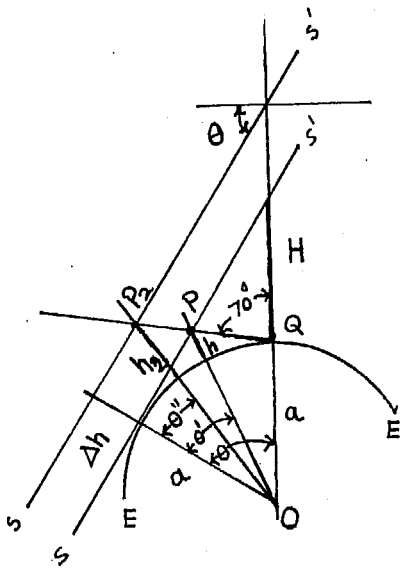

Fig.2. Schematic diagram of the solar grazing rays illuminating the twilight sky.

Fig.2 gives a schematic diagram of the sun's grazing rays illuminating the twilight sky. EE is the earth's surface. OQ the direction of the observer's zenith. QP is the direction of observation, which is 70° from the zenith in sun's meridian plane. a is radius of the earth. SS' the direction of solar radiations. θ is the depression of the centre of the sun below the horizon at the observer's zenith, Z(= 90°+θ) is the zenith distance of the sun, P is the point

where the tangential ray to the surface of the earth meets the line of observation, and P_2 is the point where the sun's grazing ray at a distance Δh from the earth's surface meets the line of observation, θ' is the depression of sun's centre below the horizon at P_1 and θ'' is that at P_2. "h" is the vertical height of P above the earth's surface and h_2 is that of P_2. H is the shadow height of the earth at the observer's zenith for sun's depression θ. No allowance has so far been made for refraction. Table 1 gives the values of h for P_1 for different values of θ.

If Δh is small, $\theta' \approx \theta''$

and $$h_2 = h + \frac{\Delta h}{\cos \theta'}$$

$$\approx h + \Delta h$$

i.e. the correction in height due to extinction of grazing rays, known as screening height is practically the same for all values of θ'.

Table 2 gives the values of θ' for different values of θ computed from the geometrical relation

$$\frac{(a+H)}{(a+h)} \cos \theta = \cos \theta' \quad \text{(Fig.2).}$$

If the screening height Δh is assumed to be 6 Km and an allowance is made for refraction in computing the

Table 1.

Height h, in kilometer of a point P vertically above the earth surface for different θ.

θ	θ'	h in km. 0	0.1	0.2	0.3	0.4	0.5	0.6	0.7	0.8	0.9
0	0.0	0.0	0.0	0.0	0.0	0.0	0.0	0.3	0.5	0.8	1.0
1	1.0	1.3	1.4	1.5	1.7	1.8	1.9	2.2	2.4	2.7	3.9
2	2.0	3.2	2.7	4.3	4.3	5.3	5.8	6.2	6.6	6.9	7.3
3	2.8	7.7	8.2	8.7	9.2	9.7	10.2	10.7	11.2	11.8	12.3
4	3.6	12.8	13.4	14.1	14.7	15.4	16.0	16.6	17.3	17.9	18.6
5	4.5	19.2	20.1	21.0	21.9	22.8	23.7	24.5	25.3	26.0	26.7
6	5.3	27.5	28.4	29.3	30.2	31.1	32.0	32.9	33.8	34.7	35.6
7	6.1	36.5	37.2	37.9	38.6	39.4	40.2	41.2	42.4	43.7	44.9
8	6.9	46.1	47.2	48.4	49.5	50.7	51.8	53.0	54.1	55.3	56.4
9	7.7	57.6	58.8	59.9	61.1	62.2	63.4	64.4	65.4	66.5	67.5
10	8.4	68.5	69.9	71.3	72.7	74.1	75.5	76.8	78.1	79.3	80.6
11	9.1	81.9	83.2	84.5	85.7	87.0	88.3	89.7	91.1	92.6	94.0
12	9.8	95.4	96.7	98.0	99.2	100.5	101.8	103.2	104.6	106.0	107.4
13	10.6	108.8	110.3	111.9	113.4	115.0	116.5	118.0	119.6	121.1	122.7
14	11.2	124.2	125.7	127.2	128.8	130.3	131.8	133.6	135.4	137.2	139.0
15	11.9	140.3	142.2	143.6	145.0	146.4	147.8	149.5	151.2	152.8	154.5

Table 2.

Values of θ' corresponding to different values of θ.

θ°	θ' in degrees									
	0'	0.1	0.2	0.3	0.4	0.5	0.6	0.7	0.8	0.9
0	0.00	0.10	0.20	0.30	0.40	0.50	0.60	0.70	0.80	0.90
1	1.00	1.10	1.20	1.30	1.40	1.50	1.60	1.70	1.80	1.90
2	2.00	2.08	2.16	2.24	2.32	2.40	2.48	2.56	2.64	2.72
3	2.80	2.88	2.96	3.04	3.12	3.20	3.28	3.36	3.44	3.52
4	3.60	3.69	3.77	3.86	3.94	4.03	4.11	4.20	4.28	4.37
5	4.45	4.54	4.62	4.71	4.79	4.88	4.96	5.05	5.13	5.22
6	5.30	5.38	5.46	5.54	5.62	5.70	5.78	5.86	5.94	6.02
7	6.10	6.18	6.26	6.34	6.42	6.50	6.58	6.66	6.74	6.82
8	6.90	6.98	7.05	7.13	7.21	7.29	7.36	7.44	7.52	7.59
9	7.67	7.74	7.81	7.88	7.95	8.02	8.09	8.16	8.23	8.30
10	8.37	8.44	8.51	8.58	8.65	8.72	8.79	8.86	8.93	9.00
11	9.07	9.14	9.22	9.29	9.36	9.44	9.51	9.58	9.65	9.73
12	9.80	9.88	9.95	10.03	10.10	10.18	10.25	10.33	10.40	10.48
13	10.55	10.62	10.68	10.75	10.81	10.88	10.94	11.01	11.07	11.14
14	11.20	11.27	11.34	11.41	11.48	11.55	11.62	11.69	11.76	11.83
15	11.90									

values of θ, the values of the height hg, which may be called the "effective shadow height", will be somewhat lowered. Table 3 gives the effective shadow heights of the lowest grazing rays of the sun illuminating the twilight sky in the direction of 70° from zenith in the sun's meridian plane.

Hulst[5] has calculated the height h at zenith of the lowest solar rays illuminating the twilight sky on the assumption that the layers of the atmosphere below 3 Km are opaque to the grazing rays. He has allowed for refraction.

Ljunghall has also calculated the effective limit of the earth-shadow. He assumed that there is no sharp limit to the earth-shadow. He calculated the limiting height at which the light, scattered from molecules below that height would be equal to the light coming from above the same limit. This limit he called the effective limit of the earth's shadow.

The effective shadow heights according to Hulst and Ljunghall are tabulated in Table 3.

4. Comparison of values of intensity with those of other investigators from zenith and from different parts of the sky

Table 4 gives the values of twilight intensity measurements at Abu made by the author in the direction of the

Table 3.

Height of the earth's shadow (allowing for refraction).

A - At zenith, according to HULST (screening height of 3 km, and $0^{o}.8$ allowance for refraction).

B - At zenith, according to Ljunghall (A limit of effective earth's shadow is that, the light, scattered from molecules below this limit, is equal to the reduction of the scattered light due to extinction of the light incident above the same limit).

C - In a direction of 70^{o} from zenith, in sun's meridian plane, according to the author (screening height of 6 km, and $0^{o}.6$ allowance for refraction).

Sun's Depressions in degrees.	Height in kilometers		
	A	B	C
0	-	11.7	-
1	3.7	14.7	6.5
2	5.6	18.7	8.0
3	8.7	24.4	10.5
4	13.9	31.6	15.0
5	21.0	40.4	21.5
6	30.0	51.2	23.5
7	41.1	65.1	36.5
8	54.0	80.0	46.0
9	69.0	97.0	56.0
10	85.5	116.5	67.5
11	106.0	138.0	79.5
12	126.0	161.0	93.5
13	150.0	187.0	107.5
14	176.0	215.0	121.5
15	204.0	245.0	135.5

sun at 70° from zenith along with the values at zenith of Dave and the values given by Ljunghall in the direction of the sun at 75° from zenith, at Helwan. The observations at Helwan were made with a red filter, mean wavelength 6350 Å, and by Dave at Abu with red filter, mean wavelength 6300 Å. The author used a red filter, the effective response of the photomultiplier and filter being at 6600 Å.

Fig.3 shows the plot of the values of twilight intensity for Abu in the direction of 70° from zenith, at zenith and at Helwan in the direction of 75° from zenith in the sun's meridian plane. The values are made to coincide at 5° sun's depression.

The following points may be noted :-

(1) The intensity at 70° from the zenith over Abu is relatively larger than the intensity at the zenith when the sun's depression is between 6° and 5°. The values at Helwan show a similar behaviour, but the difference is less pronounced.

(2) When the sun's depression is between 3° and 6°, the intensity at 70° decreases very rapidly with θ.

(3) From 6° to 11°, the rate of change of brightness is similar in all cases.

(4) From 11° to 15° the zenith intensity remains practically unaltered while the intensity at 70° still goes on decreasing.

I → INTENSITY OF LIGHT FROM CLOUDLESS SKY AT ZENITH (ABU); 70° FROM ZENITH (ABU) AND 75° FROM ZENITH (HELWAN) — ALL MADE TO COINCIDE AT $\theta = 5°$

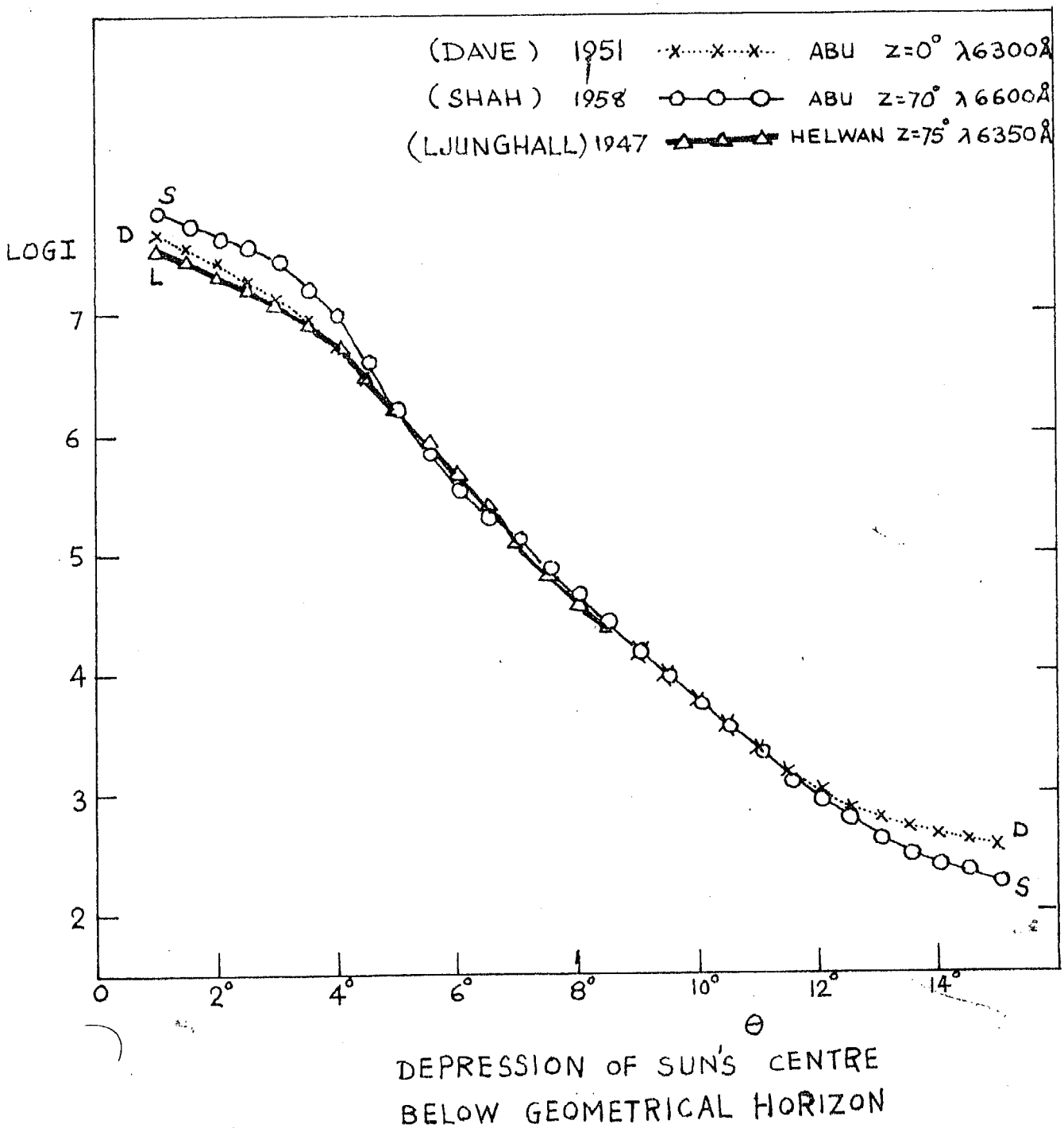

FIG - 3

III

Table 4.

Intensities of twilight sky during morning twilight from different parts of the sky (Red filter). Z = Zenith distance of the sky (towards sun).

Sun's depression	Dave Z=0°	Ljunghall Z = 75°	Abu Z=70°	Sun's depression	Dave Z=0°	Ljunghall Z = 75°	Abu Z=70°
1.0	4.64×10^{7}	3.63×10^{7}	7.41×10^{7}	8.5	2.60×10^{4}		2.69×10^{4}
1.5	3.65	2.32	5.39	9.0	1.52		1.59
2.0	2.33	2.19	4.47	9.5	1.01		1.00
2.5	1.33	1.70	3.55	10.0	6.20×10^{3}		4.47×10^{3}
3.0	1.29	1.20	2.32	10.5	3.30		3.55
3.5	3.40×10^{6}	8.32×10^{6}	1.53	11.0	2.45		2.09
4.0	5.20	5.50	1.00	11.5	1.52		1.26
4.5	3.00	3.24	4.17×10^{6}	12.0	1.01		3.31×10^{2}
5.0	1.65	1.66	1.66	12.5	7.10×10^{2}		6.03
5.5	3.50×10^{5}	3.71×10^{5}	7.03×10^{5}	13.0	6.0		4.17
6.0	4.45	4.63	3.55	13.5	5.2		3.16
6.5	2.42	2.45	2.24	14.0	4.4		2.51
7.0	1.30	1.26	1.41	14.5	3.9		2.24
7.5	7.25×10^{4}	6.76×10^{4}	7.94×10^{4}	15.0	3.6		1.66
8.0	4.23	3.55	4.63				

The difference from Dave's observations may be due to the fact that Dave's observations were made on 6300 Å (where there is the added effect of the twilight airglow), while the author's observations were on an effective wavelength of 6600 Å. and the proportion of multiple scattering to primary scattering is larger

5. Analysis

I is the intensity measured in arbitrary units as an amplified current by the photometer. To cover the large range of intensities, the amplification factor is changed by the insertion of different resistances in the input of the D.C. amplifier. The readings of the micro-ammeter are brought to the same unit of intensity by multiplying the current by the appropriate scaling factors. From the time of observation 't', the sun's depression θ at the zenith of the observer can be calculated. Owing to the large range in the value of I, it is convenient to plot log I against 't' or its equivalent θ.

In a pure dust-free atmosphere, if the intensity of sky light is assumed to be due mainly to primary scattered light, the intensity I will be proportional to the pressure p at the level of the effective shadow. But as a matter of fact, there is a certain amount of secondary and multiply scattered light added to the primary scattered radiation, and moreover, the atmosphere contains some particles of haze and ~~hydrometeors~~ condensed water-vapour which cause additional brightness in certain directions and also attenuate the direct radiation.

The effects of multiple scattering can be minimised by the use of longer wavelengths.

If a curve of $\frac{\Delta I/I}{\Delta p/p}$ or $\frac{\Delta \text{Log } I}{\Delta \text{Log } p}$ is plotted against θ, it is found that it shows significant rapid changes at some values of θ, and these are attributable to changes in the structure of the atmosphere, either of density changes or of changes in the dust content of the atmosphere.

The change of pressure with height in the atmosphere is given by the equation

$$\Delta p = - g \rho \Delta h \qquad (1)$$

where Δp is the fall of pressure corresponding to an increase in height of Δh.

Since $p = RT\rho$

we get,

$$\Delta p/p = - g \Delta h / RT \qquad (2)$$

where g is the acceleration due to gravity, and T the absolute temperature in degrees at pressure level p.

Table 5 gives the assumed values of temperature in the upper atmosphere used in making the calculations. Up to 30 Km, the temperatures are taken to be the same as those of the mean tropical atmosphere and above 30 Km, they are as in ARDC Model[7] Atmosphere.

Table 5.

Air temperature (°K) at different heights

(0-30 Km as for tropical atmosphere, ARDC atmospheres above 30Km)

h Km	0	1	2	3	4	5	6	7	8	9
0	305	297	291	284	277	270	263	255	249	242
10	235	228	220	214	208	201	194	197	200	204
20	208	212	215	218	220	222	224	227	229	232
30	235	234	237	240	243	246	249	252	255	258
40	261	264	267	270	273	276	279	281	283	283
50	283	283	283	281	280	276	271	267	262	258
60	254	249	245	240	236	232	227	223	218	214
70	210	205	201	196	192	188	183	179	174	170
80	166	166	166	166	166	166	166	166	166	166
90	166	167	168	172	176	180	184	187	191	195
100	199	203	207	210	214	218	222	235	248	267
110	287	306	325	344	363	382	401	420	439	458
120	477	496	515	533	552	571	590	609	627	646
130	665	684	702	721	739	758	776	795	813	832
140	850									

The value of h in Fig.2 is

$$h = a(\sec\theta' - 1)$$

$$= a\theta'^2/2 \text{ approximately, when } \theta' \text{ is small}$$

and $\Delta h = a\theta' \Delta\theta'$ (3)

From (2) and (3)

$$-\frac{\Delta p}{p} = \frac{g}{RT} a(\theta' \Delta\theta')$$

or $$\Delta \text{Log } p = -\frac{g}{RT} a(\theta' \Delta\theta') \quad (4)$$

(θ' measured in radians)

where R is universal gas constant. The values of $\frac{\Delta \text{Log } I}{\Delta \text{Log } p} = \frac{\Delta I \cdot RT}{I \cdot ag\theta'\Delta\theta'}$ are calculated for few days and are plotted against mean θ.

Representation of changes in sky intensity as a function of the height of the earth's shadow

Bigg[3] plotted dI/Idt against h where t is the time from sunrise or sunset and h is the height of the earth's shadow defined by the rising or setting of the sun's centre, allowing 68' for the horizontal refraction of the sun's ray. He found that there were marked peaks in the values of dI/Idt at heights varying from 10 to 20 Km and also one or two minor peaks at 75 to 90 Km.

Since there is a certain amount of uncertainty in defining the height of the earth's shadow, we considered it desirable to plot different simple functions of $\Delta I/I$ or $\Delta(\text{Log } I)$ against θ, the depression of the sun's centre below the geometrical horizon.

III

Fig.4 shows plots of Log I, Log p and ΔLog I/Δ Log p against θ on two days. The temperatures at the heights of the geometrical earth's shadow h, corresponding to θ are also plotted.

Among the other functions tried were $\Delta I/I \cdot \Delta t$ against θ, and Δ Log I/T$\cdot\Delta$Log p against θ. Fig.5 shows these three curves relating to the observations in the dawn of 27-1-53, p refers to the pressure in the atmosphere at the level of the geometrical earth's shadow without refraction.

For each value of θ, values of θ' and h_{eff}, the effective height of the earth's shadow corresponding to different assumptions regarding the screening height of the dust layer and atmospheric refraction, can be tried out.

From Figs.5, 6 and 7, it will be seen that in the curve of ΔLog I/ΔLog p against θ, the temperature structure of the earth's atmosphere is somewhat reflected, while in the curves of Δ Log I/T$\cdot\Delta$Log p against θ, and of $\Delta I/I \cdot \Delta t$, it is practically absent.

Still for the sake of simplicity we have preferred to retain the curves of ΔLog I/ΔLog p against θ.

On the right hand side of the Figs.5, 6 and 7, h_{eff}, the effective shadow height of the directly illuminated region in the direction 70° from zenith, corresponding to different depressions of the sun's centre θ, is given with an assumption

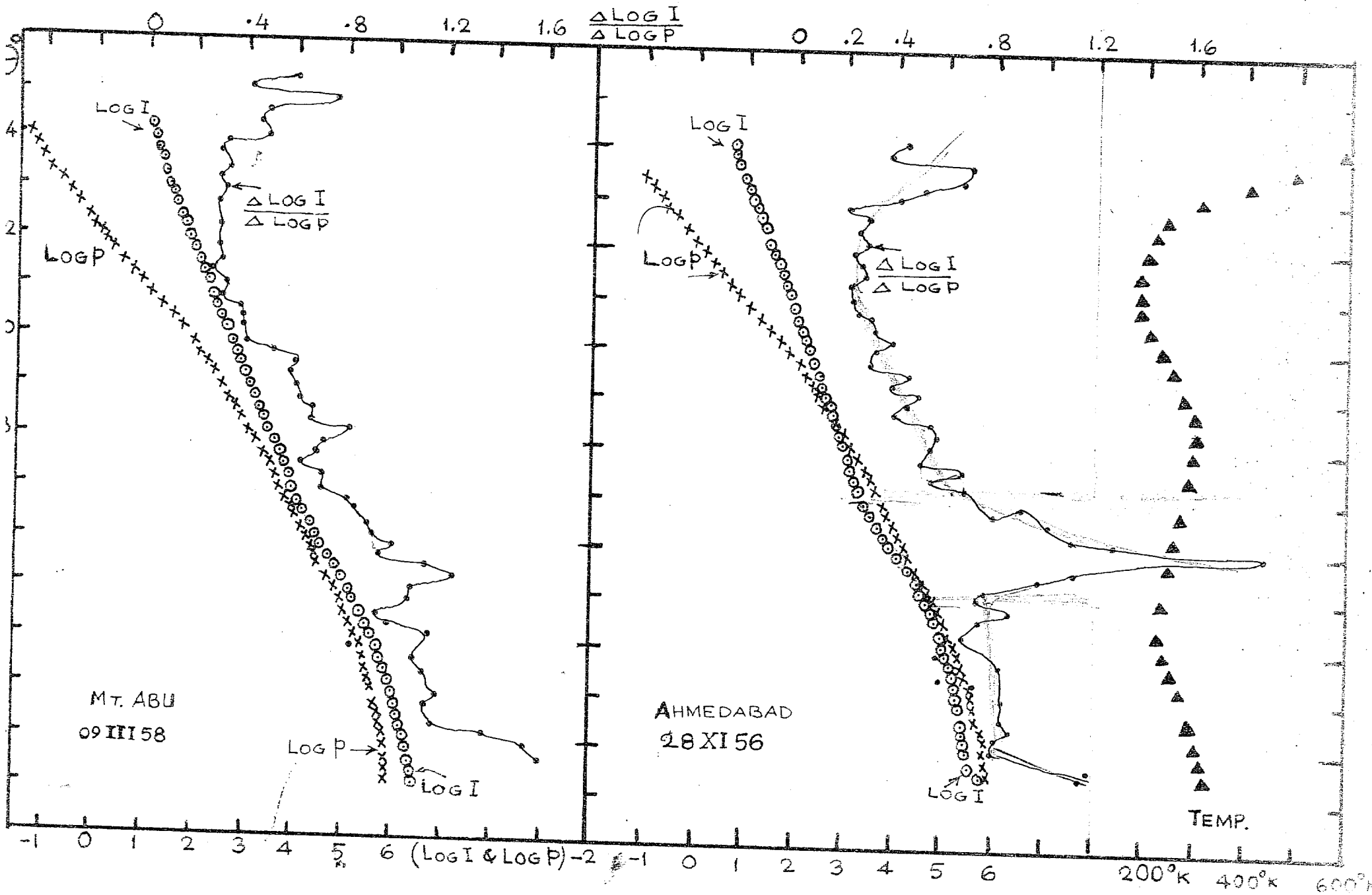
0 .4 .8 1.2 1.6 ΔLOG I / ΔLOG P
0 .2 .4 .8 1.2 1.6
LOG I
ΔLOG I / ΔLOG P
LOG P
MT. ABU
09 III 58
LOG P
LOG I
AHMEDABAD
28 XI 56
LOG I
TEMP.
-1 0 1 2 3 4 5 6 (LOG I & LOG P)
-2 -1 0 1 2 3 4 5 6
200°K 400°K 600°K

FIG. 4

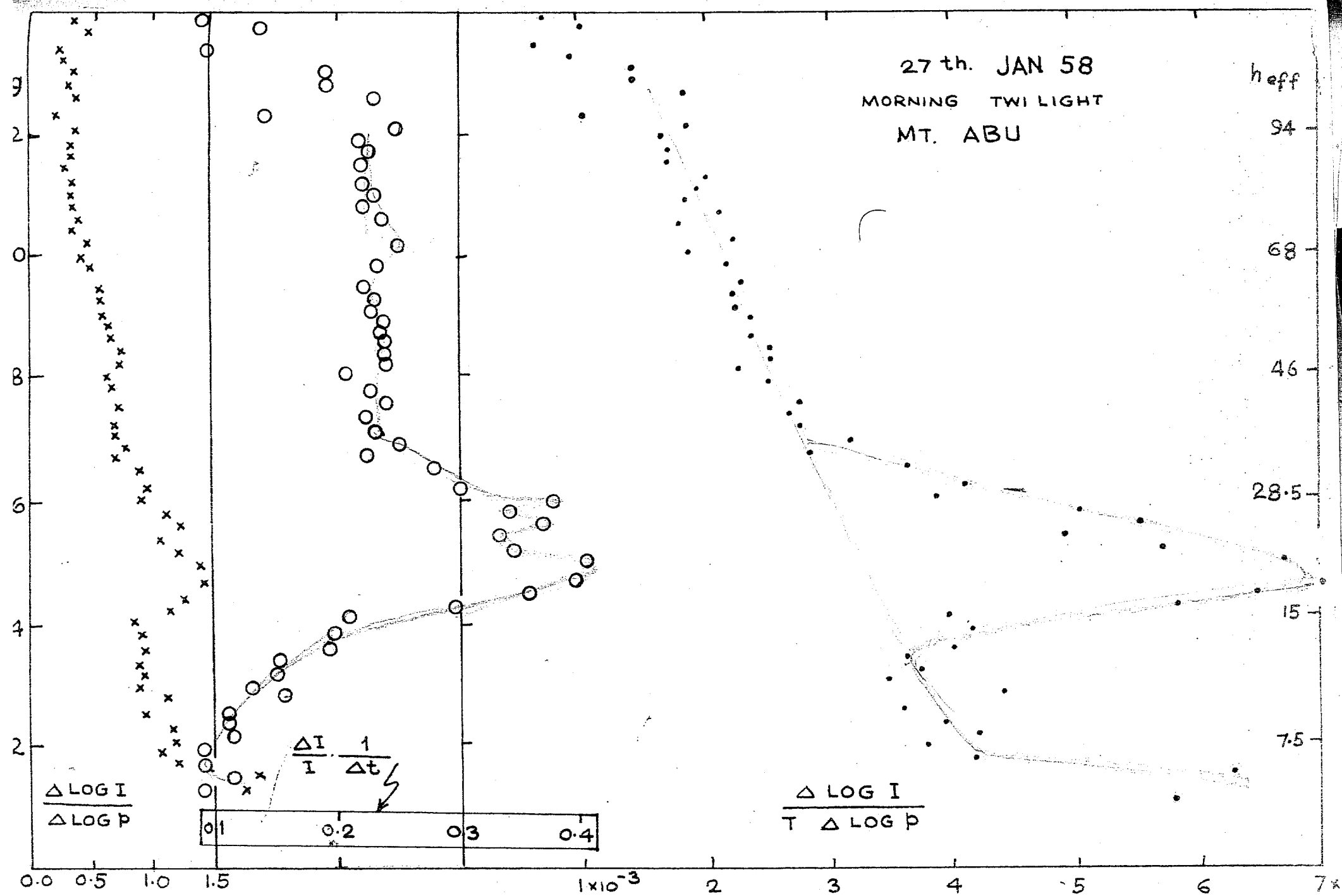
27 th. JAN 58
MORNING TWI LIGHT
MT. ABU
h eff
94
68
46
28·5
15
7·5
g
2
0
8
6
4
2
ΔI/I · 1/Δt
0·1
0·2
0·3
0·4
Δ LOG I / Δ LOG P
Δ LOG I / T Δ LOG P
0.0
0·5
1.0
1.5
1×10⁻³
2
3
4
5
6
7×

FIG. 5

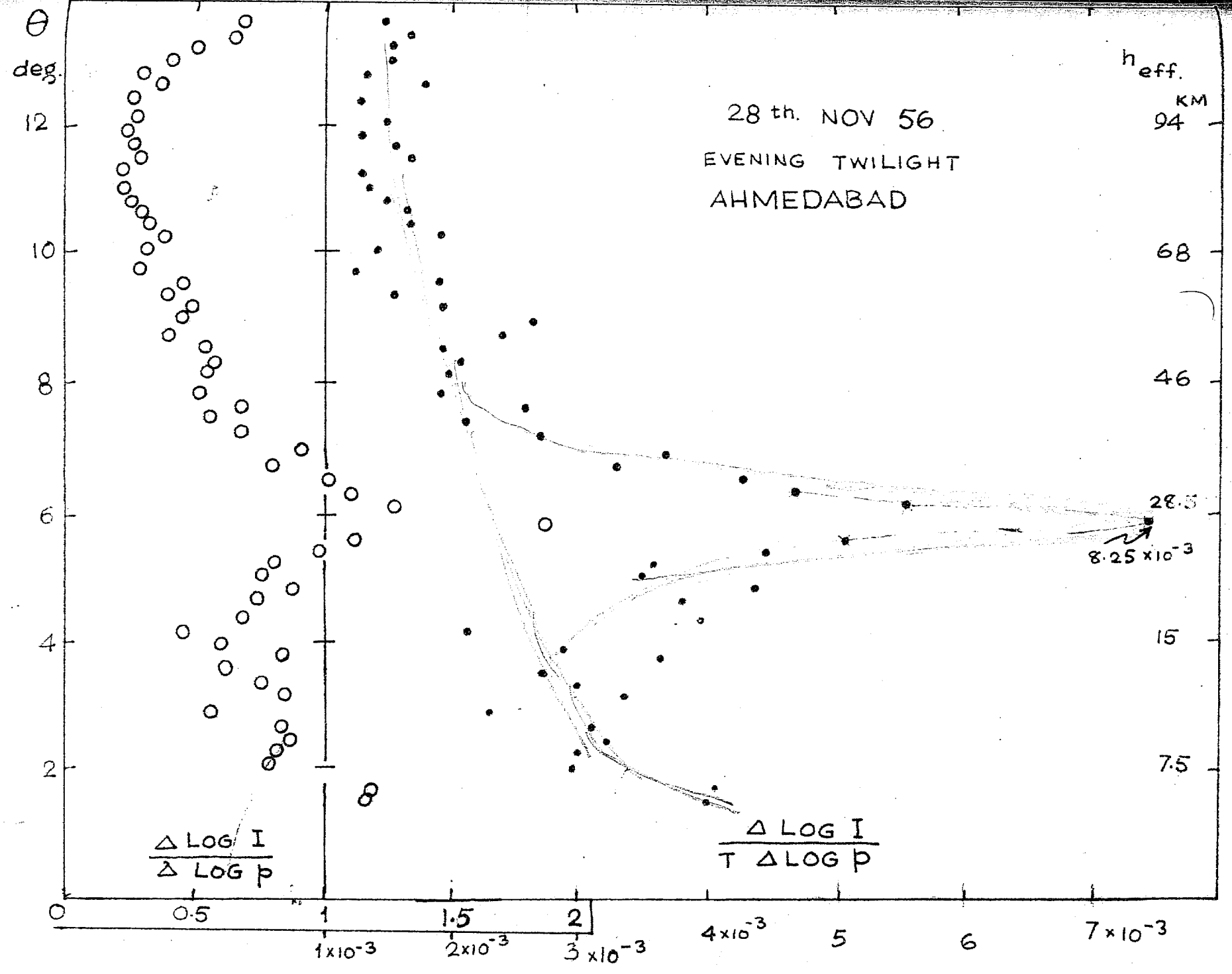
θ
deg.
12
10
8
6
4
2
0
h eff.
KM
94
68
46
28.5
15
7.5
28 th. NOV 56
EVENING TWILIGHT
AHMEDABAD
8·25 x10⁻³
Δ LOG I / Δ LOG p
Δ LOG I / T Δ LOG p
0·5
1
1.5
2
1x10⁻³
2x10⁻³
3 x10⁻³
4x10⁻³
5
6
7 x10⁻³

III

FIG.6

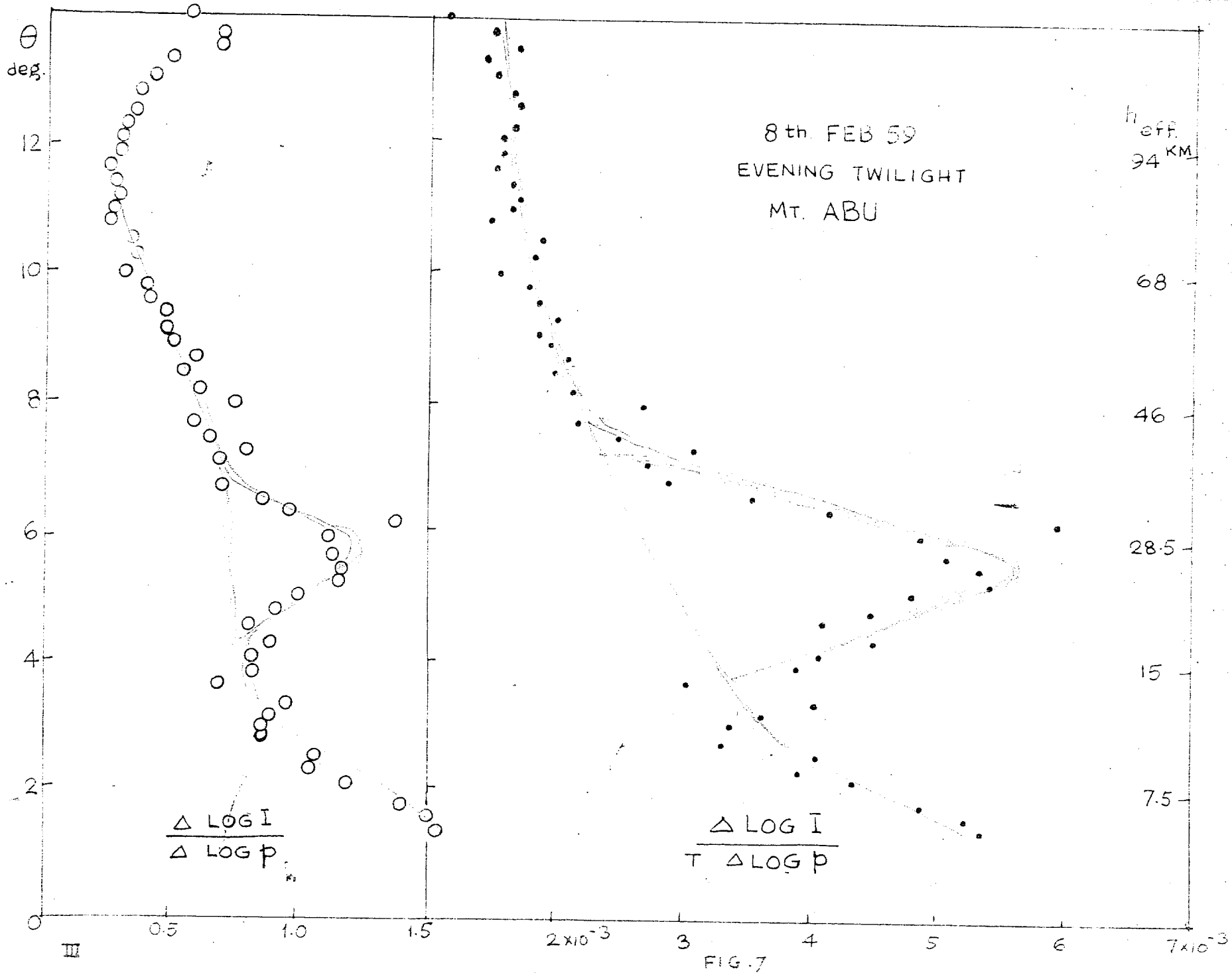
θ
deg.
12
10
8
6
4
2
0
8th FEB 59
EVENING TWILIGHT
MT. ABU
h eff.
94 KM
68
46
28·5
15
7·5
Δ LOG I
Δ LOG p
Δ LOG I
T Δ LOG p
0·5
1.0
1.5
2x10⁻³
3
4
5
6
7x10⁻³

III

FIG. 7

that the screening height is 6 Km and the allowance for refraction is $0^{\circ}.6$.

6. Presentation of results

Fig.3 represents the variation of $\Delta \text{Log } I / \Delta \text{Log } p$ against θ on a number of days in the month of January 1957-59.

The curves show the following more or less regular features, maximum between 5° and 6°, and a second feebler maximum at about $8^{\circ}.5$. The first maxima are sharp but the second less pronounced. The first maxima are sometimes divided into two or three sub-maxima, as shown on 30-1-57, 23-1-58 and 7-1-59. The minima occur at about $11^{\circ}.5$.

Figs.9 and 10 represent the variation of $\Delta \text{Log } I / \Delta \text{Log } p$ on a number of days in the month of February 1957-59. The maximum occurs as usual at θ equal to 5° to 6° and second maxima at about $8^{\circ}.5$. This is a usual feature of second maxima. Broad minima are shown at about 12°.

In March 1958 (Fig.11), the first maxima are irregular. Sometimes they are sharp and occur at 4° to 5° and second maxima at $8^{\circ}.5$. The minima occur at 12°. The variation of 4-3-58 was of peculiar nature. The first maximum occurred at about 4° sun's depression and was very sharp. The maxima on 9-3-58 was less pronounced and it occured between 5° and 6°.

In summer, many irregularities are observed in the curves and strong haze occurs at lower levels (Figs.12 and 13).

The first maxima occurred at values of sun's depression below 5° i.e. the whole layer seems to descend. On 13 and 14 June 1958, they were found at 4° sun's depression. The height of occurrence of first maxima recovers in the month of Nov-Dec. 1958 (Figs.14 & 15) and again they occur at $\theta = 5^{\circ}$ to 6° of sun's depression below the horizon. The second maxima occur between 8° and $8^{\circ}.5$ and minima occur at $11^{\circ}.5$.

7. Discussion

Junge et al[9,10] (1961) in their study of stratospheric aerosols by direct observation of the particles collected by means of balloon-borne inertial impactors at Bismarck N.D. and Omaha, found that the vertical distribution of stratospheric particles within a radius range of 0.1 μ to 1.0 μ, consistently showed a maximum in the stratosphere showing a broad maximum in between 15-23 Km. They suggested that these aerosol layers were identical with the layers responsible for the purple glow of twilight and the haze layers observed by fliers in the stratosphere. They also showed that on the upper side of a stratospheric aerosol layer, there is very pronounced stratification. This twilight phenomenon had been observed and studied for many years, particularly by Gruner (1958). The characteristics of the purple glow, especially the time of its

appearance as a function of the sun's depression below horizon, allow an estimation of the height of the scattering layer to be made, which is given by Gruner to be in the neighbourhood of 25 Km.

From our observations, it is found that the first maximum occurs at about 5° to 6° sun's depression which is equivalent to a layer at a height of 20-25 Km. Sometimes, these maxima are found to be at about 4° to 5° sun's depression, which corresponds to 15-20 Km. This means the whole layer of dust descends to a lower level in the atmosphere. Sometimes, thin layers of dust occur which are revealed by two to three maxima on the $\Delta \text{Log } I / \Delta \text{Log } P$ curve - when the tangential rays of the sun cross the lower boundary of a dust layer, the intensity falls abruptly and when the ray clears out, the intensity recovers to its previous normal value, with a slight decrease. Such are the cases occurring on 7-1-59, 3-12-58, 16-5-58 and 23-1-58. The first scattering layer varies from 15-30 Km. The lowest heights occur in June, and the highest in Nov-Dec.

A second layer is found at about 50 Km. in all the curves irrespective of season. Sometimes it is sharp and sometimes it is less pronounced. The minima occur at a height of 80-90 Km near the height where the temperature is also minimum.

III

References

1. Ramanathan K.R. & Dave J.V., Annals of IGY, 5, 23 (1957).
2. Cabannes J., J.Phys.Radium, 7, 260 (1927).
3. Ljunghall Arvid, "The intensity of twilight and its connection with the density of the atmosphere" Meddelande Fran Lunds Astronomiska Observatorium, Ser.II, Nr.125, (1949).
4. Hulst H.C., "Atmosphere of the Earth and Planets" by Gerard P. Kuiper, (1947).
5. Khwostikov I.A. & Megrolishvili T.G., Ind.J.Met. and Geophy., 11, 4, 347 (1960).
6. Dave J.V., M.Sc.Thesis submitted to the Bombay University (1952).
7. "Handbook of Geophysics", United Air Force Air Research and Development Command, The MacMillan Co., New York (1960).
8. Bigg E.K., Ind.J.Met. & Geophy., 10, 2, 185 (1959).
9. Junge C.E., Chagnon C.W. & Manson J.E., Geophy.Res. Directorate (ARDC) Bedford, Massachusetts (1960).
10. Junge C.E. & Chagnon C.W., J.Met., 18, 746 (1961).

SECTION II

APPENDIX

Relative change in intensity of twilight sky, in the direction 70° from zenith in sun's meridian plane during evening twilight at Mt.Abu for different θ. (Red filter)

31-10-58

θ	ΔI/I	θ	ΔI/I	θ	ΔI/I	θ	ΔI/I
1.0	0.14	4.3	0.19	7.6	0.21	11.0	0.10
1.2	0.13	4.5	0.32	7.8	0.23	11.2	0.22
1.4	0.08	4.8	0.47	8.1	0.22	11.5	0.20
1.7	0.10	5.0	0.44	8.3	0.22	11.7	0.18
1.9	0.10	5.2	0.36	8.5	0.20	11.9	0.25
2.1	0.11	5.4	0.34	8.7	0.20	12.1	0.18
2.3	0.12	5.6	0.35	9.0	0.21	12.4	0.21
2.5	0.11	5.9	0.30	9.2	0.19	12.6	0.26
2.8	0.12	6.1	0.25	9.4	0.22	12.8	0.25
3.0	0.11	6.3	0.30	9.6	0.20	13.0	0.35
3.2	0.16	6.5	0.30	9.9	0.20	13.3	0.30
3.4	0.13	6.7	0.25	10.1	0.25	13.5	0.39
3.7	0.15	7.0	0.25	10.3	0.23	13.7	0.25
3.9	0.16	7.2	0.21	10.6	0.22	13.9	0.10
4.1	0.22	7.4	0.23	10.8	0.21		

Relative change in intensity of twilight sky, in the direction 70° from zenith in sun's meridian plane during evening twilight at Mt.Abu for different θ. (Red filter)

3-11-58

θ	△I/I	θ	△I/I	θ	△I/I	θ	△I/I
1.2	0.09	4.7	0.23	8.2	0.23	11.7	0.20
1.4	0.10	4.9	0.27	8.4	0.18	11.9	0.21
1.6	0.10	5.1	0.30	8.6	0.24	12.2	0.17
1.3	0.10	5.3	0.32	8.9	0.20	12.4	0.19
2.0	0.10	5.6	0.34	9.1	0.20	12.6	0.20
2.3	0.11	5.3	0.33	9.3	0.22	12.8	0.19
2.5	0.11	6.0	0.34	9.5	0.20	13.0	0.20
2.7	0.13	6.2	0.33	9.7	0.25	13.3	0.23
2.9	0.15	6.4	0.31	10.0	0.21	13.5	0.19
3.1	0.14	6.7	0.29	10.2	0.14	13.7	0.17
3.4	0.15	6.9	0.26	10.4	0.20	13.9	0.08
3.6	0.19	7.1	0.22	10.6	0.19	14.1	0.21
3.3	0.19	7.3	0.24	10.8	0.16	14.4	0.13
4.0	0.18	7.5	0.19	11.1	0.21	14.6	0.12
4.2	0.21	7.8	0.21	11.3	0.18		
4.5	0.22	8.0	0.21	11.5	0.20		

Relative change in intensity of twilight sky, in the direction 70° from zenith in sun's meridian plane during evening twilight at Mt.Abu for different θ. (Red filter)

10-12-58

θ	ΔI/I	θ	ΔI/I	θ	ΔI/I	θ	ΔI/I
1.2	0.10	4.5	0.24	7.8	0.21	11.1	0.23
1.4	0.10	4.7	0.27	8.0	0.20	11.3	0.16
1.6	0.10	4.9	0.28	8.2	0.21	11.5	0.19
1.8	0.10	5.1	0.32	8.4	0.20	11.7	0.17
2.0	0.11	5.3	0.34	8.6	0.20	11.9	0.21
2.2	0.11	5.5	0.36	8.8	0.19	12.1	0.17
2.4	0.12	5.7	0.32	9.0	0.21	12.4	0.23
2.6	0.11	5.9	0.37	9.3	0.17	12.6	0.15
2.8	0.13	6.2	0.34	9.5	0.21	12.8	0.16
3.0	0.12	6.4	0.29	9.7	0.21	13.0	0.12
3.2	0.17	6.6	0.25	9.9	0.18	13.2	0.19
3.4	0.18	6.8	0.27	10.1	0.21	13.4	0.15
3.6	0.18	7.0	0.18	10.3	0.19	13.6	0.11
3.8	0.17	7.2	0.23	10.5	0.17	13.8	0.14
4.1	0.26	7.4	0.18	10.7	0.19	14.0	0.08
4.3	0.22	7.6	0.27	10.9	0.19	14.2	0.09

Relative change in intensity of twilight sky, in the direction 70° from zenith in sun's meridian plane during evening twilight at Mt.Abu for different θ. (Red filter)

8-2-59

θ	ΔI/I	θ	ΔI/I	θ	ΔI/I	θ	ΔI/I
1.0	0.09	4.3	0.23	7.7	0.19	11.2	0.20
1.2	0.10	4.6	0.23	8.0	0.25	11.4	0.21
1.4	0.09	4.8	0.25	8.2	0.20	11.7	0.20
1.6	0.11	5.1	0.29	8.5	0.19	11.9	0.21
1.8	0.11	5.3	0.32	8.7	0.21	12.1	0.21
2.0	0.11	5.5	0.36	8.9	0.19	12.3	0.21
2.3	0.11	5.7	0.34	9.1	0.19	12.6	0.22
2.5	0.12	6.0	0.35	9.4	0.21	12.8	0.23
2.8	0.12	6.2	0.43	9.6	0.20	13.1	0.21
3.0	0.12	6.4	0.31	9.8	0.20	13.3	0.19
3.2	0.14	6.6	0.27	10.0	0.18	13.5	0.24
3.4	0.17	6.8	0.22	10.3	0.21	13.7	0.21
3.7	0.13	7.1	0.22	10.5	0.22	14.0	0.15
3.9	0.19	7.3	0.26	10.8	0.13	14.2	0.18
4.1	0.21	7.5	0.22	11.0	0.20	14.4	0.18

Relative change in intensity of twilight sky, in the direction 70° from zenith in sun's meridian plane during evening twilight Mt.Abu for different θ. (Red filter)

5-1-59

θ	ΔI/I	θ	ΔI/I	θ	ΔI/I	θ	ΔI/I
1.2	0.09	.3	0.19	7.4	0.22	10.6	0.18
1.4	0.09	.6	0.24	7.7	0.21	10.8	0.19
1.6	0.10	.8	0.25	7.9	0.21	11.0	0.20
1.8	0.11	.0	0.23	8.1	0.20	11.2	0.18
2.0	0.12	.2	0.29	8.3	0.20	11.4	0.18
2.2	0.13	.4	0.32	8.5	0.20	11.6	0.19
2.4	0.09	.6	0.31	8.8	0.20	11.8	0.18
2.6	0.14	.8	0.34	9.0	0.20	12.0	0.23
2.8	0.13	.0	0.31	9.2	0.19	12.2	0.16
3.0	0.15	.2	0.29	9.4	0.21	12.4	0.19
3.2	0.14	.4	0.27	9.6	0.19	12.6	0.18
3.5	0.19	.6	0.21	9.8	0.17	12.9	0.17
3.7	0.12	.8	0.27	10.0	0.24	13.1	0.16
3.9	0.13	.0	0.24	10.2	0.19	13.3	0.14
4.1	0.20	.2	0.20	10.4	0.18	13.5	0.11
						13.7	0.18